Symmetric Achromatic Variability:
A New and Totally Unexpected Phenomenon

Anthony Readhead
Caltech

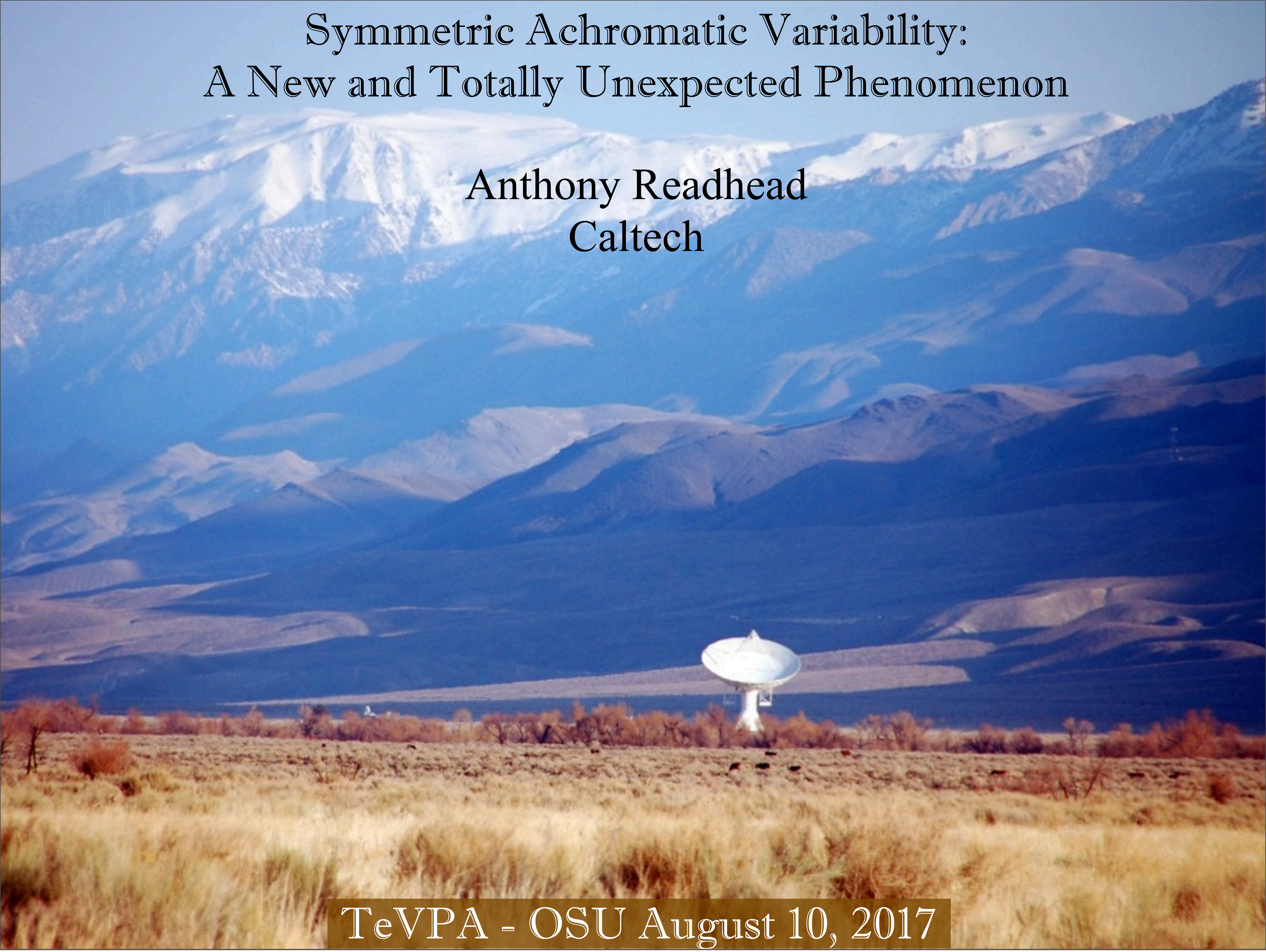

TeVPA - OSU August 10, 2017

Traditionally there have been two ways of detecting gravitational lensing:

1. Multiple Images

2. Time Delayed Variations

We believe there is now a third,
until now totally unsuspected, way:

3. **Symmetric Achromatic Variability**
That not only gives us a totally new approach to gravitational lensing but, also provides microarcsecond resolution on some active galactic nuclei - i.e. a factor 30-100x better resolution than mm VLBI

Symmetric Achromatic Variability in Active Galaxies -
A Powerful New Gravitational Lensing Probe?
arXiv:1702.06582

The Peculiar Light Curve of J1415+1320 -
A Case Study in Extreme Scattering Events
arXiv:1702.05519

H. K. Vedantham[1*], A. C. S. Readhead[1], T. Hovatta[2,3,4],
T. J. Pearson[1], R. D. Blandford[5], M. A. Gurwell[6],
A. Lähteenmäki[2], W. Max-Moerbeck[7], V. Pavlidou[8],
V. Ravi[1], R. A. Reeves[9], J. L. Richards[1],
M.Tornikoski[2], J. A. Zensus[6]

To be published in ApJ next week (8/15/17)

Symmetric Achromatic Variability in Active Galaxies - A Powerful New Gravitational Lensing Probe?
arXiv:1702.06582

The Peculiar Light Curve of J1415+1320 - A Case Study in Extreme Scattering Events
arXiv:1702.05519

Harish Vedantham

H. K. Vedantham[1*], A. C. S. Readhead[1], T. Hovatta[2,3,4], T. J. Pearson[1], R. D. Blandford[5], M. A. Gurwell[6], A. Lähteenmäki[2], W. Max-Moerbeck[7], V. Pavlidou[8], V. Ravi[1], R. A. Reeves[9], J. L. Richards[1], M.Tornikoski[2], J. A. Zensus[6]

To be published in ApJ next week (8/15/17)

40 m Telescope 15 GHz monitoring program since 2008 in support of *Fermi*-GST: ~1830 objects twice a week. This program has amassed ~12,000 object-years on Active Galaxies and the OVRO data have been used in a paper per month in refereed journals for the last 8 years - now up to 95 papers using this data with no sign of a drop off

The field of radio AGN monitoring began with the discovery of quasars and has been going on now for half a century

The field of radio AGN monitoring began with the discovery of quasars and has been going on now for half a century

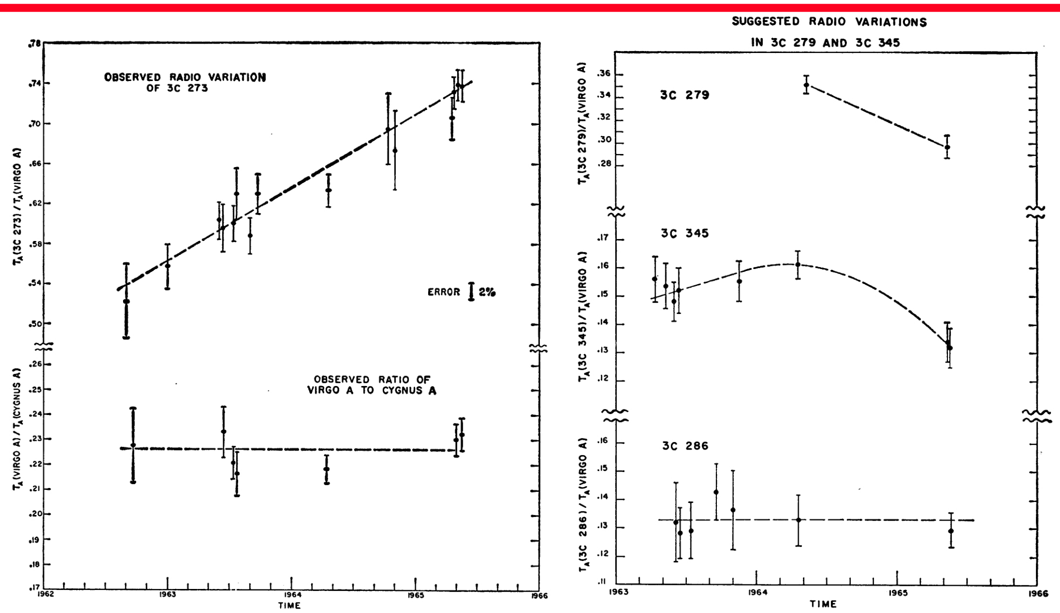

Fig. 1 (left). The ratio of the corrected antenna temperature, T_A, at 8000 Mc/sec of the quasi-stellar source 3C 273 to that of Virgo A, showing the observed 40-percent increase in the radio emission over a nearly three-year period. The measured ratio of Virgo A to Cygnus A shows no variation over the same period. Fig. 2 (right). Evidence for possible variations in the radio emissions of the quasi-stellar sources 3C 279 and 3C 345 at 8000 Mc/sec, and for a lack of variation in the quasi-stellar source 3C 286. Like 3C 273, which shows variations, both 3C 279 and 3C 345 have flat radio spectra at 8000 Mc/sec.

Dent 1965, Science, 148, 1458

Lack of synchrotron self-absorption as shown by their spectra give a lower limit to the size of the emitting regions which is >> the light-travel time associated with the flux density variations.

The field of radio AGN monitoring began with the discovery of quasars and has been going on now for half a century

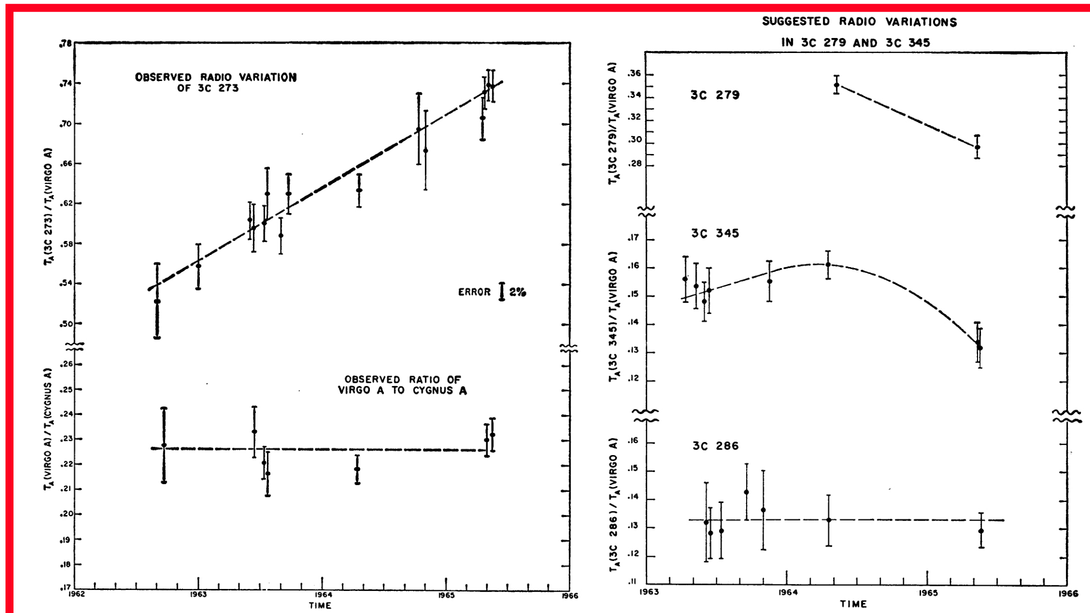

Fig. 1 (left). The ratio of the corrected antenna temperature, T_A, at 8000 Mc/sec of the quasi-stellar source 3C 273 to that of Virgo A, showing the observed 40-percent increase in the radio emission over a nearly three-year period. The measured ratio of Virgo A to Cygnus A shows no variation over the same period. Fig. 2 (right). Evidence for possible variations in the radio emissions of the quasi-stellar sources 3C 279 and 3C 345 at 8000 Mc/sec, and for a lack of variation in the quasi-stellar source 3C 286. Like 3C 273, which shows variations, both 3C 279 and 3C 345 have flat radio spectra at 8000 Mc/sec.

Dent 1965, Science, 148, 1458

Lack of synchrotron self-absorption as shown by their spectra give a lower limit to the size of the emitting regions which is >> the light-travel time associated with the flux density variations.

Rees1966, Nature, 211, 468

APPEARANCE OF RELATIVISTICALLY EXPANDING RADIO SOURCES

1. Explained rapid variability in PEGRS
2. **Predicted superluminal motion**

The first unification paper

Rees 1967, MNRAS, 135,345

The field of radio AGN monitoring began with the discovery of quasars and has been going on now for half a century

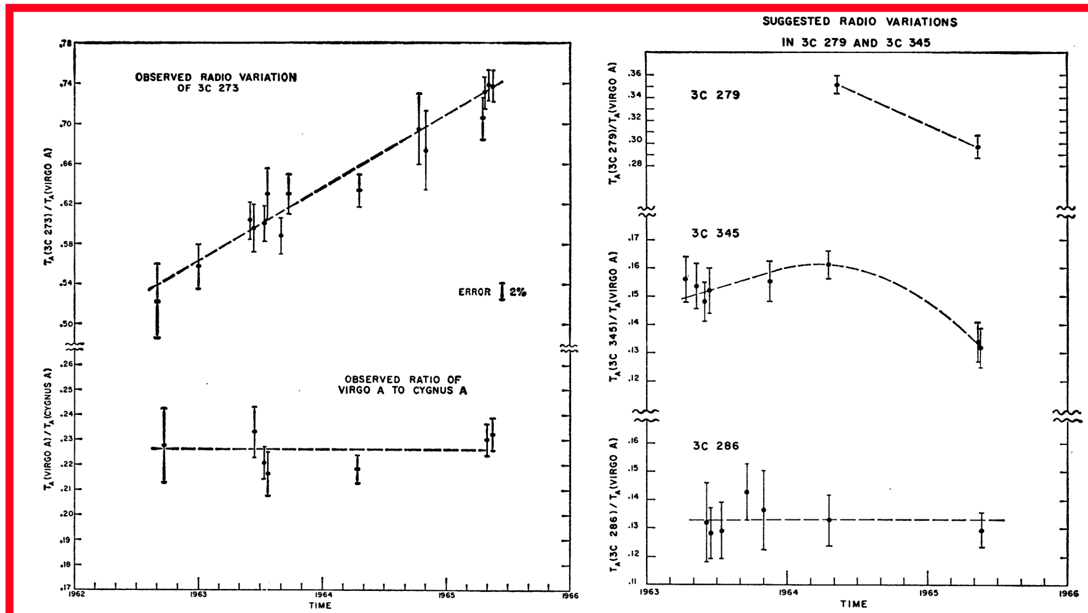

Fig. 1 (left). The ratio of the corrected antenna temperature, T_A, at 8000 Mc/sec of the quasi-stellar source 3C 273 to that of Virgo A, showing the observed 40-percent increase in the radio emission over a nearly three-year period. The measured ratio of Virgo A to Cygnus A shows no variation over the same period. Fig. 2 (right). Evidence for possible variations in the radio emissions of the quasi-stellar sources 3C 279 and 3C 345 at 8000 Mc/sec, and for a lack of variation in the quasi-stellar source 3C 286. Like 3C 273, which shows variations, both 3C 279 and 3C 345 have flat radio spectra at 8000 Mc/sec.

Dent 1965, Science, 148, 1458

Lack of synchrotron self-absorption as shown by their spectra give a lower limit to the size of the emitting regions which is >> the light-travel time associated with the flux density variations.

Rees1966, Nature, 211, 468

APPEARANCE OF RELATIVISTICALLY EXPANDING RADIO SOURCES

1. Explained rapid variability in PEGRS
2. **Predicted superluminal motion**

The first unification paper

Rees 1967, MNRAS, 135,345

STUDIES IN RADIO SOURCE STRUCTURE

Gubbay, Legg, Robertson, Moffet, Ekers, Seidel 1969 Nature 224, 1094

Moffet, Gubbay, Robertson & Legg 1972 IAUS, 44, 228

(conference was in 1970 - proceedings 2 years later)

Cohen et al. 1971, ApJ, 170, 207

Whitney et al. 1971, Science, 173, 225

The field of radio AGN monitoring began with the discovery of quasars and has been going on now for half a century

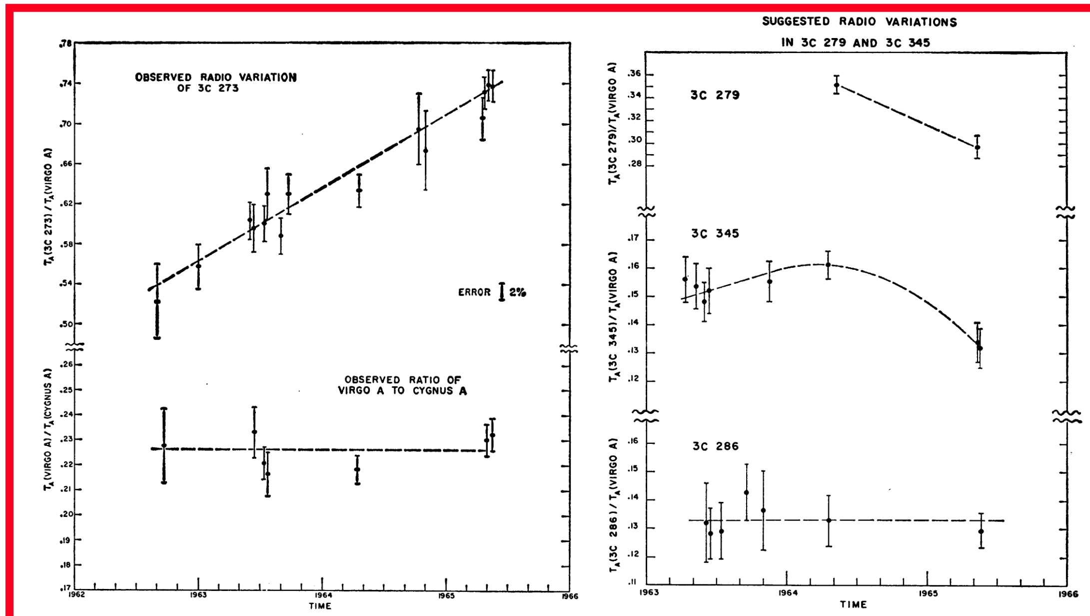

Fig. 1 (left). The ratio of the corrected antenna temperature, T_A, at 8000 Mc/sec of the quasi-stellar source 3C 273 to that of Virgo A, showing the observed 40-percent increase in the radio emission over a nearly three-year period. The measured ratio of Virgo A to Cygnus A shows no variation over the same period. Fig. 2 (right). Evidence for possible variations in the radio emissions of the quasi-stellar sources 3C 279 and 3C 345 at 8000 Mc/sec, and for a lack of variation in the quasi-stellar source 3C 286. Like 3C 273, which shows variations, both 3C 279 and 3C 345 have flat radio spectra at 8000 Mc/sec.

Dent 1965, Science, 148, 1458
Lack of synchrotron self-absorption as shown by their spectra give a lower limit to the size of the emitting regions which is >> the light-travel time associated with the flux density variations.

Rees1966, Nature, 211, 468

APPEARANCE OF RELATIVISTICALLY EXPANDING RADIO SOURCES

1. Explained rapid variability in PEGRS
2. Predicted superluminal motion

The first unification paper

Rees 1967, MNRAS, 135,345

STUDIES IN RADIO SOURCE STRUCTURE

Gubbay, Legg, Robertson, Moffet, Ekers, Seidel 1969 Nature 224, 1094

Moffet, Gubbay, Robertson & Legg 1972 IAUS, 44, 228

(conference was in 1970 - proceedings 2 years later)

Cohen et al. 1971, ApJ, 170, 207

Whitney et al. 1971, Science, 173, 225

Since AGN monitoring has been going on for 50 years it is surprising, to say the least, to find a strong signature that has not been noticed before, although it has been detected before but not recognized because it is masked by intrinsic variability

Calibrators

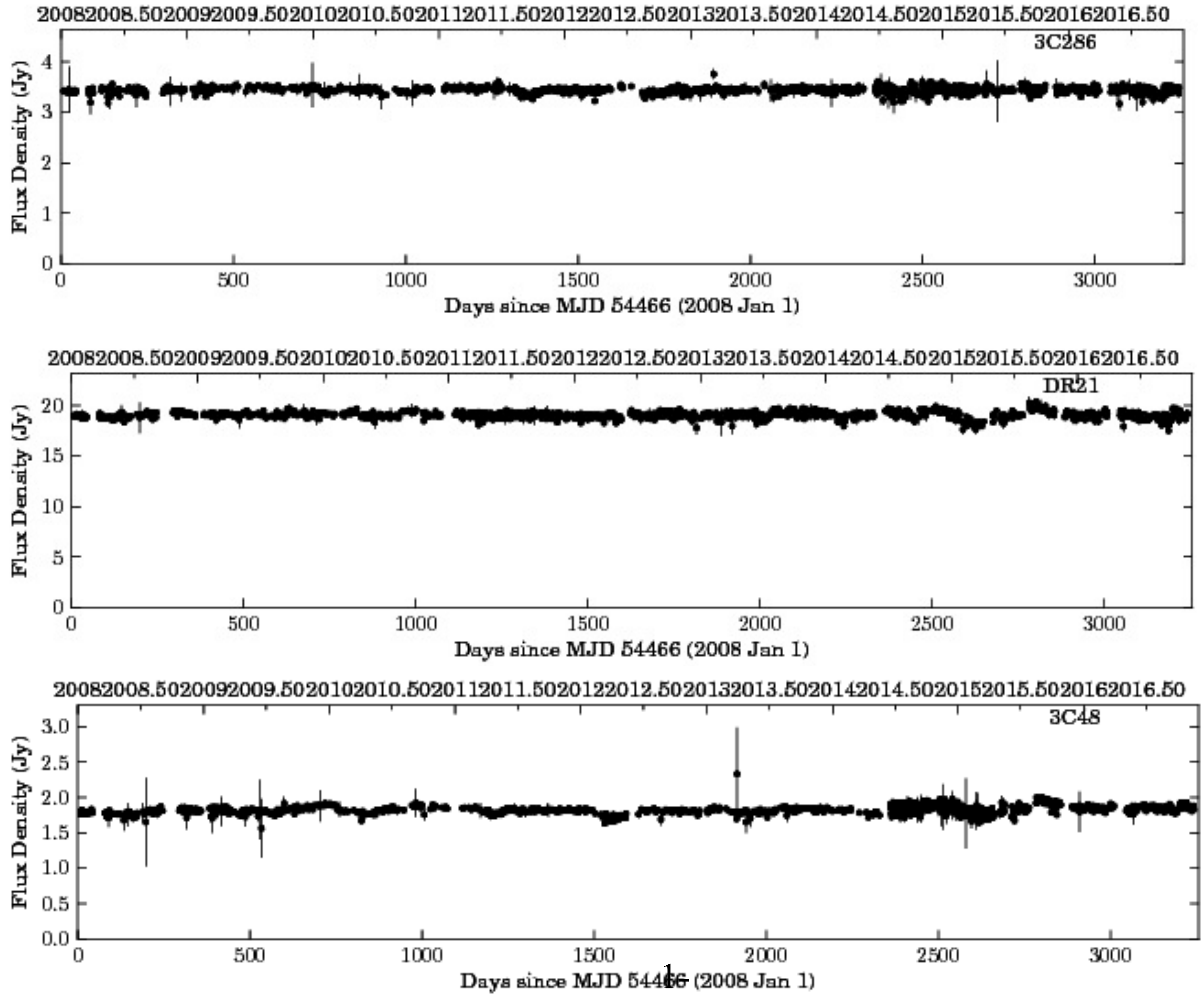

1-σ error bars, absolute flux density scale accuracy 5%

[Data made public within ~1 month of observations at http://www.astro.caltech.edu/ovroblazars/](http://www.astro.caltech.edu/ovroblazars/)

Strong Sources (> 1 Jy)

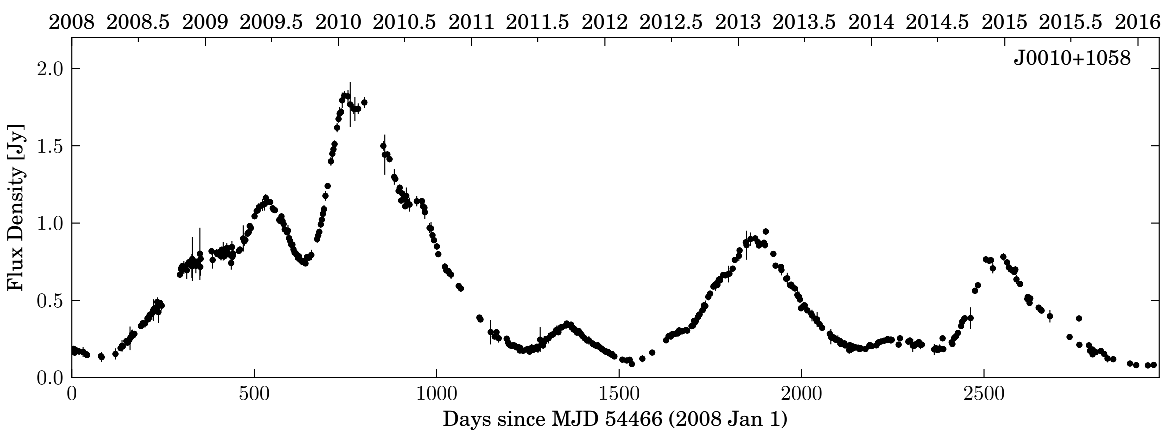

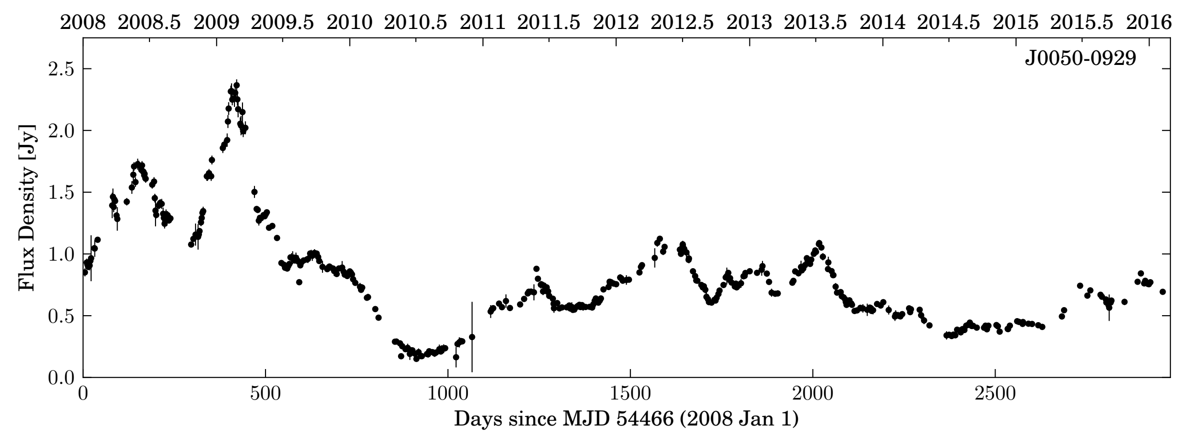

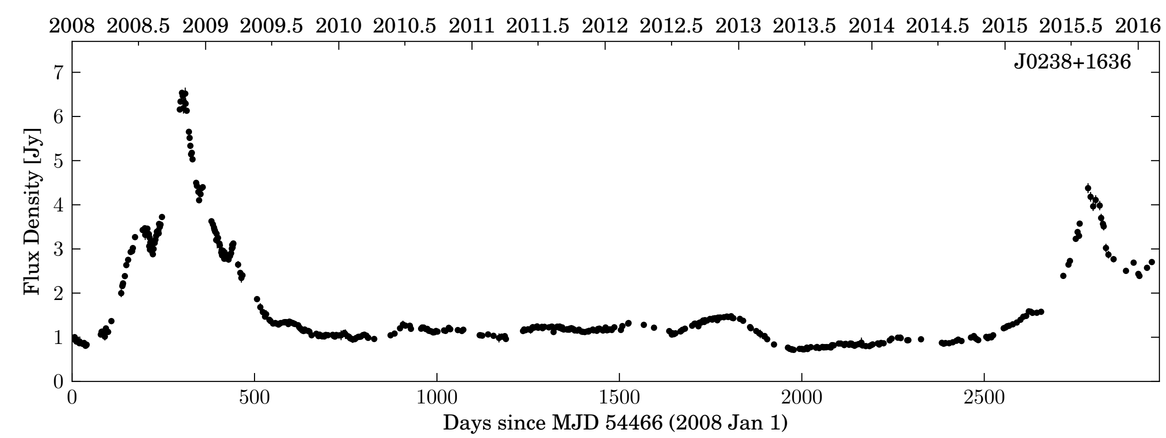

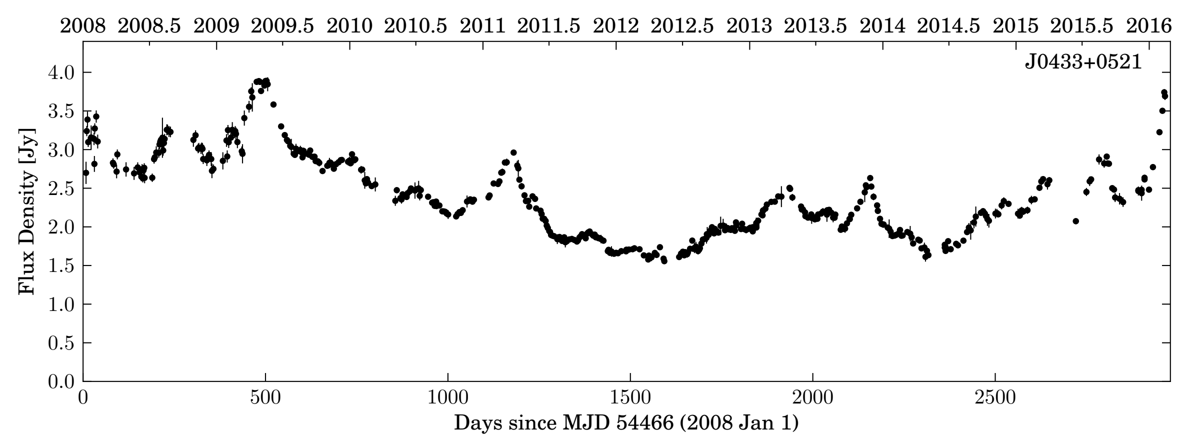

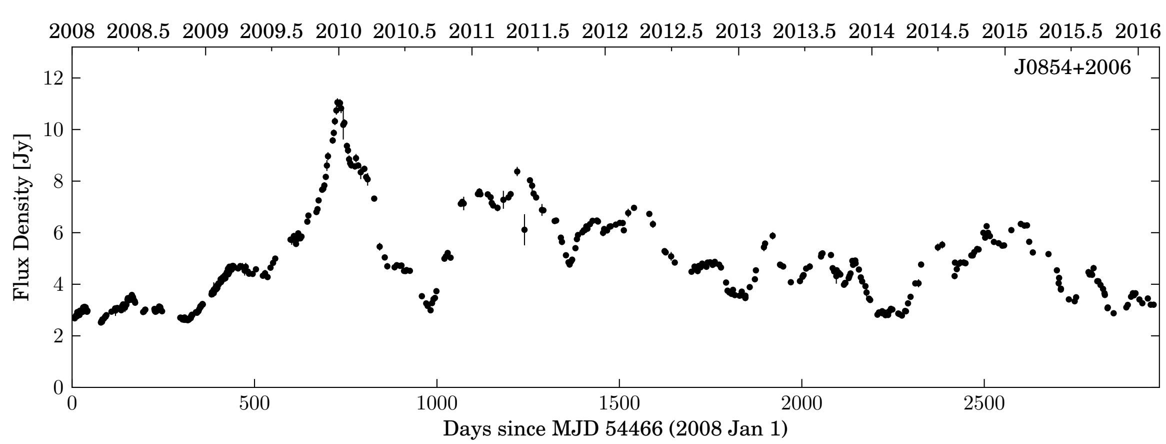

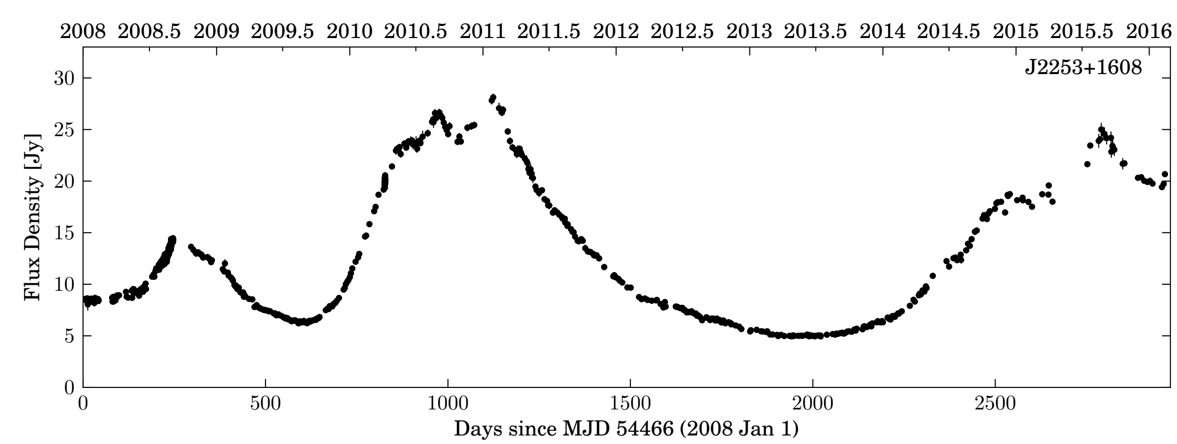

Weaker Sources (0.1 Jy - 1 Jy)

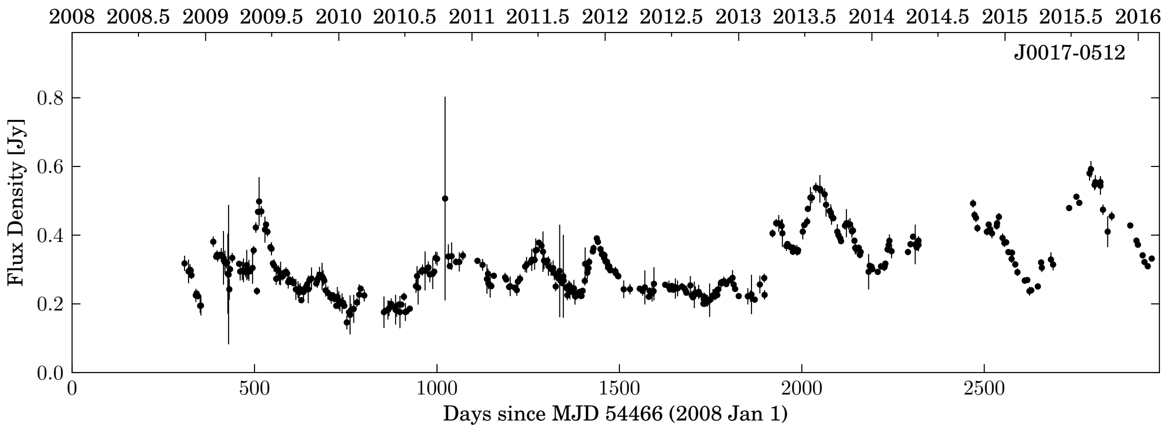

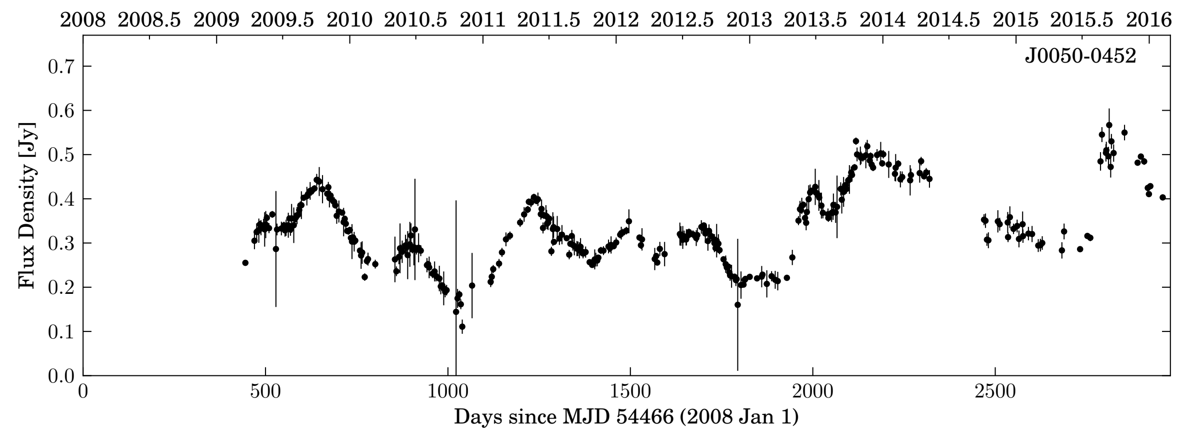

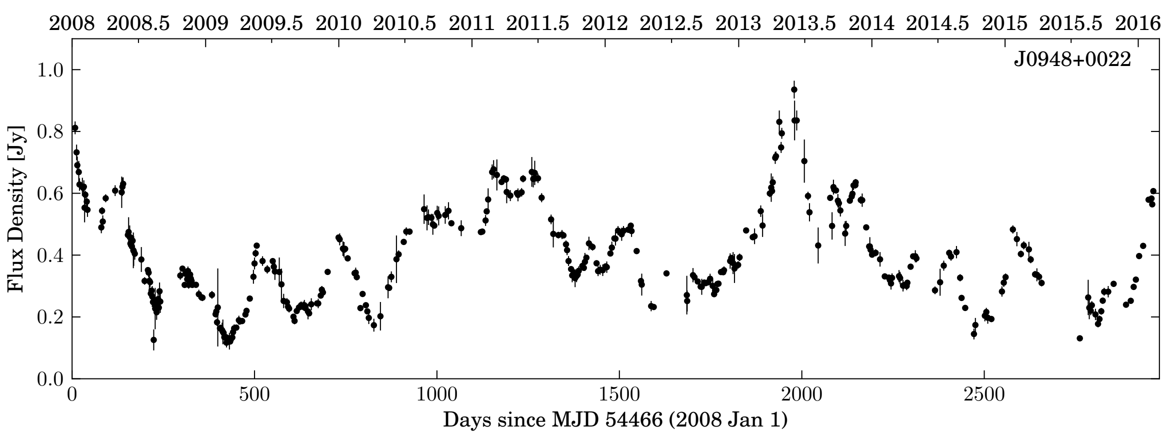

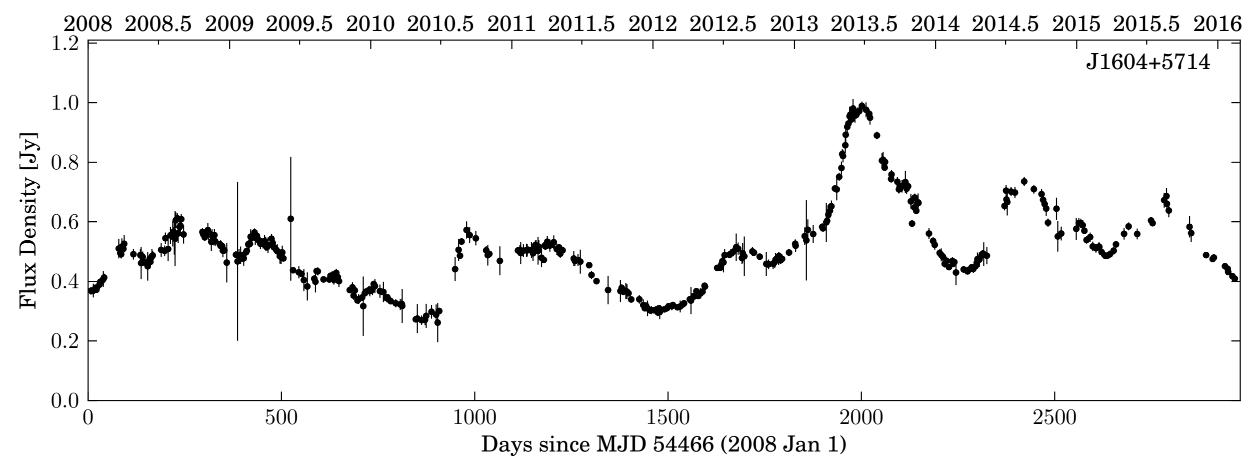

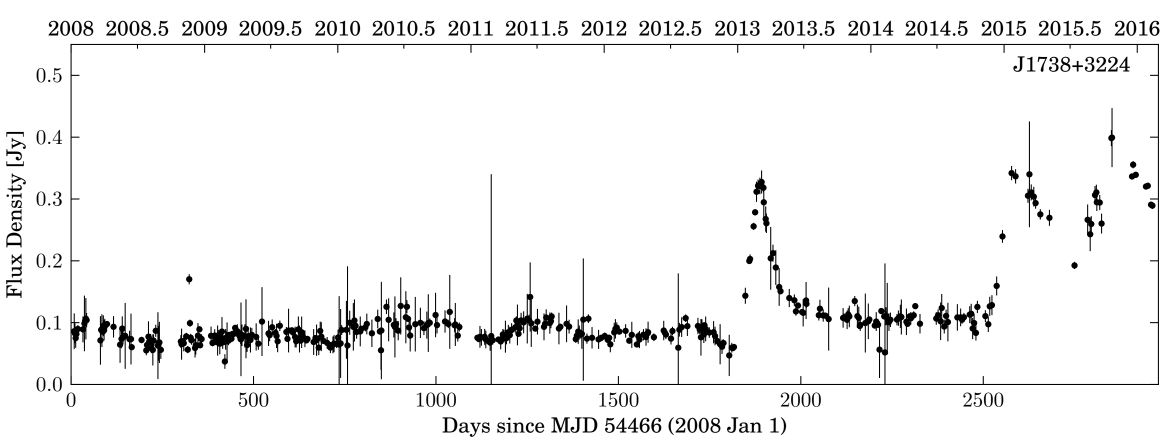

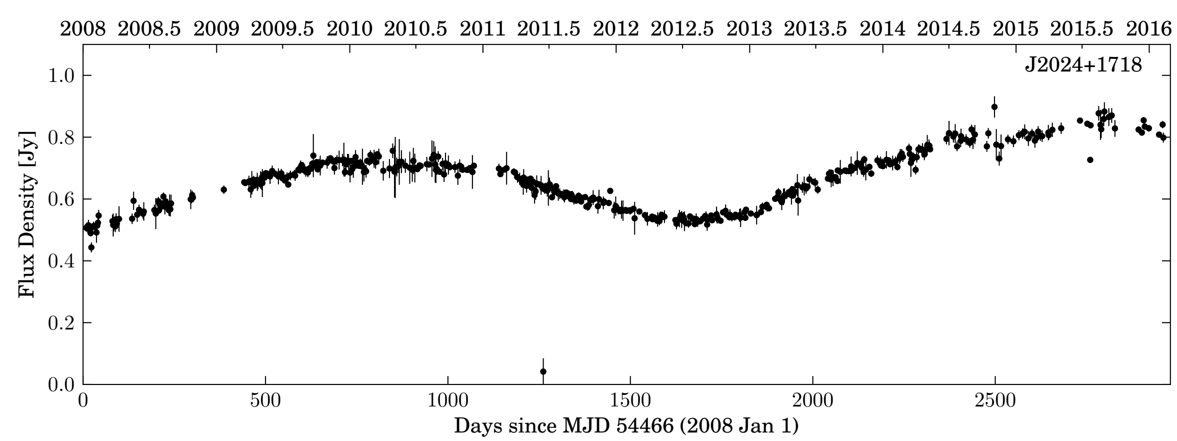

Under-sampled

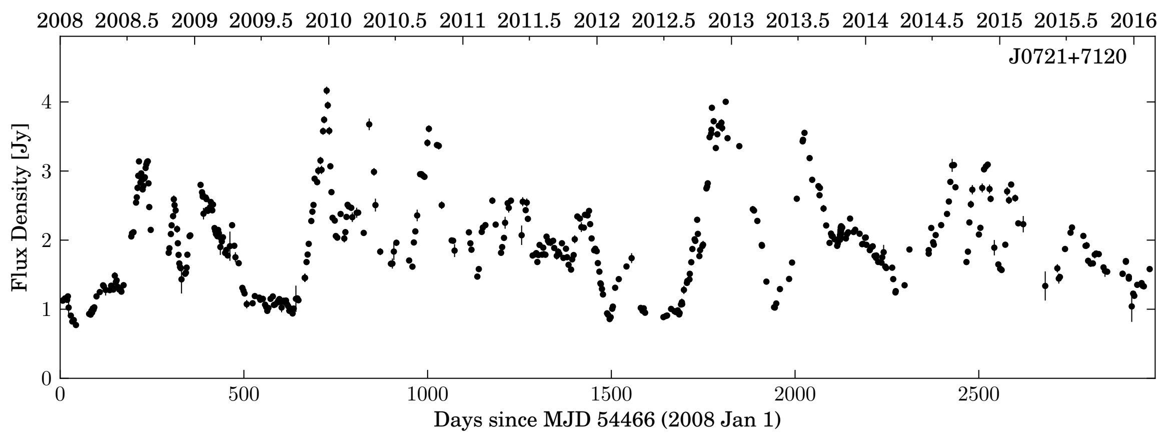

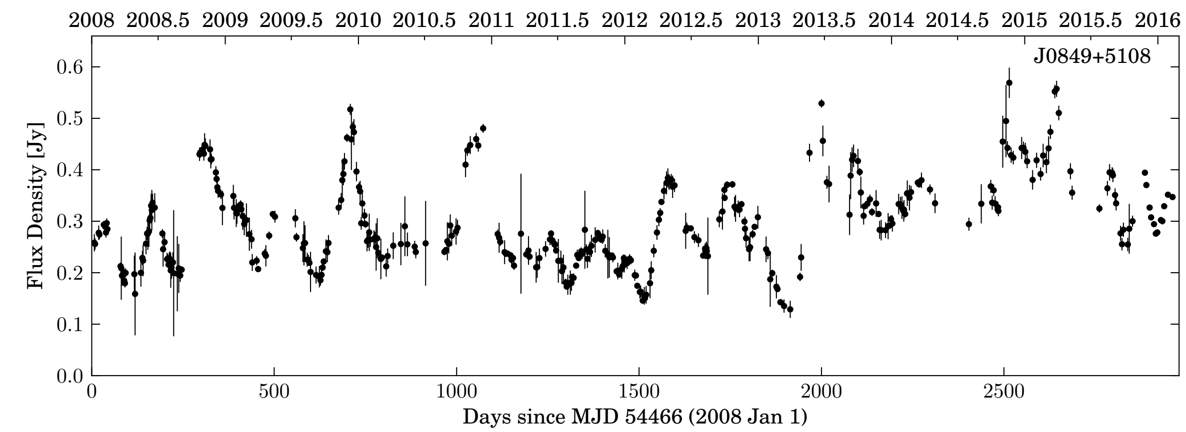

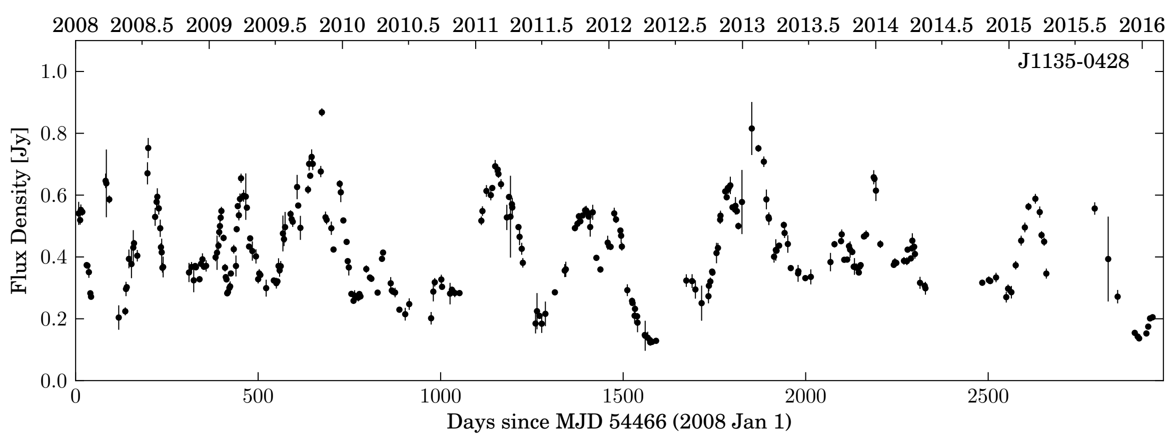

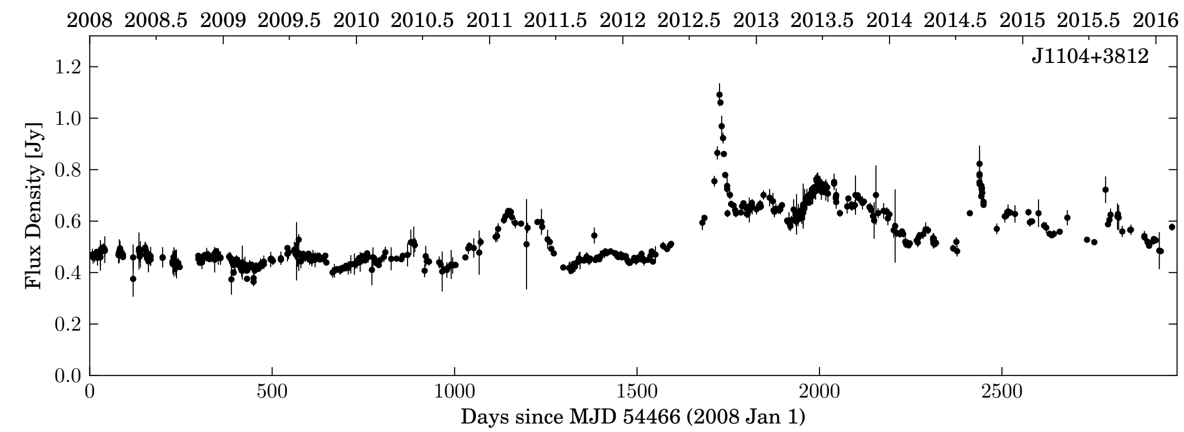

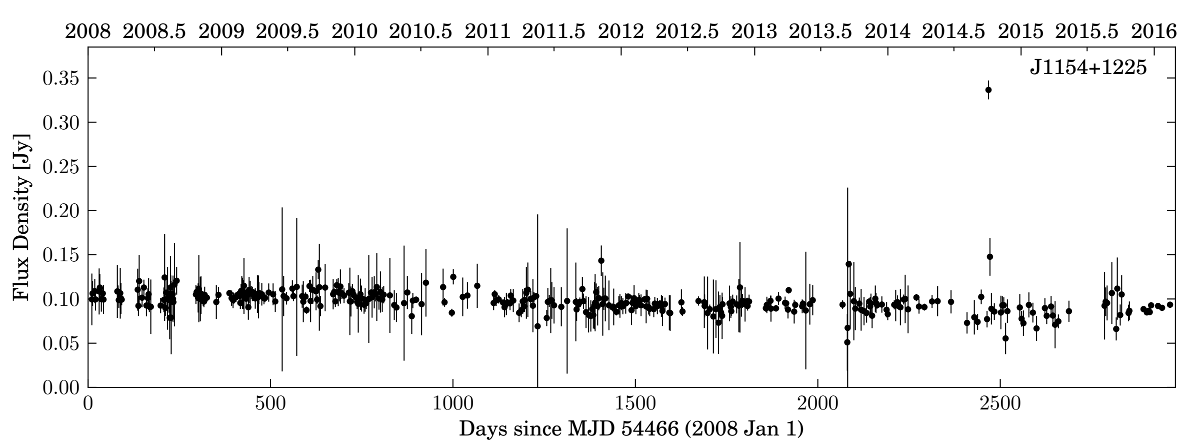

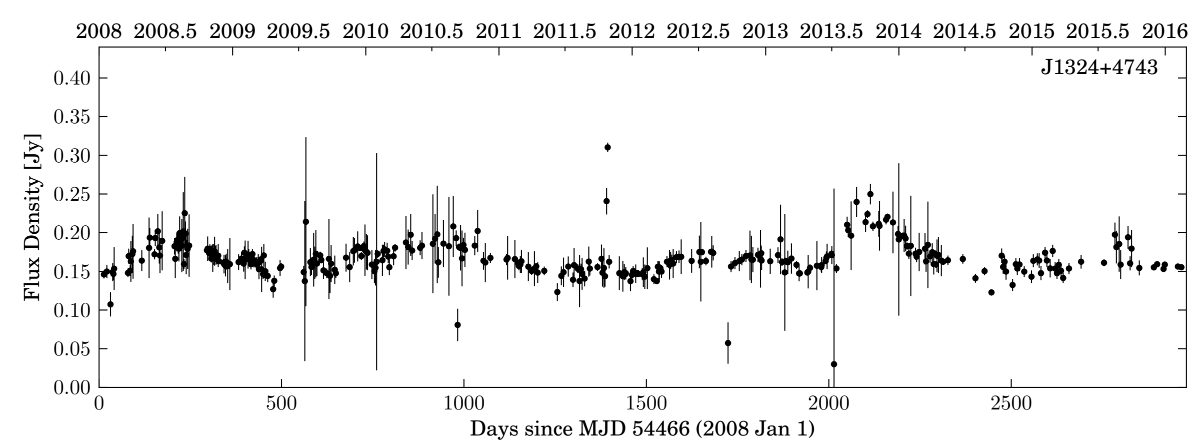

We have a sample of a dozen of such highly variable objects that we are monitoring on AMI

Particularly Interesting Objects

Quasi-Periodic Oscillators (J1359+4011 & PG1553+113)

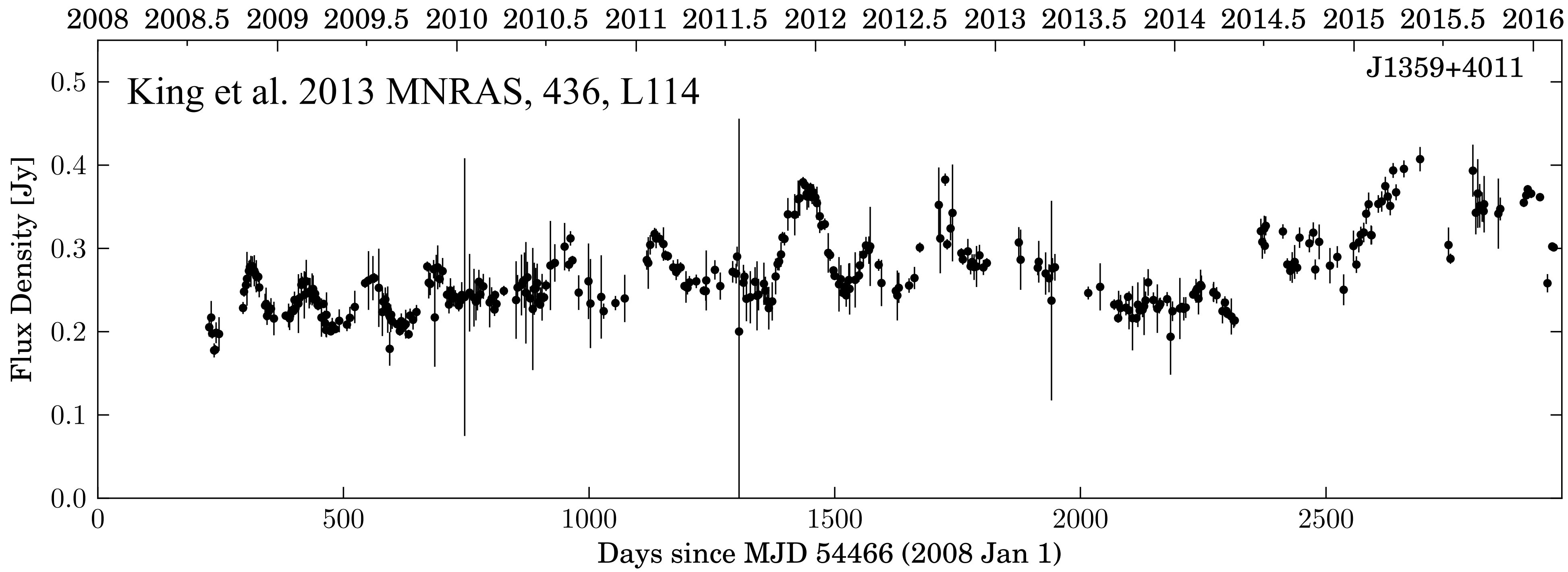

PG1553+113

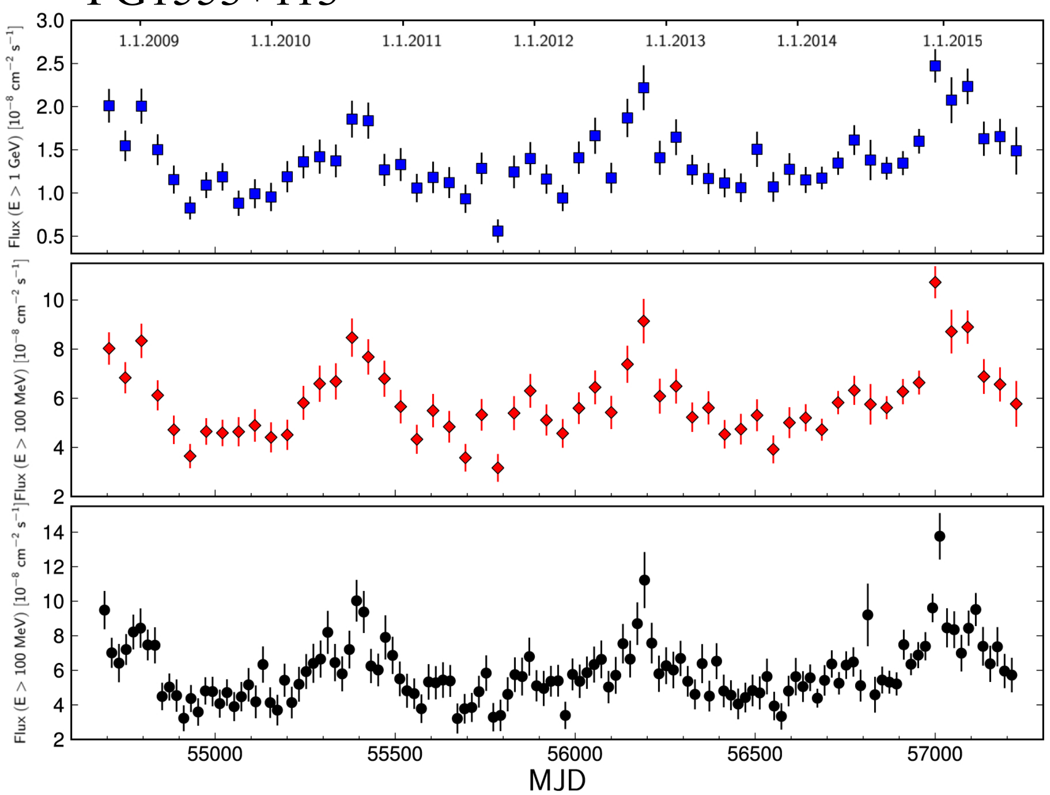

Ackermann et al. 2015 ApJ, 813, L41

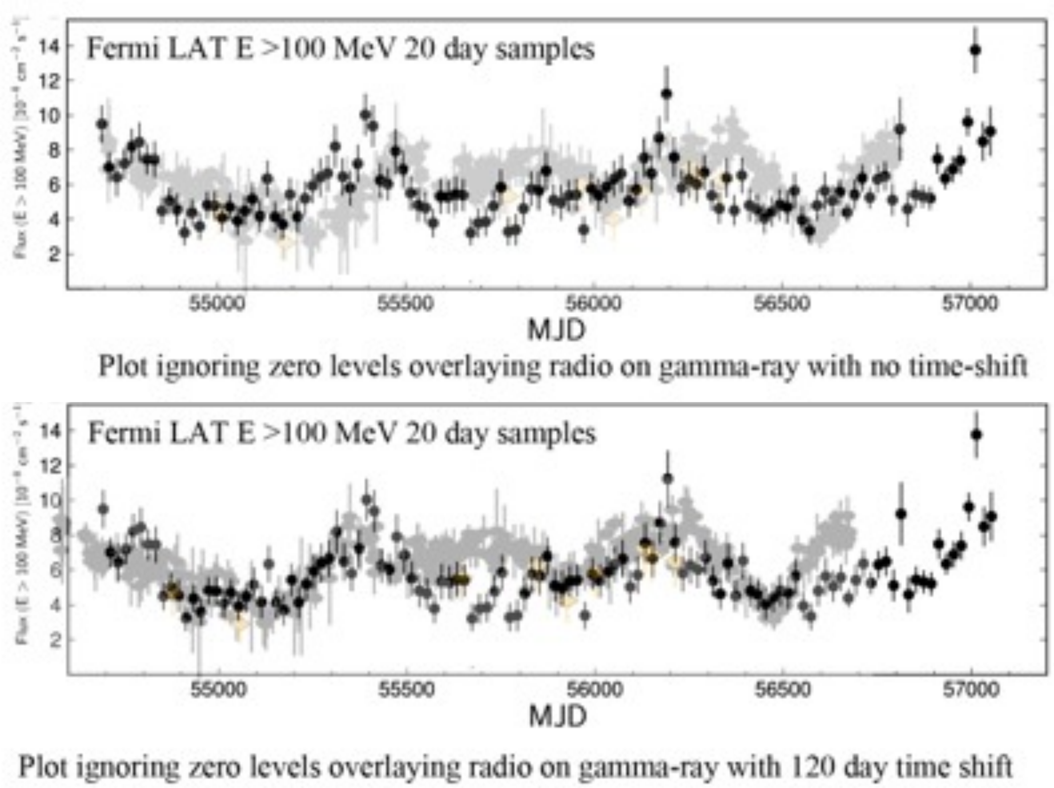

Fermi (black) overlaid on OVRO (grey)

AGN analogue of the short-period (0.01-450 Hz) QPOs seen in micro-quasars? Periods scale directly with mass, as expected. Or thermal instabilities in the “inner” accretion disc?

Extreme Scattering Events (ESEs)

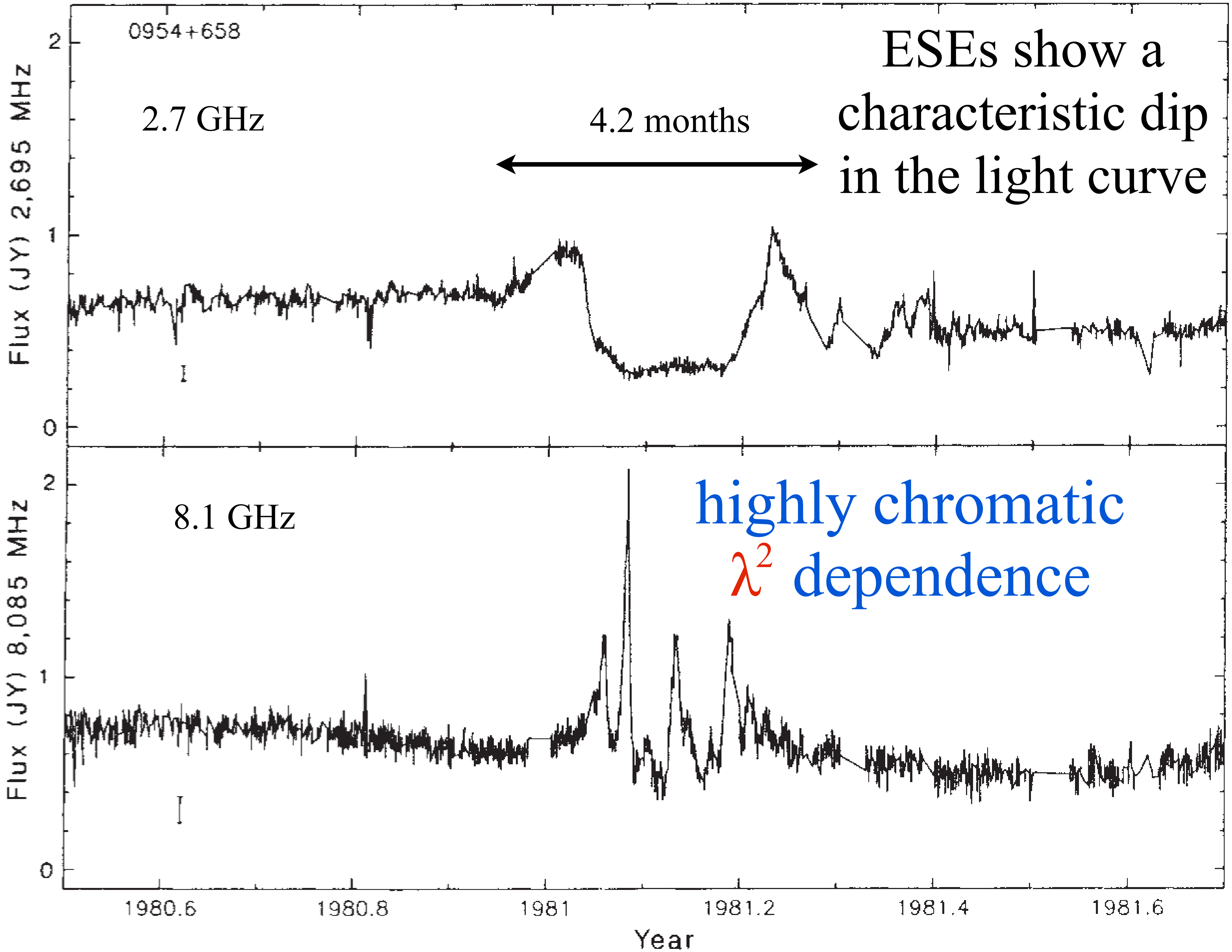

Fiedler, Dennison, Johnston & Hewish 1987 Nature 326, 625

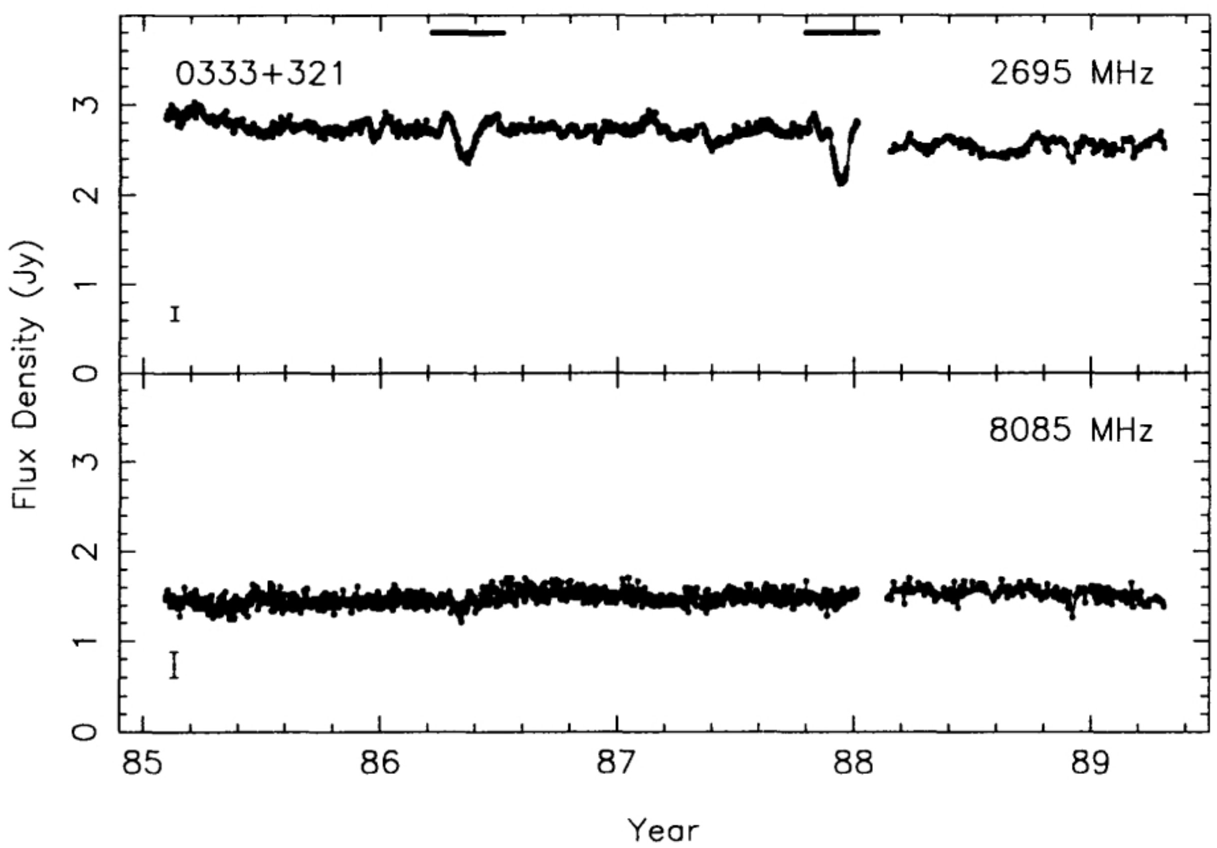

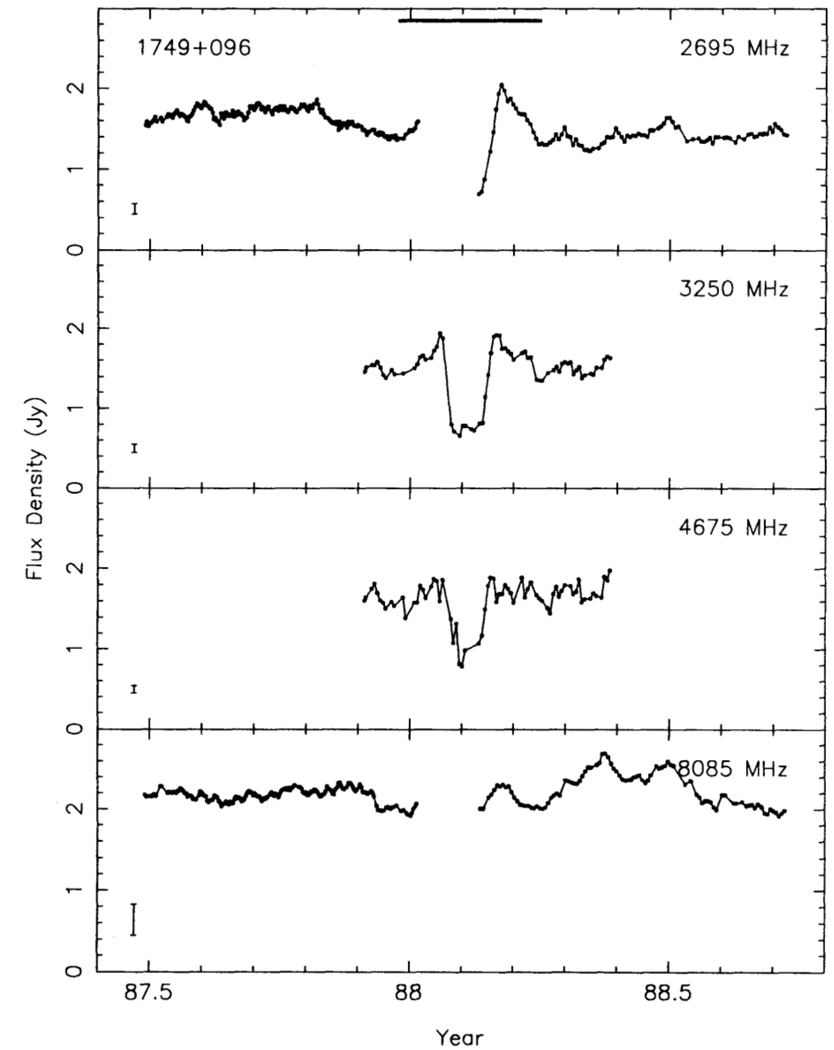

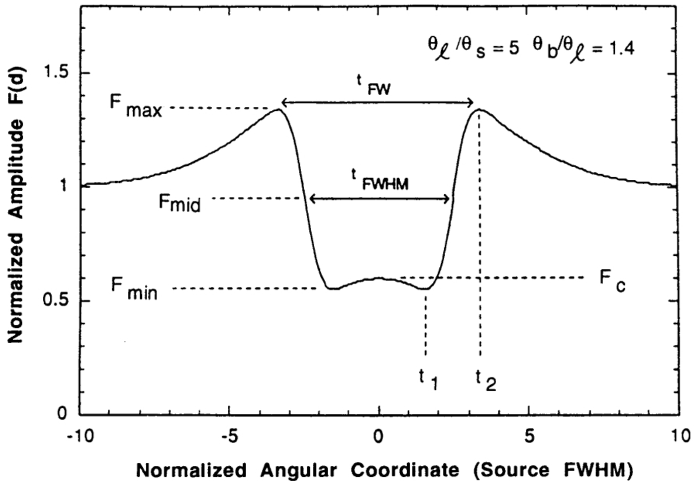

FIG. 3*a*

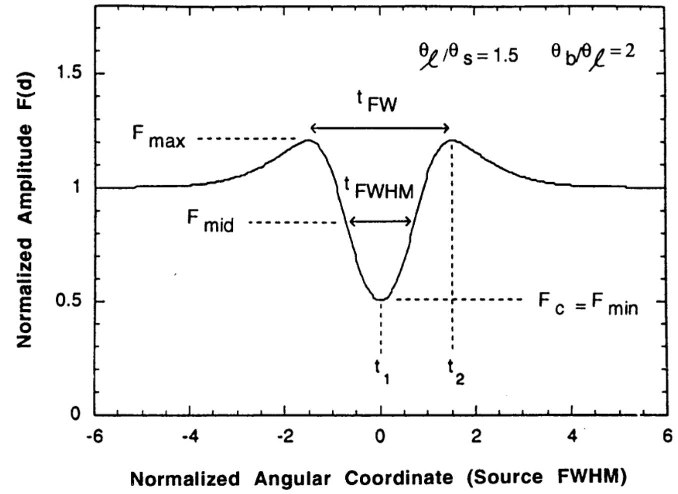

FIG. 3*b*

FIG. 3.—Model light curves of an ESE based on a band-shaped lens, where the size of the lens is (*a*) larger than the extent of the background source and (*b*) smaller than the background source. The components of an ESE are labeled. The ratios refer to the width θ_l of the lens, the FWHM θ_s of the background source, and the FWHM θ_b of the broadening function resulting from the electron density turbulence in the lens. The normalized amplitudes, $F(u_y)$, in (*a*) and (*b*) were obtained by evaluating eq. (A5) in Appendix A.

ESEs are rare events: Fiedler et al. ApJ 1994, 430, 581
In 430 object-years of data 8 U-shaped dips were seen at 2695 MHz and
0 U-shaped dips were seen at 8085 MHz - so at high radio frequencies U-shaped dips are **VERY RARE!**

But we did see a small number of U-shaped events in our 12,000 objects hours of observing on the 40 m, but only one had been published until this month:

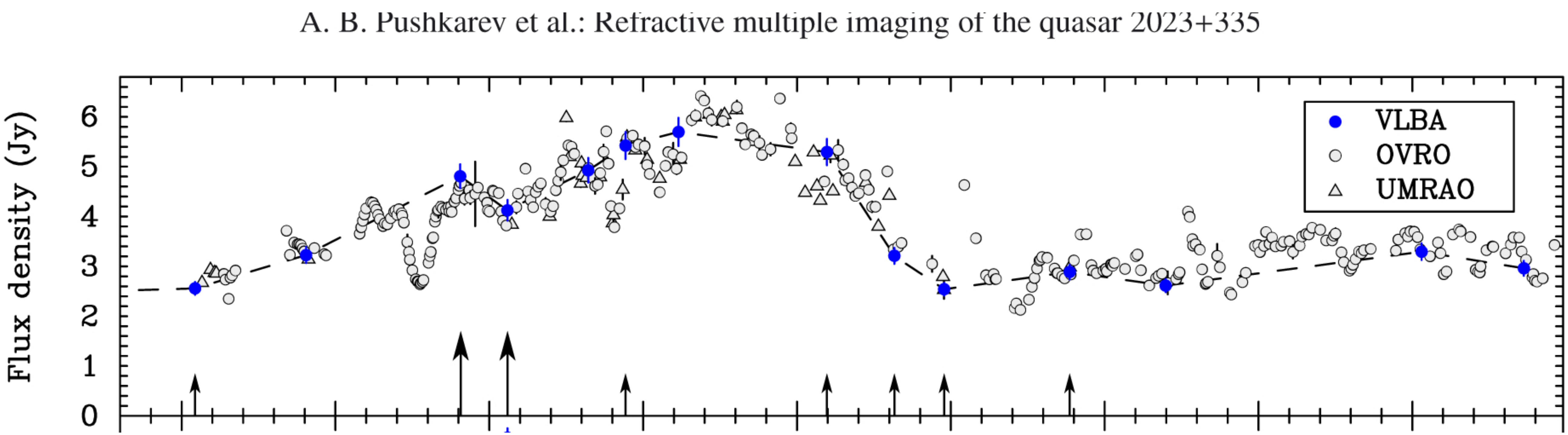

Pushkarev et al 2013, A&A, 555, A80.

An Extreme Scattering Event in J1415+1320 (PKS 1413+135)?

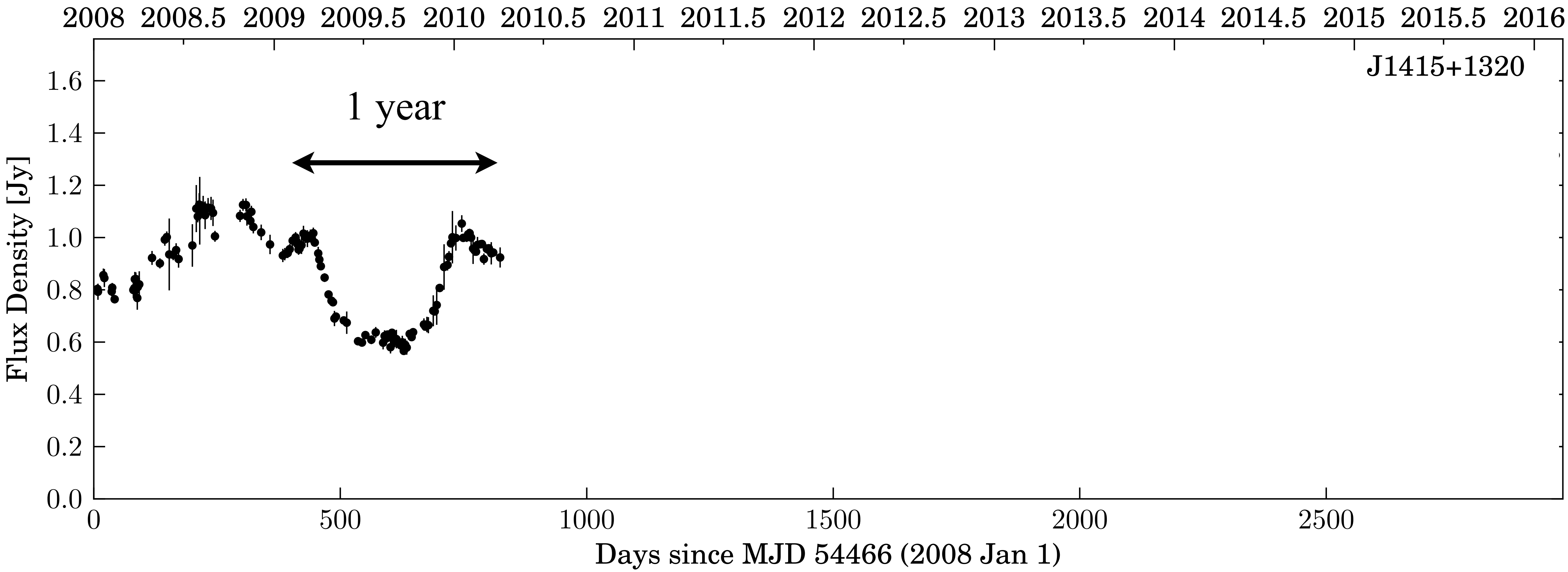

An Extreme Scattering Event in J1415+1320 (PKS 1413+135)?

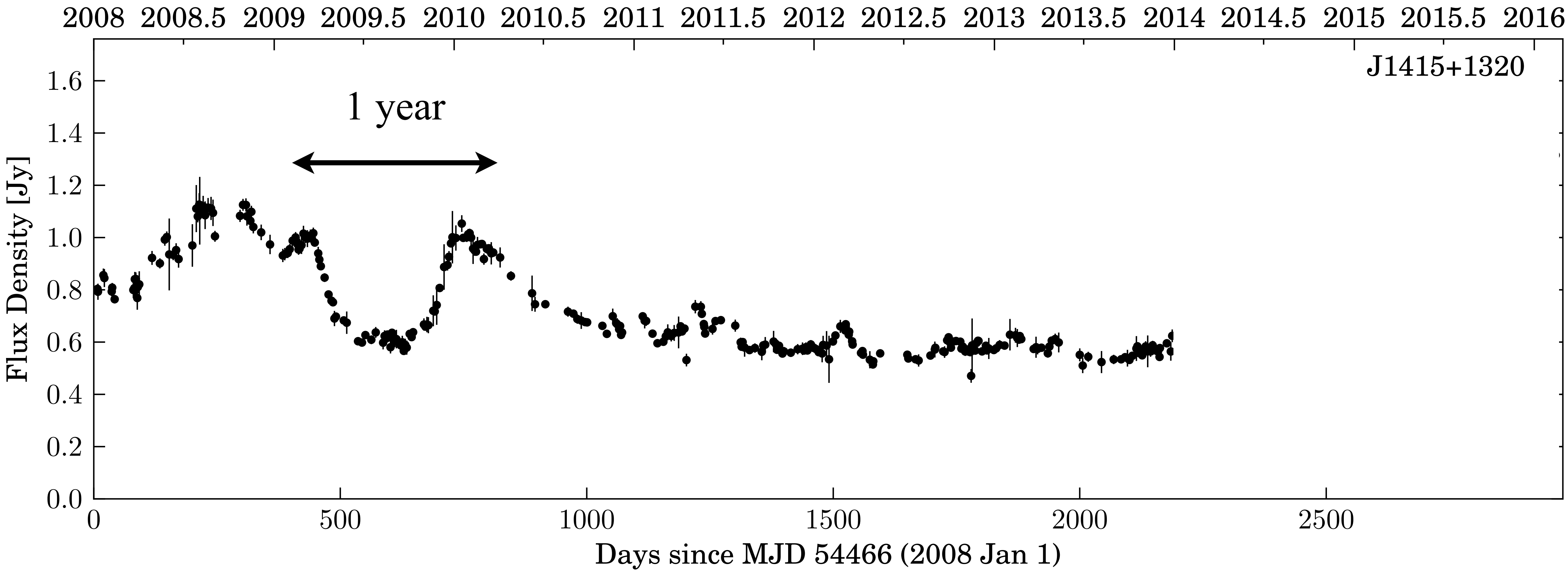

An Extreme Scattering Event in J1415+1320 (PKS 1413+135)?

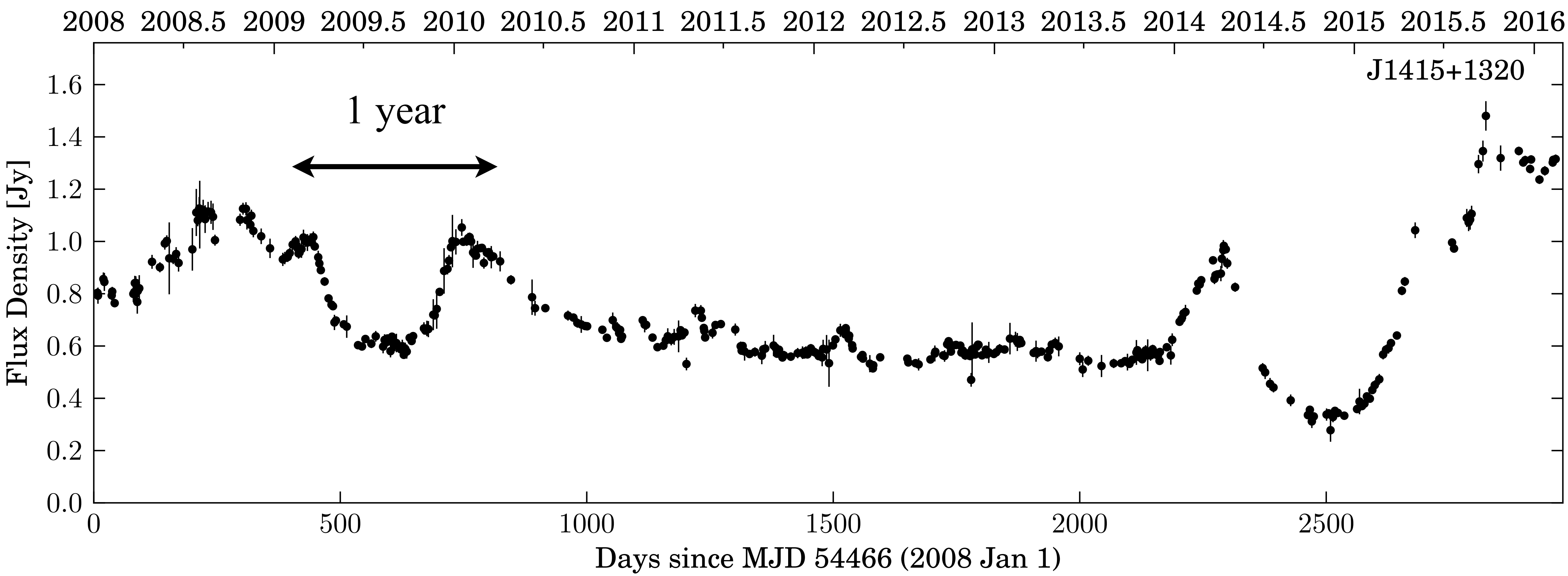

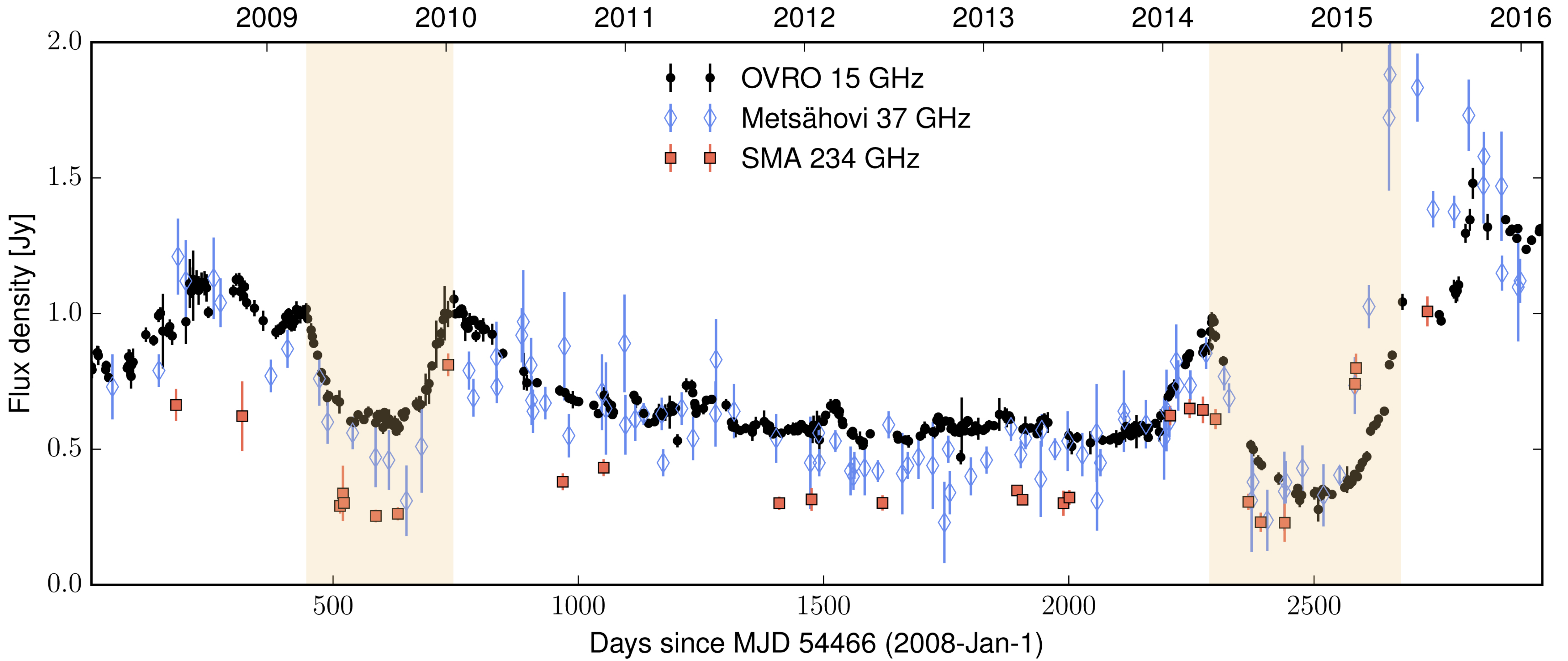

It cannot be an ESE - it’s highly achromatic from 15 GHz to 234 GHz

The Peculiar Light Curve of J1415+1320 - A Case Study in Extreme Scattering Events arXiv:1702.05519

H. K. Vedantham[1*], A. C. S. Readhead[1], T. Hovatta[2,3,4], T. J. Pearson[1], R. D. Blandford[5], M. A. Gurwell[6], A. Lähteenmäki[2], W. Max-Moerbeck[7], V. Pavlidou[8], V. Ravi[1], R. A. Reeves[9], J. L. Richards[1], M.Tornikoski[2], J. A. Zensus[6]

J1415+1320 (PKS1413+135)

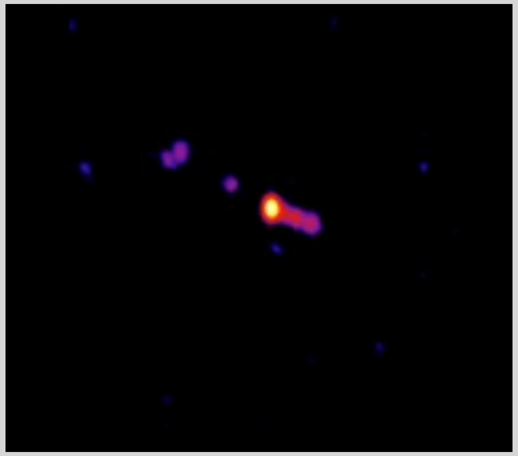

radio source at
z~0.5

edge-on Sa
spiral galaxy
at z = 0.247

OVRO
40 m Telescope

J1415+1320 (PKS1413+135)

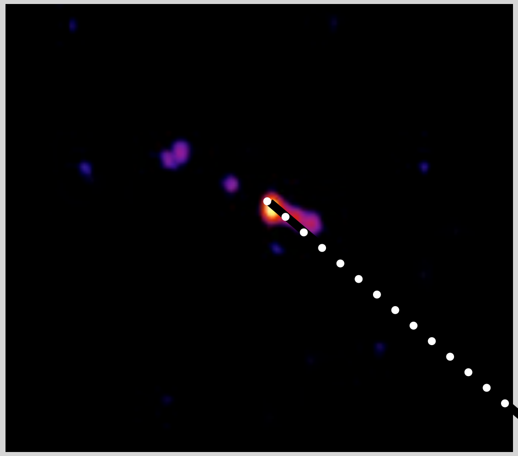

radio source at
z~0.5

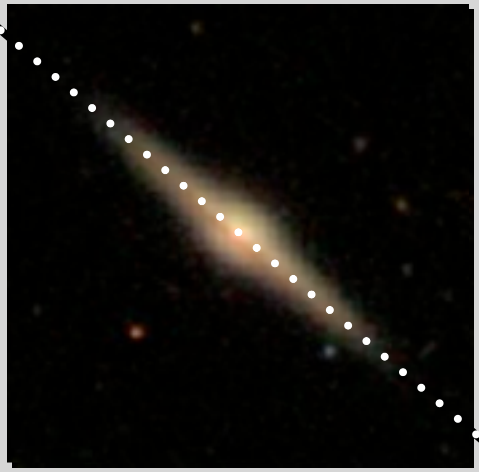

edge-on Sa
spiral galaxy
at z = 0.247

OVRO
40 m Telescope

J1415+1320 (PKS1413+135)

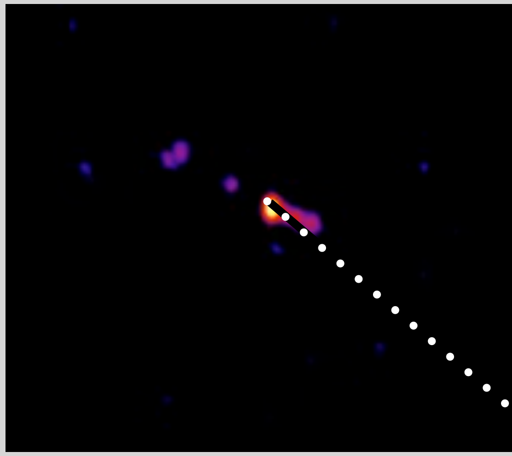

radio source at
z~0.5

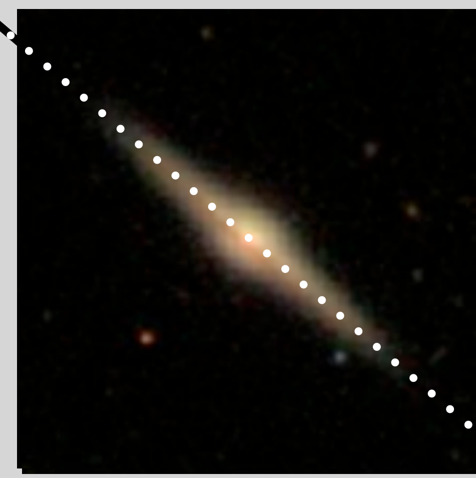

edge-on Sa
spiral galaxy
at z = 0.247

We believe that the SAV we are observing are due to lensing by ~10^3 - 10^4 solar mass condensates in the edge-on Sa galaxy
These condensates need to have a surface density integrated through the galaxy of 10^4 solar masses per square pc

OVRO
40 m Telescope

J1415+1320 (PKS1413+135)

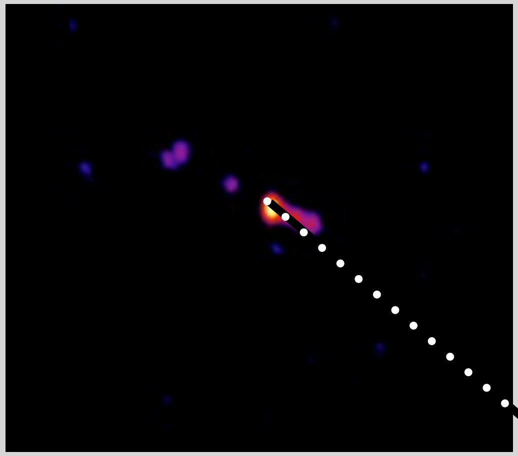

radio source at
z~0.5

As successive components are ejected along the jet they pass behind the intervening lens system moving at apparent speed ~c and repeatedly trace out a ~1-year flux density variation due to magnification by the lens

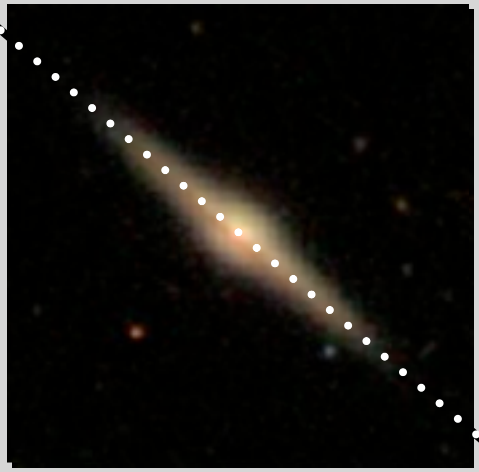

edge-on Sa
spiral galaxy
at z = 0.247

We believe that the SAV we are observing are due to lensing by ~10^3 - 10^4 solar mass condensates in the edge-on Sa galaxy These condensates need to have a surface density integrated through the galaxy of 10^4 solar masses per square pc

OVRO
40 m Telescope

J1415+1320 (PKS1413+135)

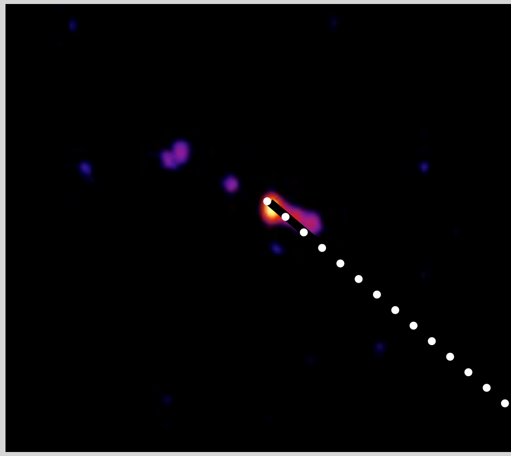

radio source at
z~0.5

There are currently two ways of detecting gravitational lensing:

1. multiple images
2. time delays between variations seen along the different lines of sight to the different images

As successive components are ejected along the jet they pass behind the intervening lens system moving at apparent speed ~c and repeatedly trace out a ~1-year flux density variation due to magnification by the lens

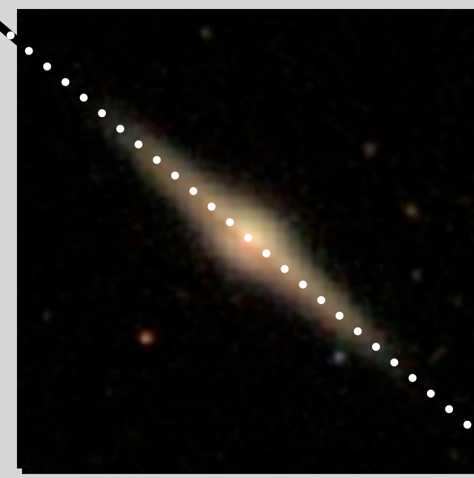

edge-on Sa
spiral galaxy
at z = 0.247

We believe that the SAV we are observing are due to lensing by $\sim10^3$ - 10^4 solar mass condensates in the edge-on Sa galaxy
These condensates need to have a surface density integrated through the galaxy of 10^4 solar masses per square pc

OVRO
40 m Telescope

J1415+1320 (PKS1413+135)

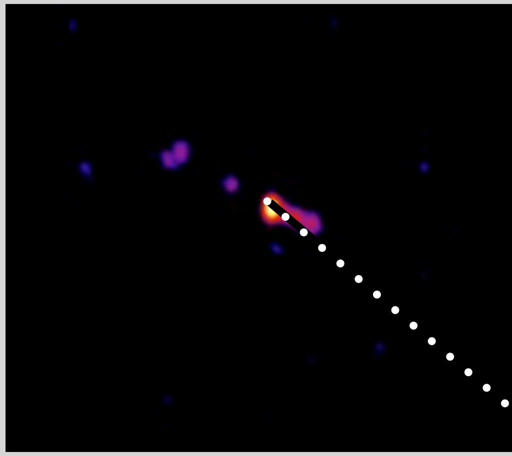

radio source at
z~0.5

There are currently two ways of detecting gravitational lensing:

1. multiple images
2. time delays between variations seen along the different lines of sight to the different images

As successive components are ejected along the jet they pass behind the intervening lens system moving at apparent speed ~c and repeatedly trace out a ~1-year flux density variation due to magnification by the lens

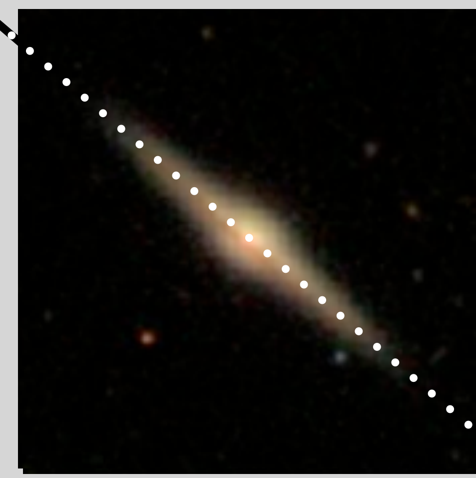

edge-on Sa
spiral galaxy
at z = 0.247

We believe that the SAV we are observing are due to lensing by ~10^3 - 10^4 solar mass condensates in the edge-on Sa galaxy
These condensates need to have a surface density integrated through the galaxy of 10^4 solar masses per square pc

OVRO
40 m Telescope

If SAV is due to gravitational lensing it will provide a third method for the detection of gravitational lensing as well as micro-arcsecond resolution of AGN - a factor 30 to 100 times better than is available now through mm VLBI, which could only be matched by mm VLBI from space

Papers suggesting that some, or all, variability in AGN is due to gravitational lensing (refs in red specifically J1415+1320)

this is not an exhaustive list

Chang & Refsdal 1979 Nature, 282, 561
Narasimha, Subramanian & Chitre 1984 MNRAS, 210,79
Subramanian, Chitre & Narasimha, 1985 ApJ, 289, 37
Ostriker & Vietri 1985 Nature, 318, 446 & 1990 Nature 344,45
Schneider & Weiss 1987 A&A, 171, 49
Stickel et al. 1988 A&A, 198, L13
Gopal-Krishna & Subramanian 1991 Nature, 349, 766
Subramanian & Gopal-Krishna 1991 A&A, 248, 55
Carilli et al. 1992 ApJ, 400, L13
Stocke et al. 1992 ApJ, 400, L17
Perlman et al. 1994 ApJ, 424, L69
Gopal-Krishna & Subramanian 1996 A&A, 315, 343
Webb et al. 2000 AJ, 120, 41

Papers suggesting that some, or all, variability in AGN is due to gravitational lensing (refs in red specifically J1415+1320)

this is not an exhaustive list

Chang & Refsdal 1979 Nature, 282, 561
Narasimha, Subramanian & Chitre 1984 MNRAS, 210,79
Subramanian, Chitre & Narasimha, 1985 ApJ, 289, 37
Ostriker & Vietri 1985 Nature, 318, 446 & 1990 Nature 344,45
Schneider & Weiss 1987 A&A, 171, 49
Stickel et al. 1988 A&A, 198, L13
Gopal-Krishna & Subramanian 1991 Nature, 349, 766
Subramanian & Gopal-Krishna 1991 A&A, 248, 55
Carilli et al. 1992 ApJ, 400, L13
Stocke et al. 1992 ApJ, 400, L17
Perlman et al. 1994 ApJ, 424, L69
Gopal-Krishna & Subramanian 1996 A&A, 315, 343
Webb et al. 2000 AJ, 120, 41

These papers suggested that J1415+1320 is a background source because:

1. this is a BL Lac object and these are very rarely, if ever, associated with spiral galaxies
2. it has an extremely red spectrum, presumably due to high extinction in foreground Sa galaxy
3. if an AGN were buried in the Sa galaxy it would heat the copious dust and gas around the nucleus and we would see a bright mid infra-red point source and bright narrow line emission, which are not seen

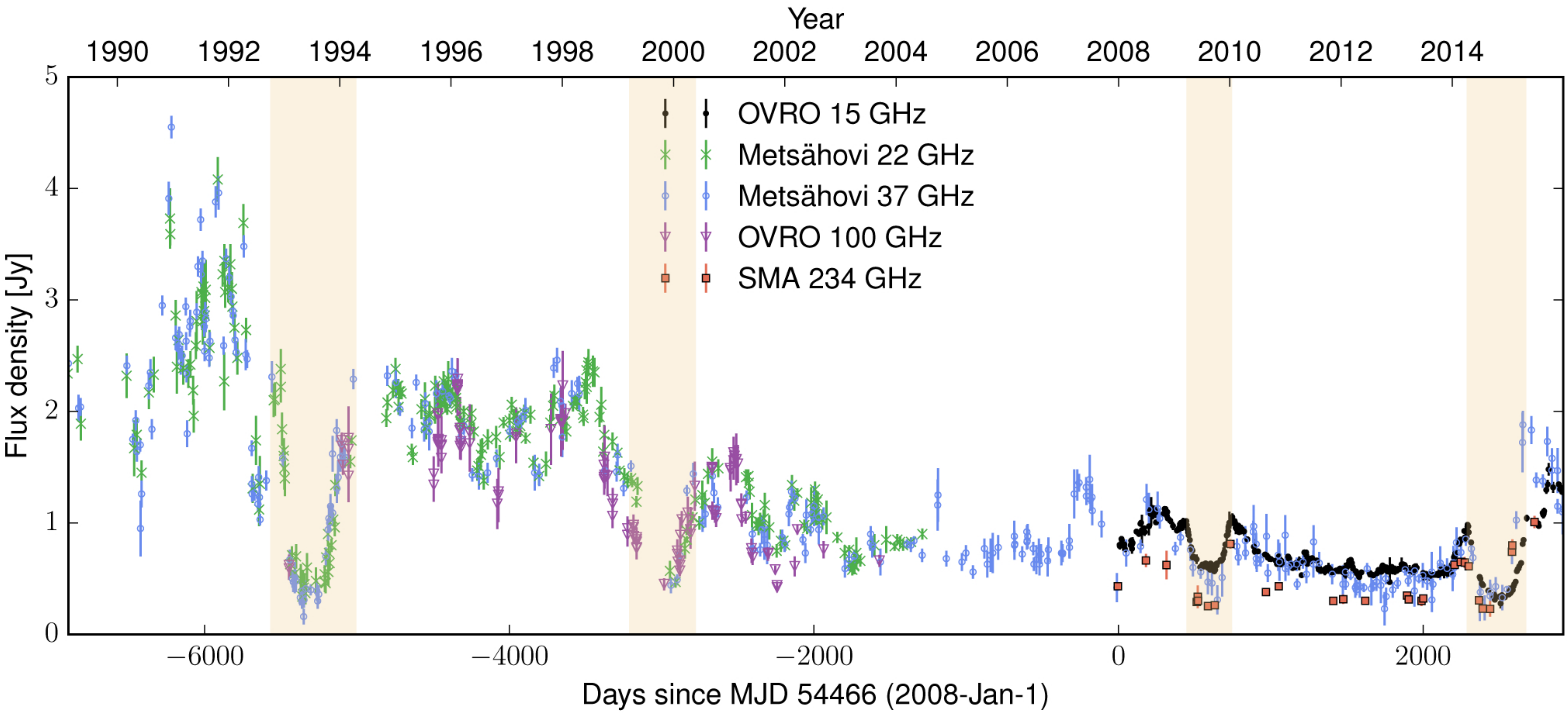

It appears that we've been somewhat lucky (or unlucky if nature is just teasing us) and that the reasons that we've been able to pick out the SAV in J1415+1320 are:

1. the high sensitivity and
2. high cadence, of our 40 m Telescope observations, combined with
3. the relatively low level of intrinsic activity in the object between 2008 and 2016

1158 objects in complete sample 981 of them of sufficient quality to look for U-features:

two independent searches - 10 features (in 7 objects) ~1% probability of seeing a feature in any object in 8 years.

We see three more features in J1415+1320 over 27 years (probability = $4x10^{-3}$)
and we see three features in J0310+3014 over 8 years (probability = 10^{-3})

Unless nature is teasing us it seems highly unlikely that these are just random juxtapositions of two “flares”

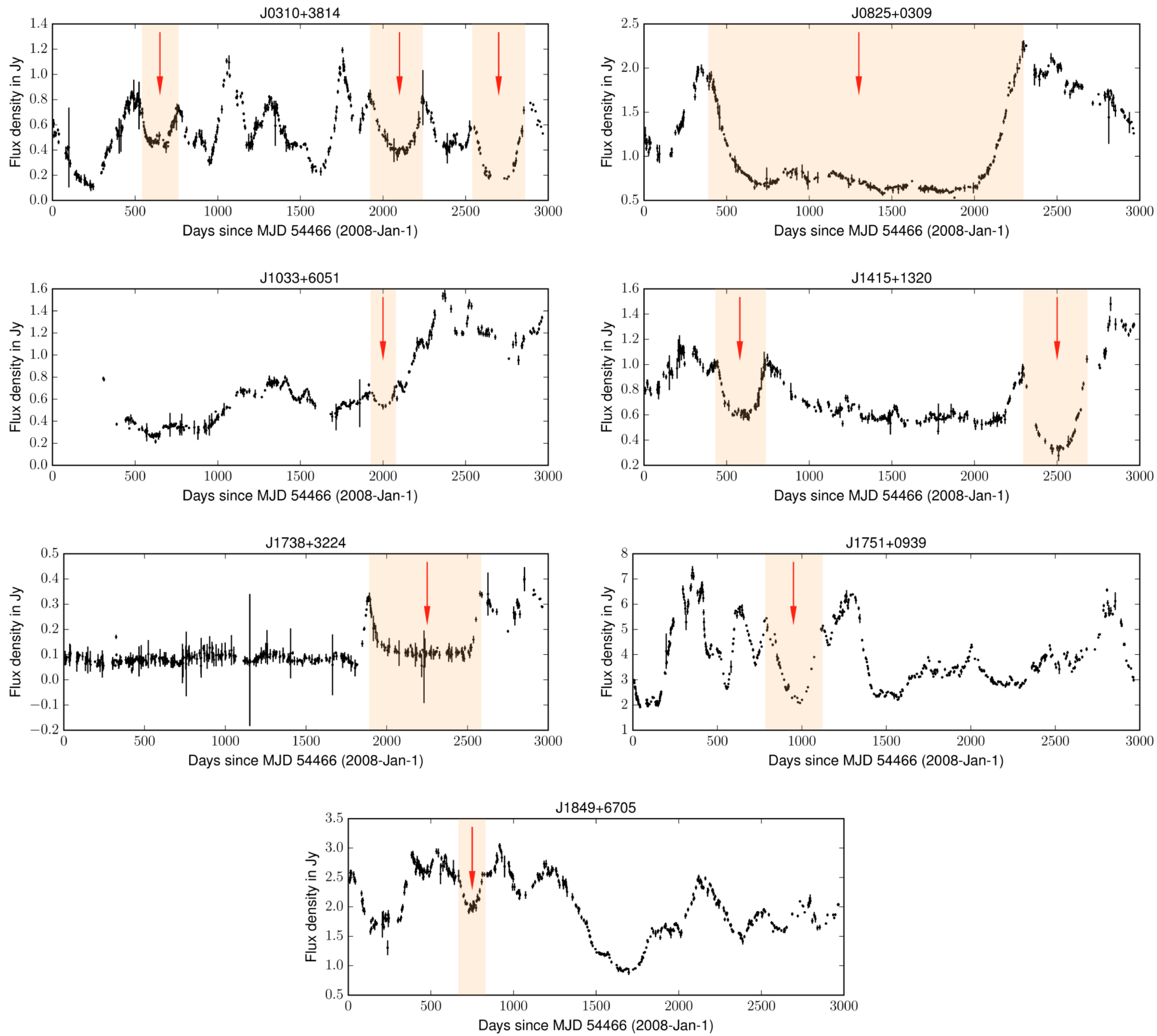
J0310+3814
J0825+0309
J1033+6051
J1415+1320
J1738+3224
J1751+0939
J1849+6705
Flux density in Jy
Days since MJD 54466 (2008-Jan-1)

Could these features be due to a pair of forward-reverse shocks, such as those modeled in GRBs?

The symmetry is then hard to explain
(see e.g. Kobayashi & Zhang 2003 ApJ, 582, L75)

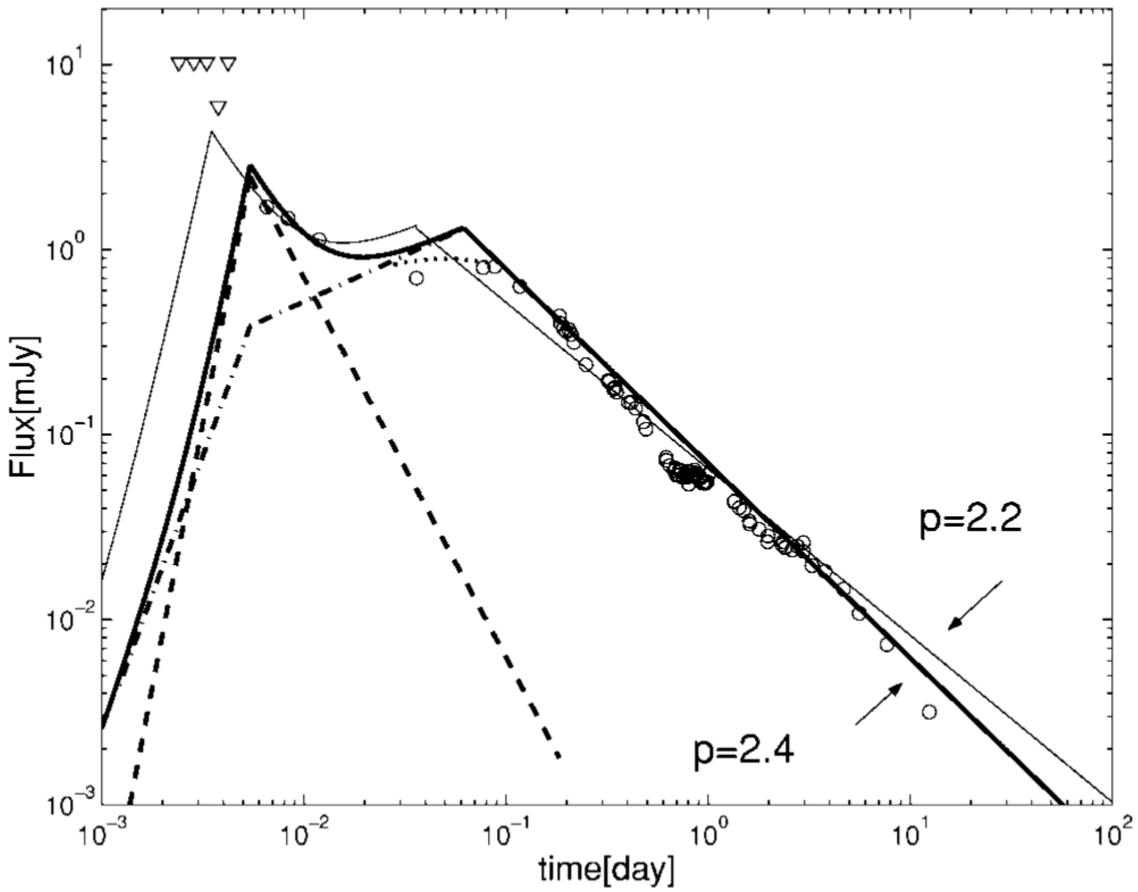

FIG. 1.—Optical light curve: Modeling with $p = 2.4$, forward shock emission (*dash-dotted line*), reverse shock emission (*dashed line*), total flux (*thick solid line*), and accurate spectrum mode (*dotted line*), $\epsilon_B = 3.0 \times 10^{-3}$, $\epsilon_e = 0.28$. $n = 0.45$ protons cm^{-3}, $\eta = 120$, and $E = 5.6 \times 10^{52}$ ergs. Modeling with $p = 2.2$ and total flux (*thin solid line*), $\epsilon_B = 3.0 \times 10^{-3}$, $\epsilon_e = 0.32$. $n = 0.45$ protons cm^{-3}, $\eta = 140$, and $E = 5.6 \times 10^{52}$ ergs. Measurements are shown as circles, and upper limits as triangles. Data are from Bersier et al. 2002b; Fox 2002; Halpern et al. 2002a, 2002b; Holland et al. 2002a, 2002b; Malesani et al. 2002a, 2002b; Masetti et al. 2002; Matsumoto et al. 2002a, 2002b; Mirabal et al. 2002a, 2002b; Oksanen & Aho 2002; Oksanen et al. 2002; Sahu et al. 2002; Stanek et al. 2002; Stefanon et al. 2002; Torii et al. 2002; Uemura et al. 2002; Weidinger et al. 2002; Winn et al. 2002; and Zharikov et al. 2002, following the calibration of Henden 2002.

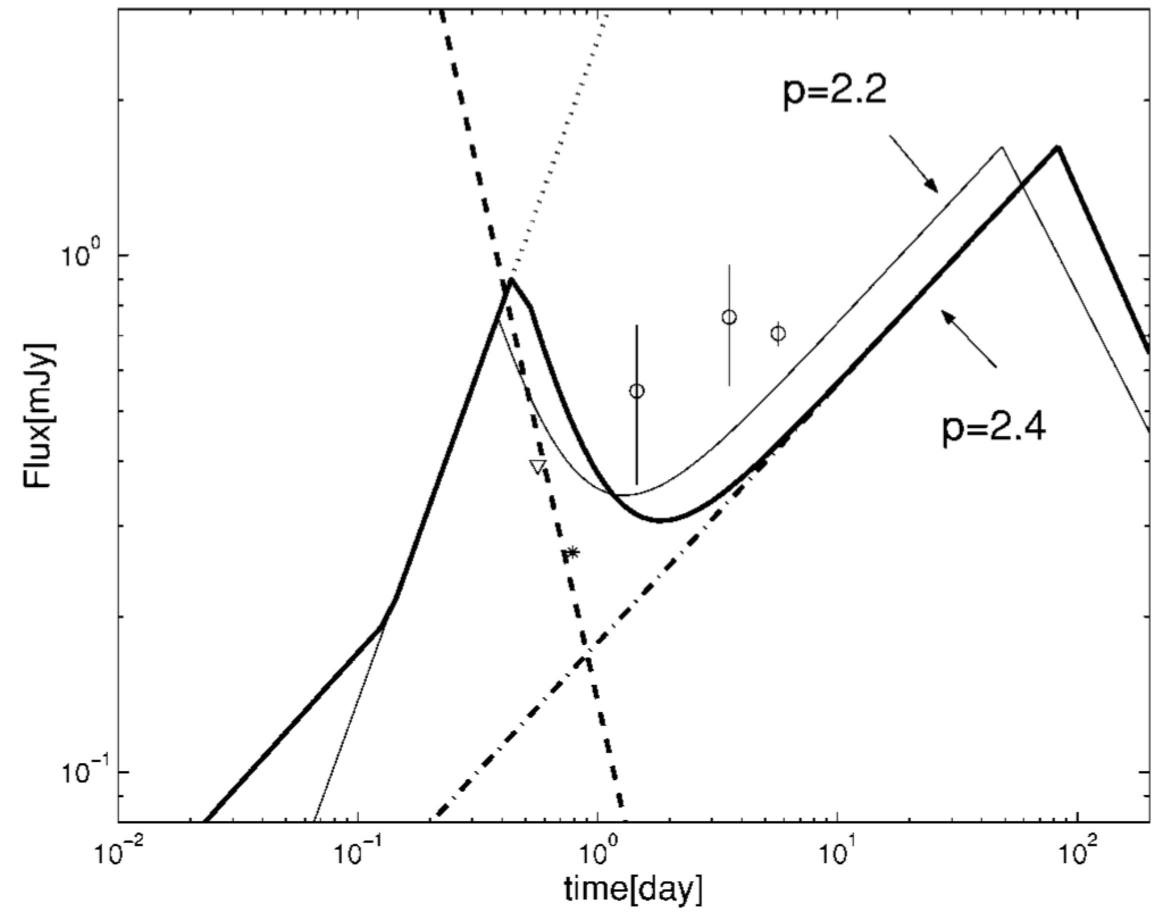

FIG. 2.—Radio light curve: Modeling with $p = 2.4$, forward shock emission (*dash-dotted line*), reverse shock emission (*dashed line*), self-absorption limit (*dotted line*), and total flux (*thick solid line*). Modeling with $p = 2.2$ and total flux (*thin solid line*). The parameters are the same as in Fig. 1. Measurements are shown as circles with error bars and as an asterisk, and the upper limit as a triangle. Data are from Frail & Berger 2002; Pooley 2002a, 2002b, 2002c; and Berger et al. 2002.

A simple elliptical circular mass distribution

(as projected on the sky)

gives an "astroid" caustic pattern

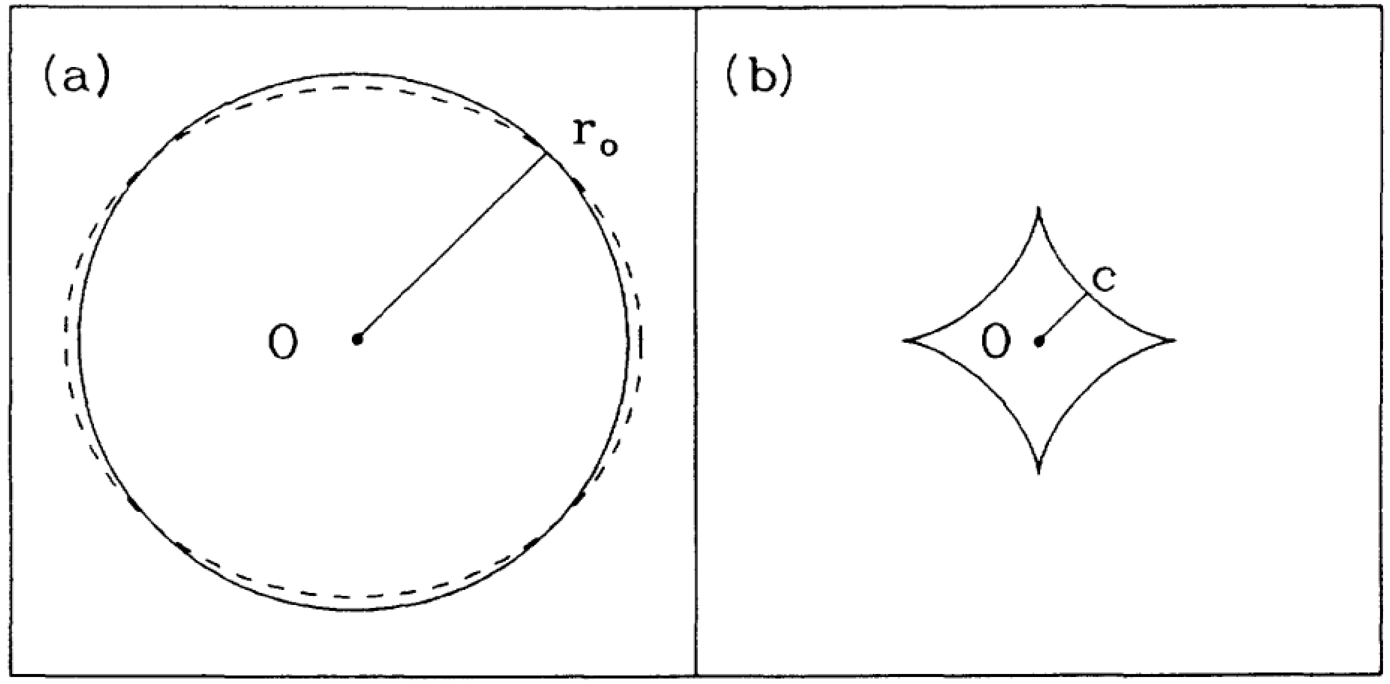

FIG. 2. Influence of noncircular perturbations. (a) Image plane. A circular lens will produce a critical circle (solid line) radius r_o. When a noncircular perturbation is applied, in this case proportional to $\cos 2\phi$, the critical circle is deformed into an ellipse (dashed line). (b) Source plane. The perturbation modifies the caustic from a degenerate point at O to a curve $\mathbf{c}(\phi)$, in this case a four-cusped asteroid.

Blandford & Kovner 1988 Phys. Rev., 38, 4028

A simple elliptical circular mass distribution

(as projected on the sky)

gives an "astroid" caustic pattern

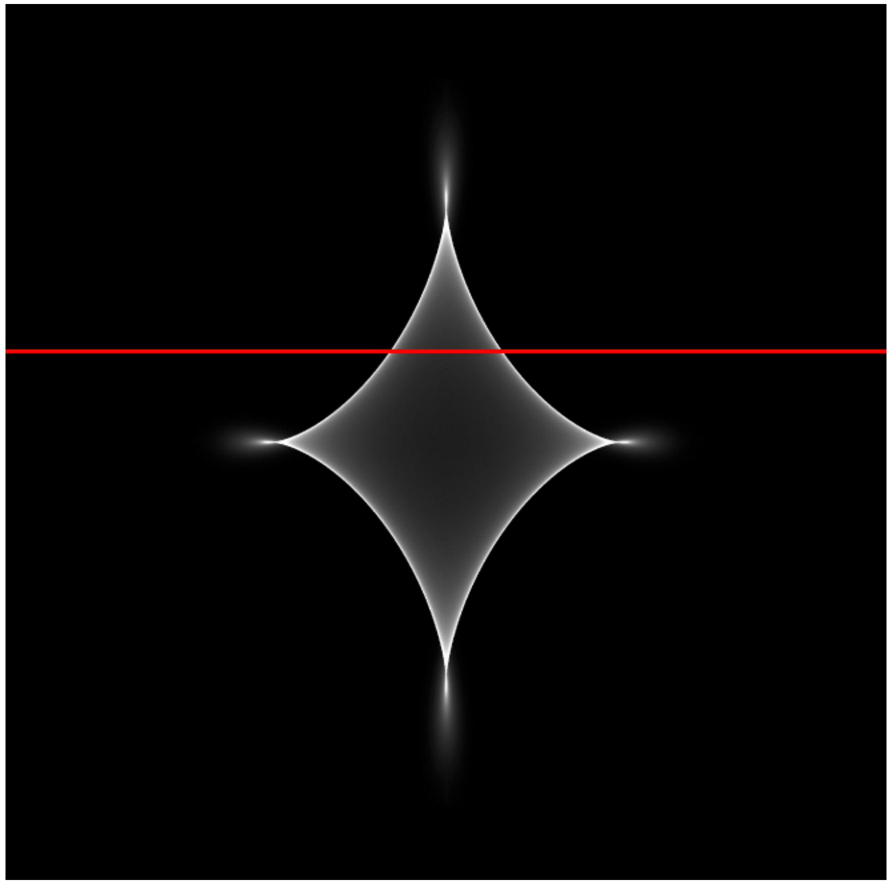

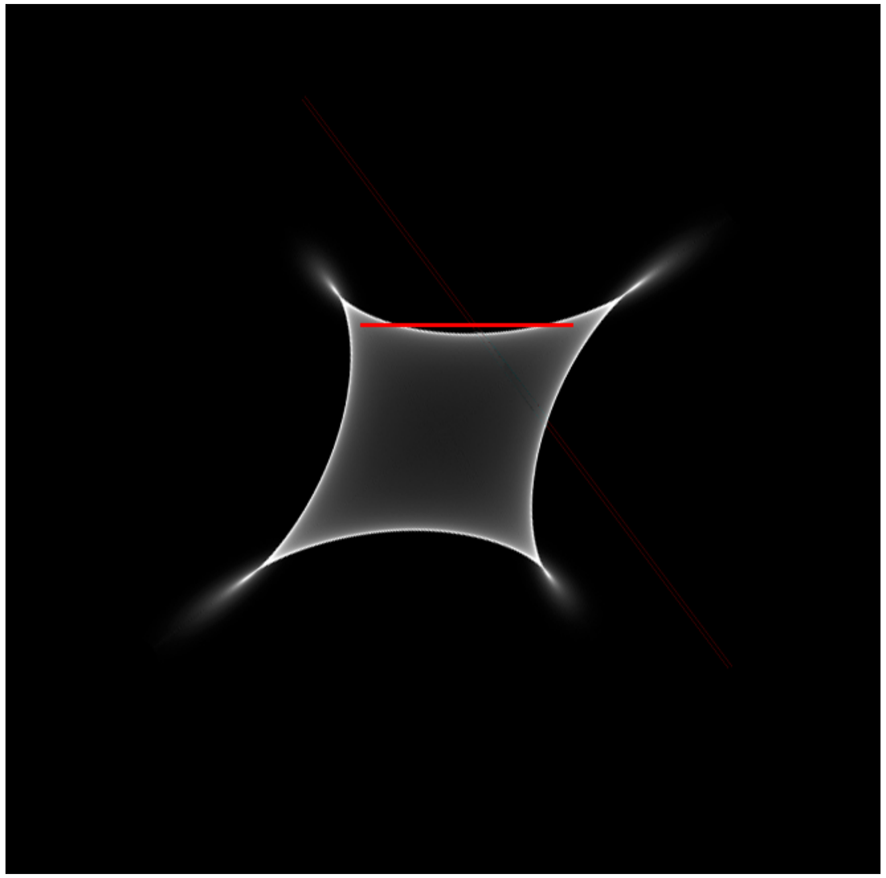

A simple elliptical circular mass distribution

(as projected on the sky)

gives an "astroid" caustic pattern

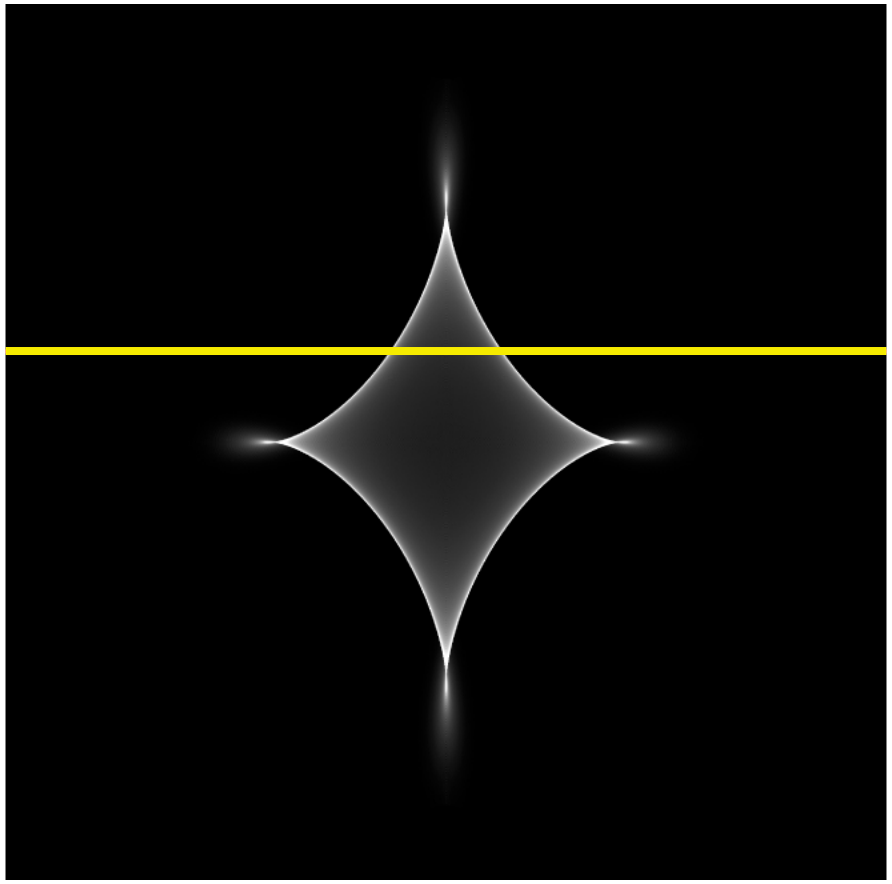

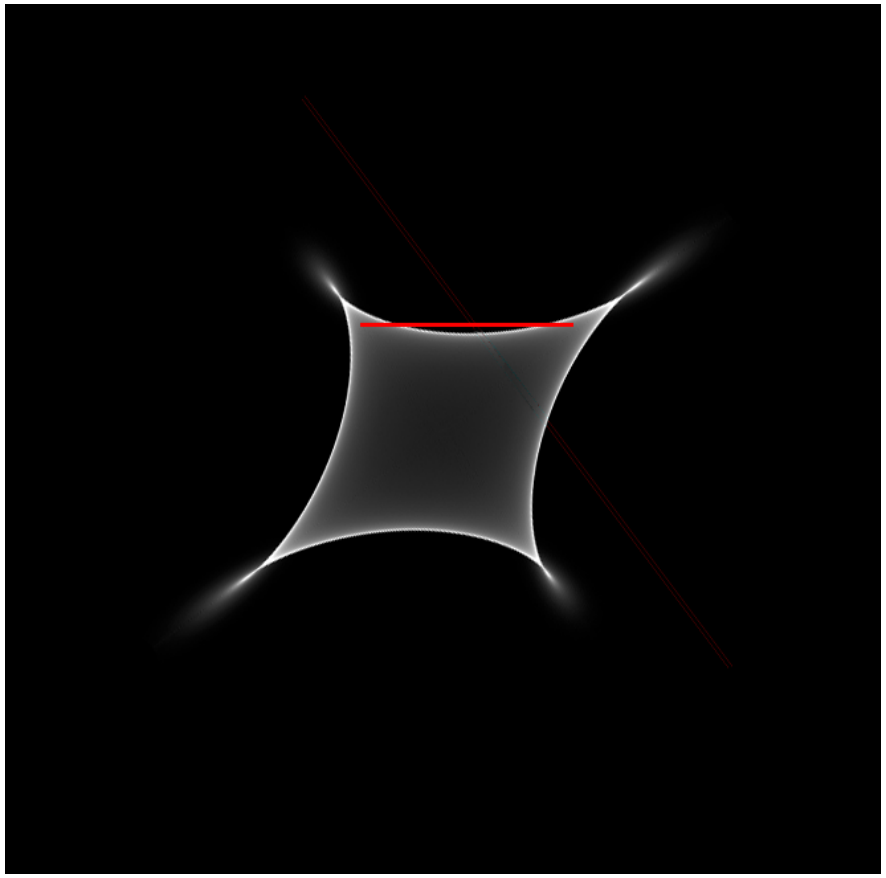

Fast Rise-Slow Decline
followed by
Slow Rise-Fast Decline
FRSD-SRFD:
"Crater Symmetry"

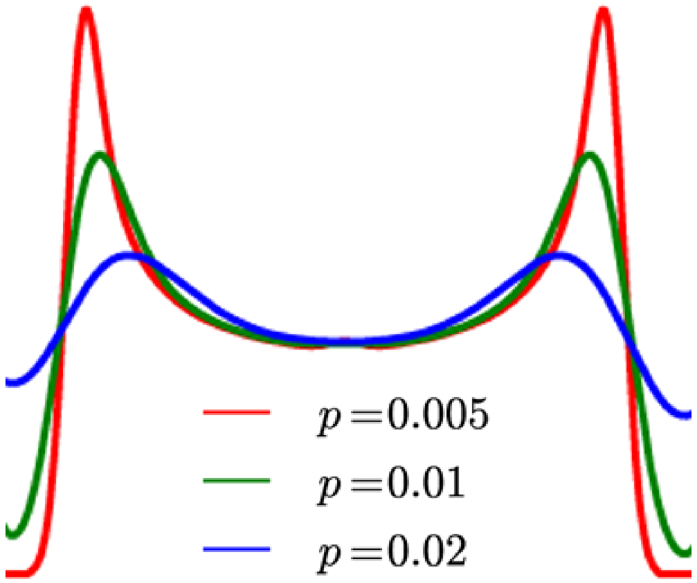

A simple elliptical circular mass distribution

(as projected on the sky)

gives an "astroid" caustic pattern

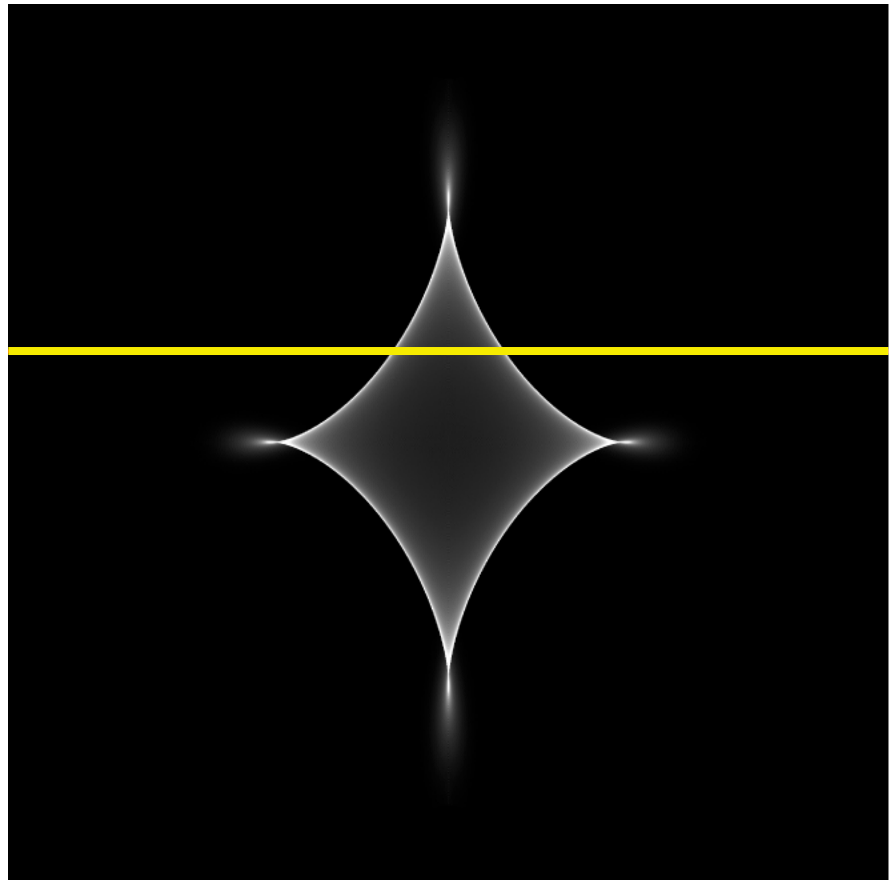

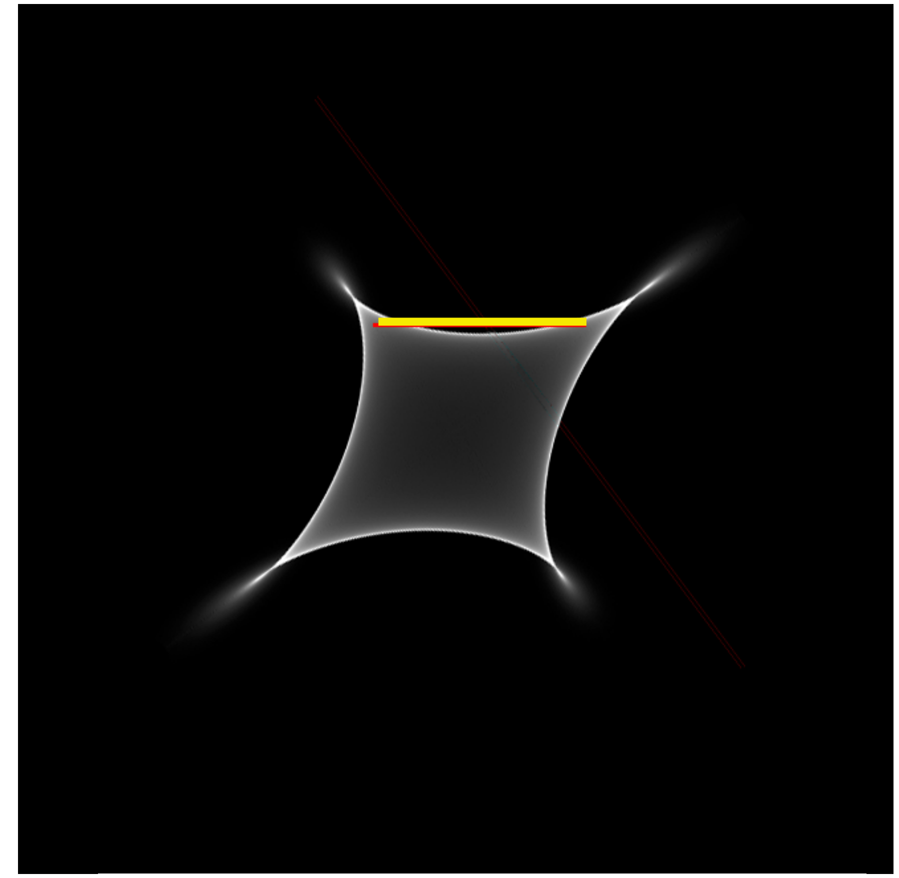

Fast Rise-Slow Decline
followed by
Slow Rise-Fast Decline
FRSD-SRFD:
"Crater Symmetry"

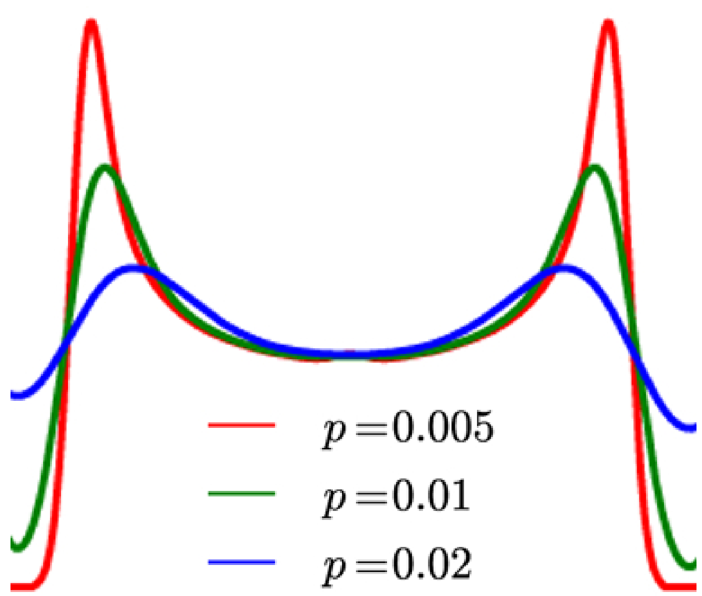

Slow Rise-Fast Decline
followed by
Fast Rise-Slow Decline
SRFD-FRSD:
"Volcano Symmetry"

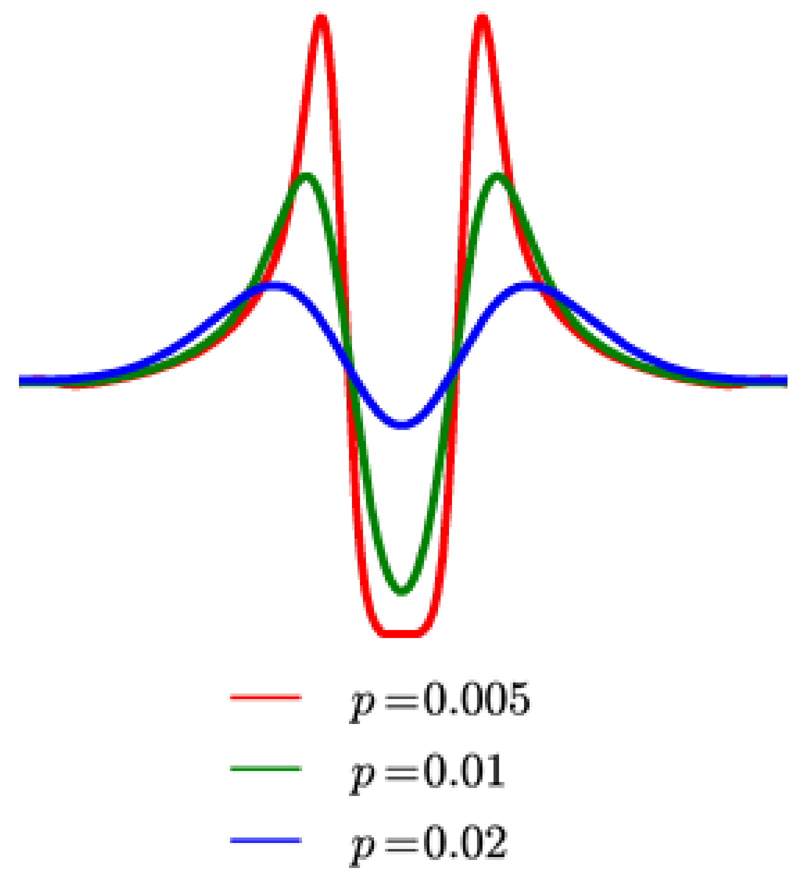

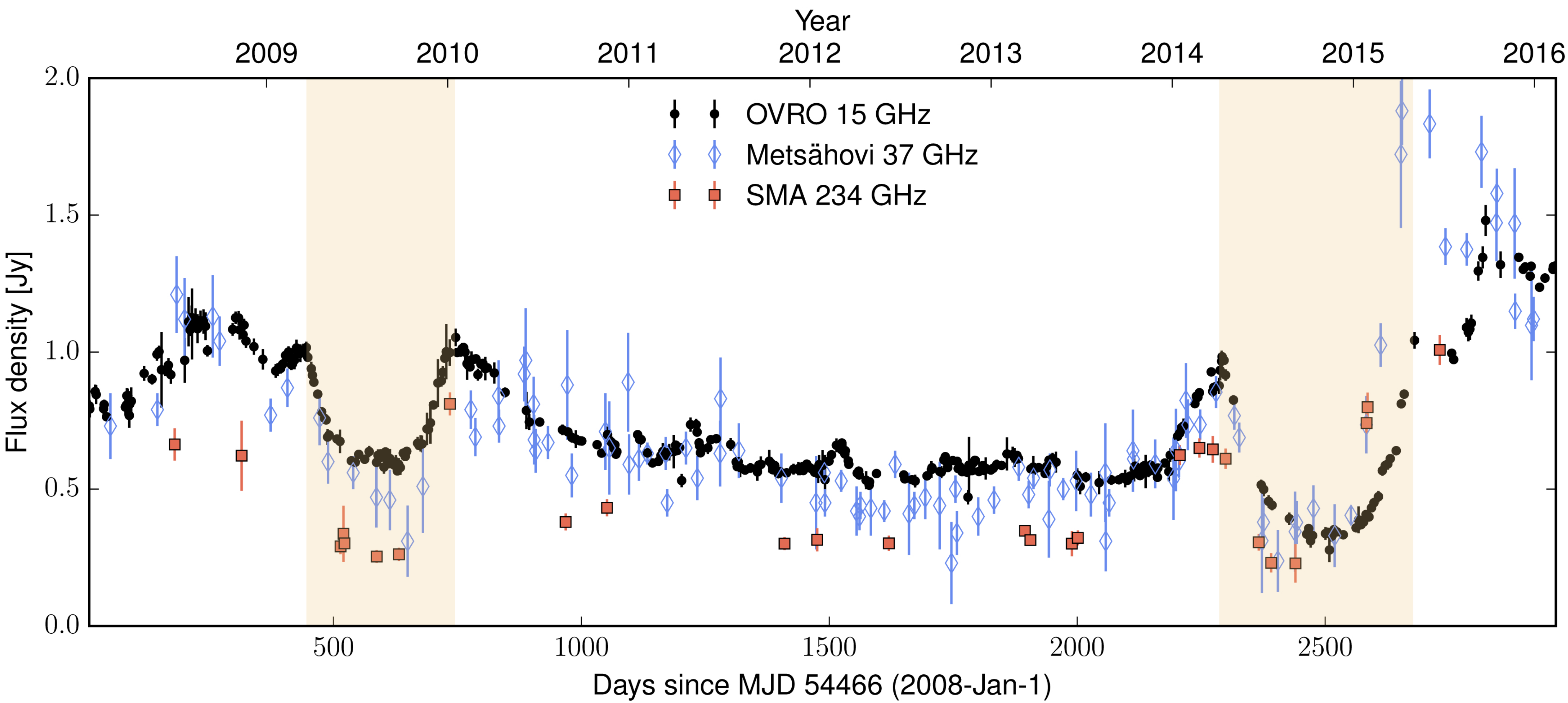
Year
2009
2010
2011
2012
2013
2014
2015
2016
2.0
1.5
1.0
0.5
0.0
Flux density [Jy]
OVRO 15 GHz
Metsähovi 37 GHz
SMA 234 GHz
500
1000
1500
2000
2500
Days since MJD 54466 (2008-Jan-1)

These are both volcano symmetries

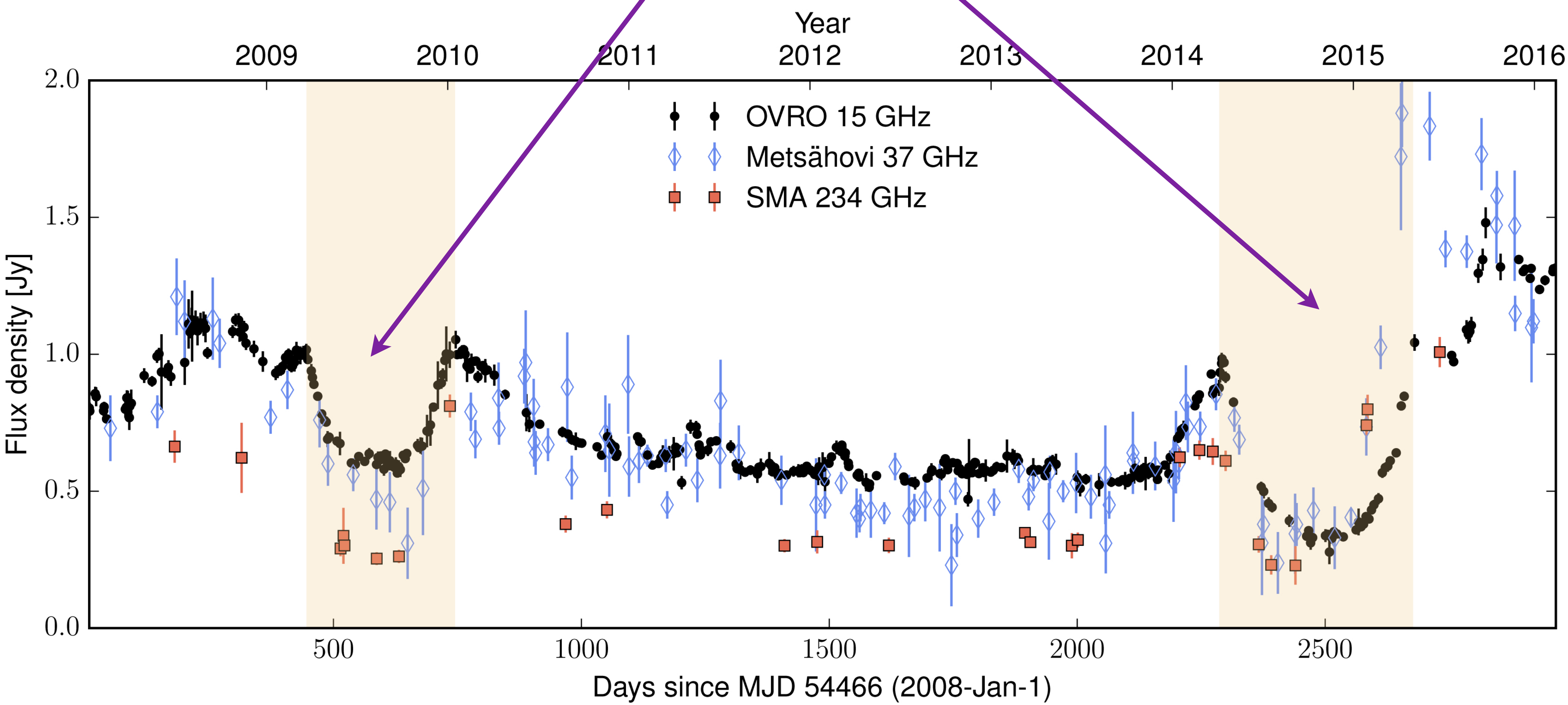

Blandford & Kovner 1988 Phys. Rev., 38, 4028

A simple elliptical circular mass distribution

(as projected on the sky)

gives an "astroid" caustic pattern

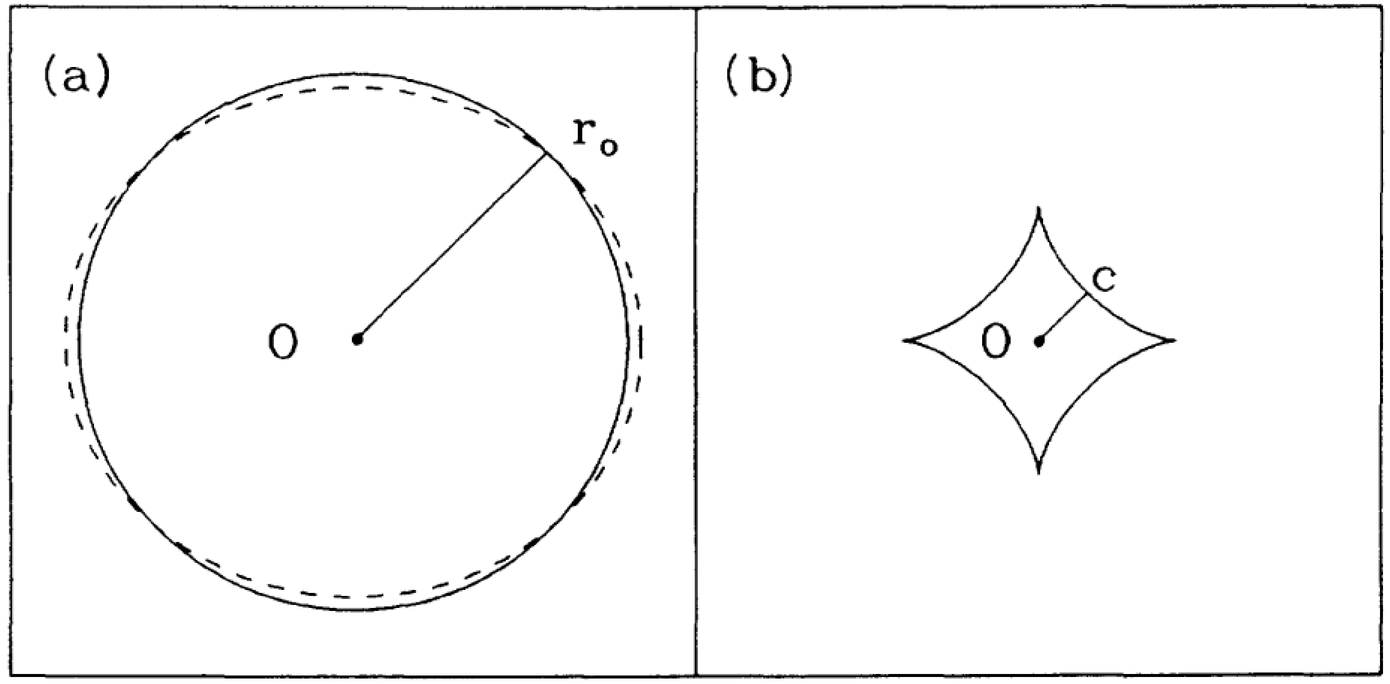

FIG. 2. Influence of noncircular perturbations. (a) Image plane. A circular lens will produce a critical circle (solid line) radius r_o. When a noncircular perturbation is applied, in this case proportional to $\cos 2\phi$, the critical circle is deformed into an ellipse (dashed line). (b) Source plane. The perturbation modifies the caustic from a degenerate point at O to a curve $\mathbf{c}(\phi)$, in this case a four-cusped asteroid.

Blandford & Kovner 1988 Phys. Rev., 38, 4028

A simple elliptical circular mass distribution

(as projected on the sky)

gives an “astroid” caustic pattern

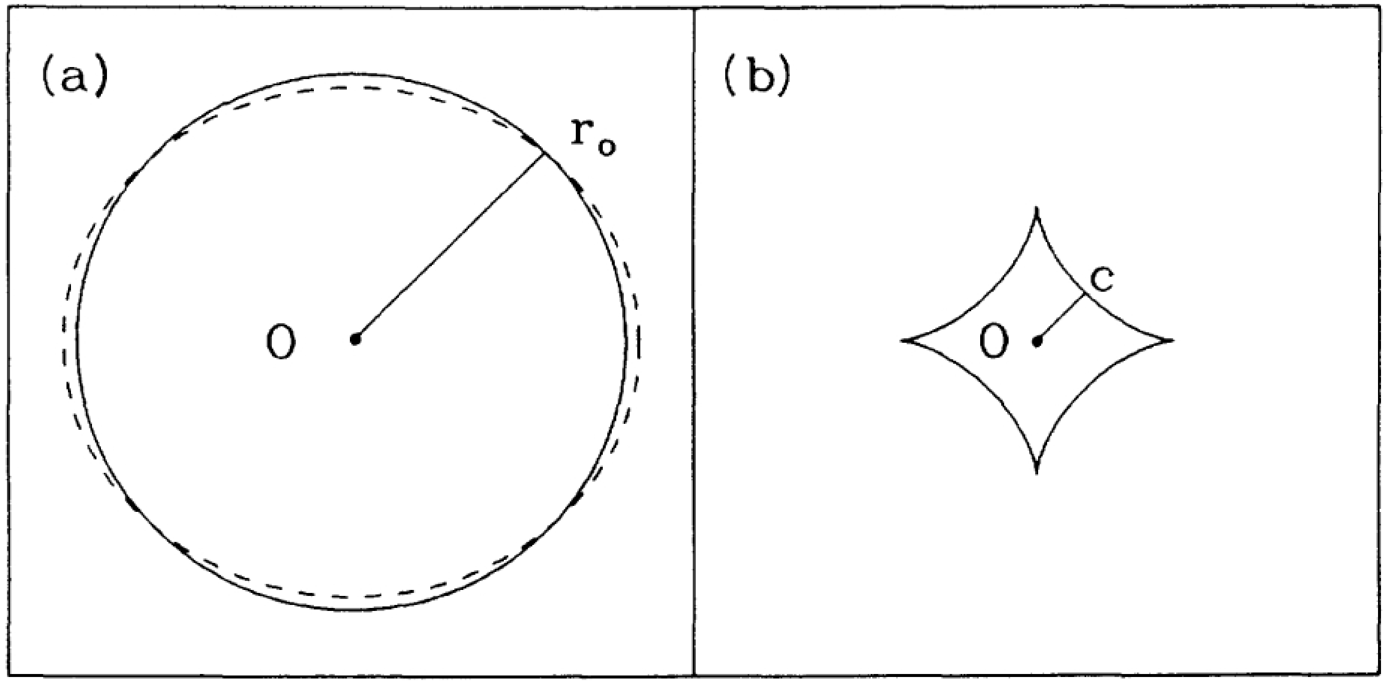

FIG. 2. Influence of noncircular perturbations. (a) Image plane. A circular lens will produce a critical circle (solid line) radius r_o. When a noncircular perturbation is applied, in this case proportional to $\cos 2\phi$, the critical circle is deformed into an ellipse (dashed line). (b) Source plane. The perturbation modifies the caustic from a degenerate point at O to a curve $\mathbf{c}(\phi)$, in this case a four-cusped asteroid.

But this is a very simple gravitational potential perturbation!
What happens if we’re looking through a galaxy and there are several condensations along the line of sight?
(they don’t have to be gravitationally bound)

e.g. if there are two condensations and we add the underlying potential of the galaxy

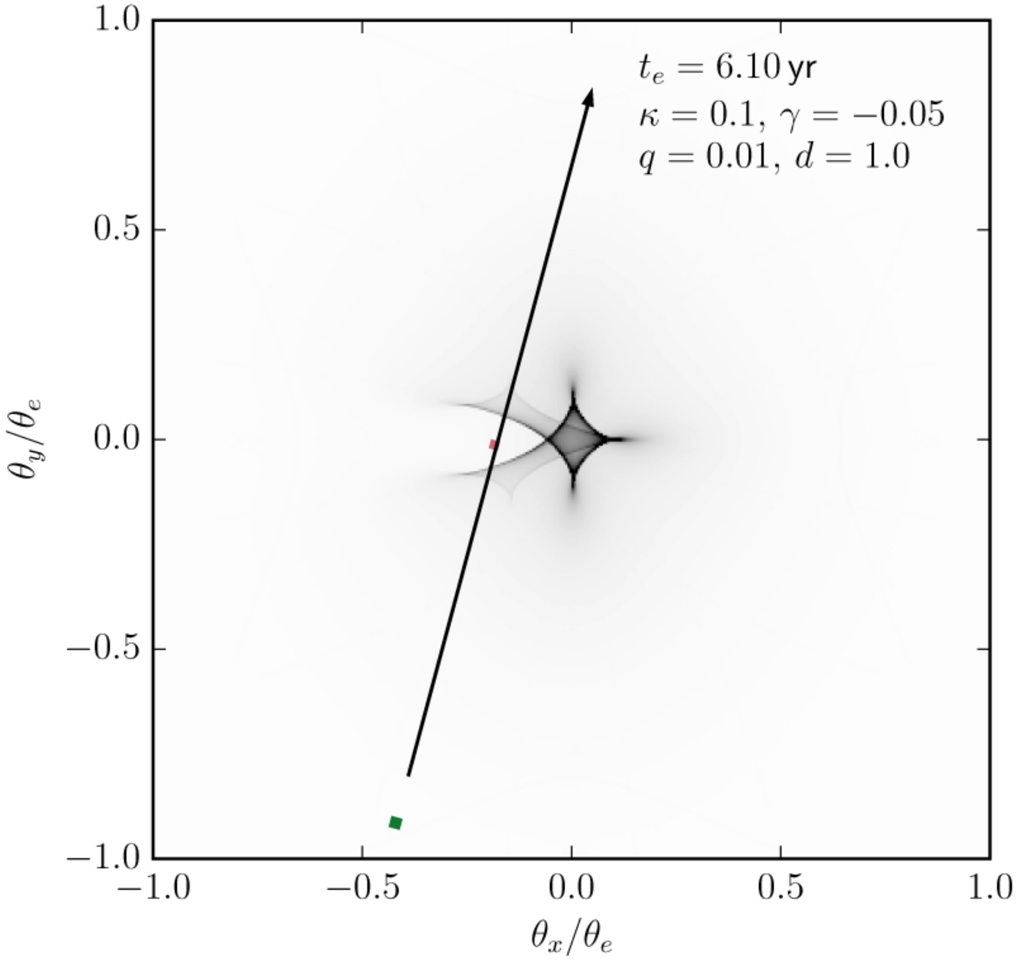

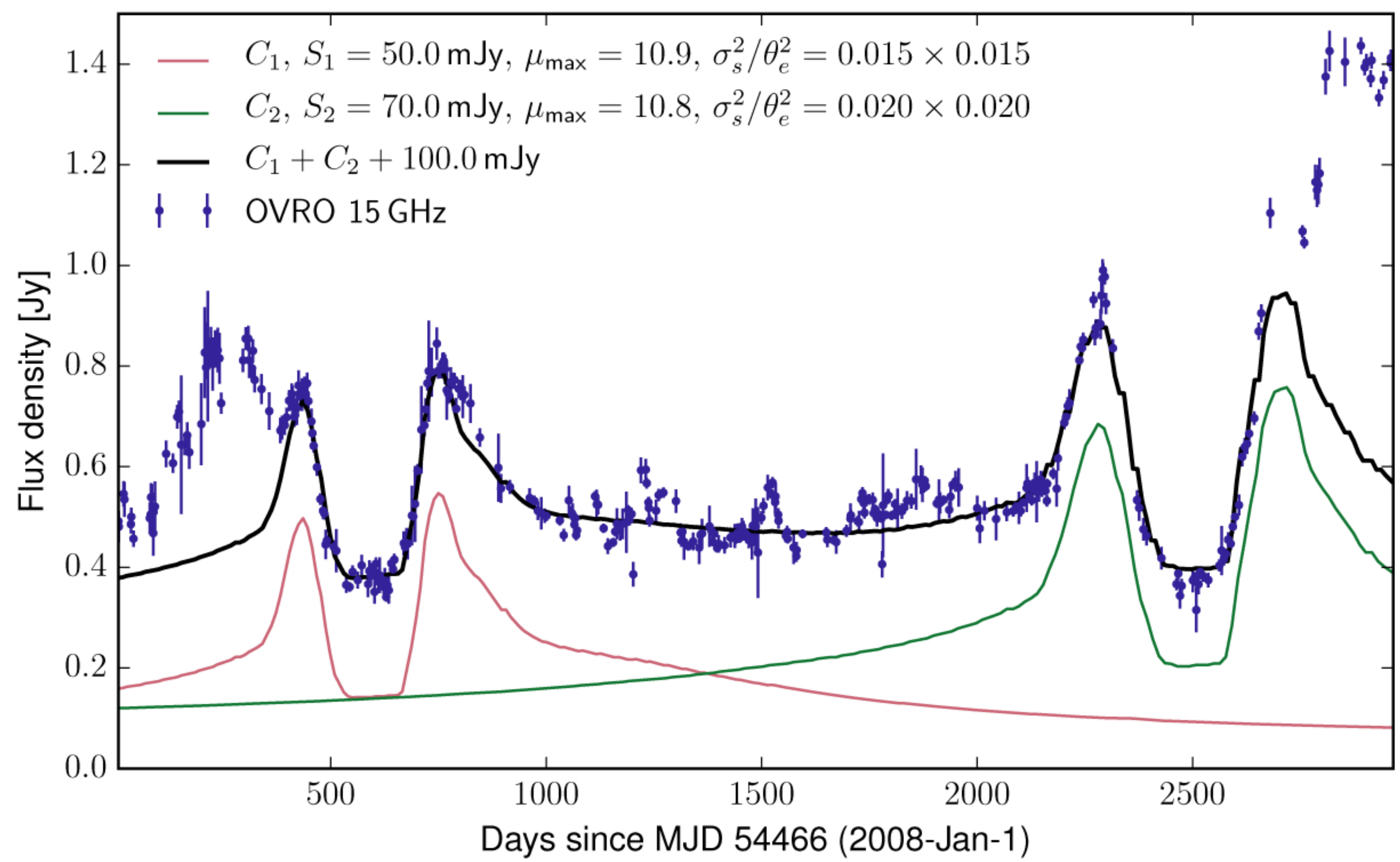

Note that the binary mass ratio is q = 0.01 so that we only need one mass condensation of 10^3 - 10^4 solar masses in the spiral and another mass of 10^1 - 10^2 solar masses *anywhere along the line of sight through the disc of the spiral galaxy* to produce such a binary gravitational lens

i.e. once you have a single 10^3 - 10^4 solar mass condensate along the line of sight through the galaxy then any e.g. stellar masses greater than about 10 solar masses along the line of sight through the galaxy will turn it into a caustic network

The Einstein radius is:

$$\theta_{\rm E} = (4GM/c^2 D)^{1/2}$$
$$\approx 90\,(M/10^3\,M_\odot)^{1/2}(D/1\,{\rm Gpc})^{-1/2}\ \mu{\rm as}.$$

Which for a high redshift (z~1) object

$$\sim 100(v_\perp/c)(t/1{\rm yr})\,\mu{\rm as}$$

It is important to note that it is the **combination** of the lensing **mass** (here ~ 10^3 - 10^4 solar masses), which produces a milli-lens with Einstein radius around 100 µarcsec, and the **distance** and **speed** of the background component, which are z~1 and v~c, that **together** give rise to a variation that can be seen on a timescale of a few months to a few years, and hence the whole lensing pattern can be observed before the component fades, as would happen if the background component were moving at the usual peculiar velocities we see in galaxies.

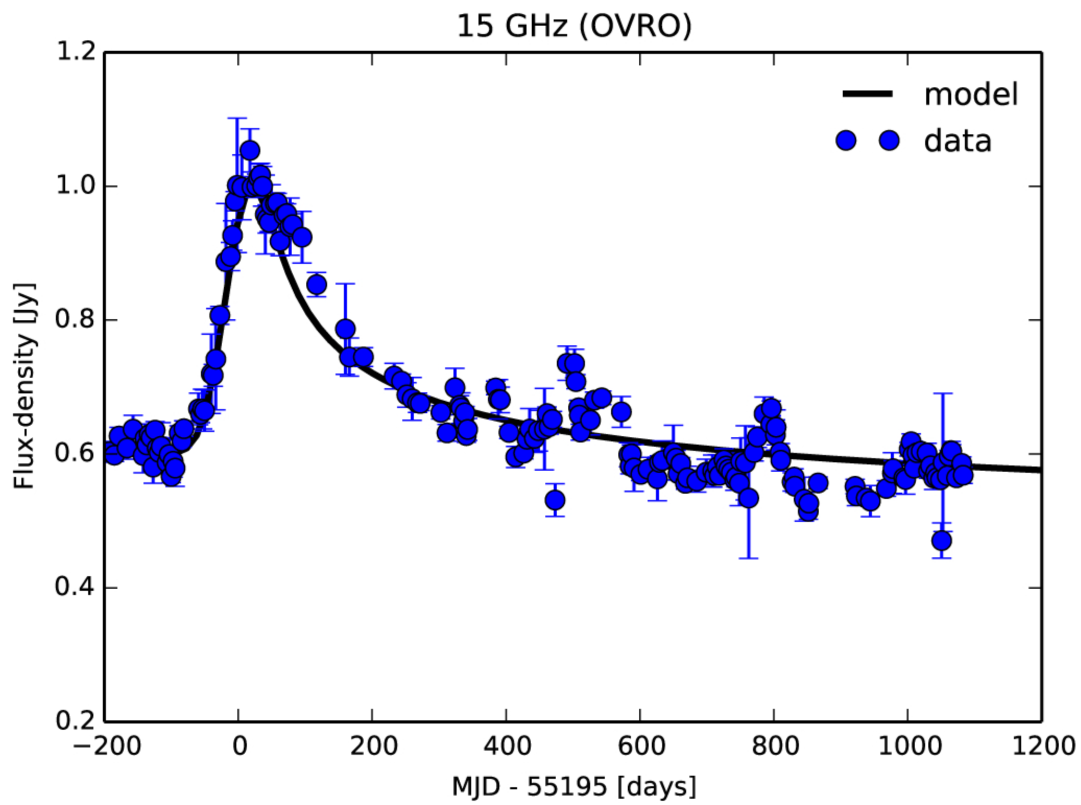

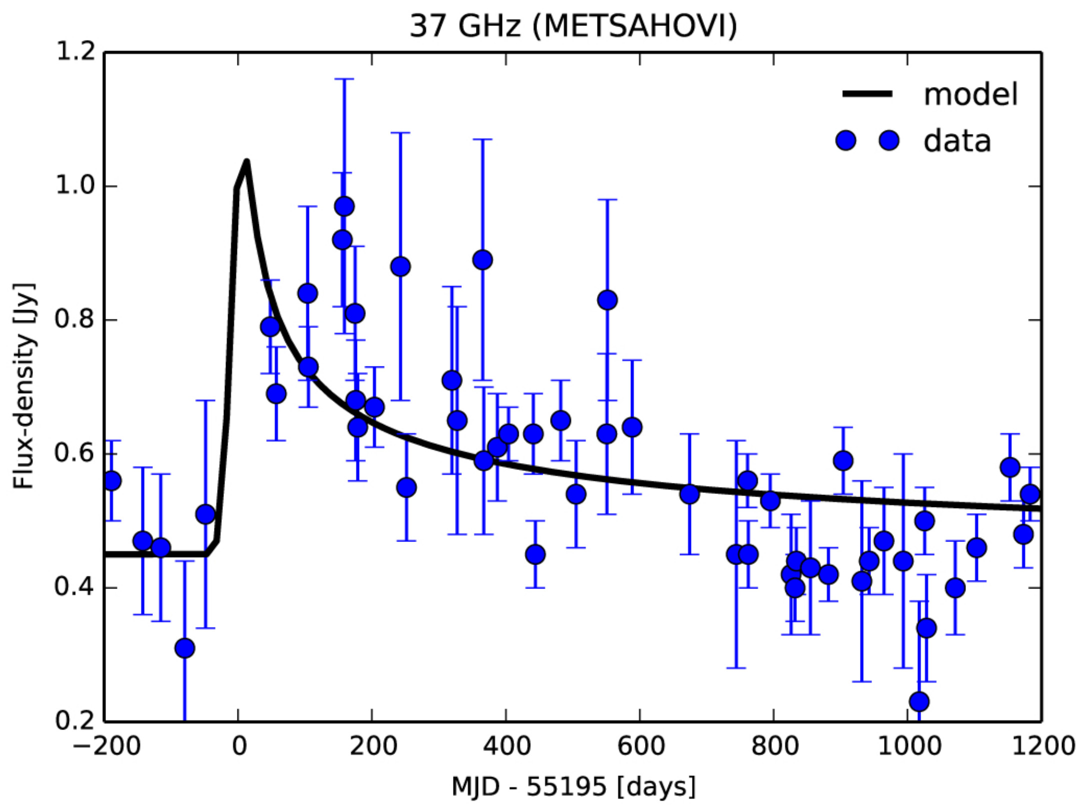

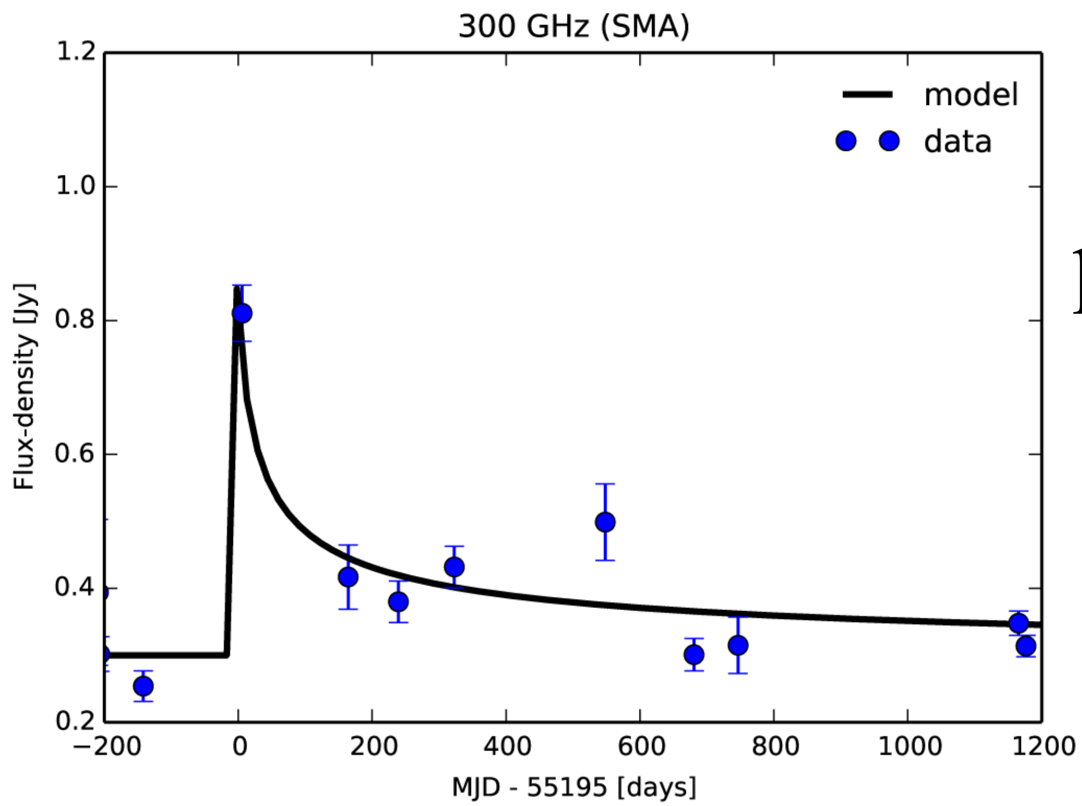

At this stage all one can say is that the fits to the high sensitivity-high cadence 15 GHz data are very good, whereas the fits to the more noisy 37 GHz and less frequently sampled 234 GHz data are not implausible

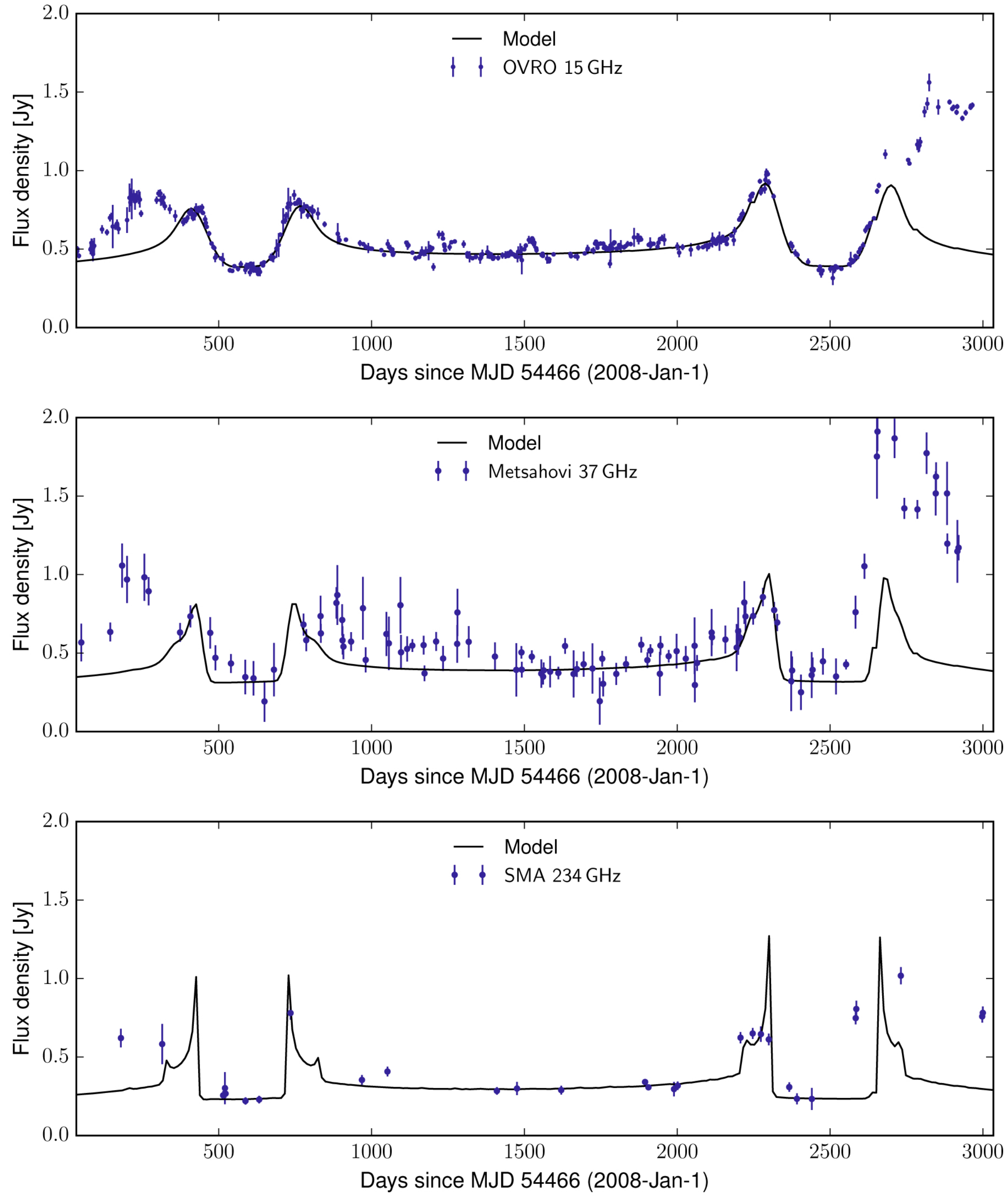

Figure S6: Multifrequency model light curves over plotted on data at 15, 37, and 234 GHz.

Curious things do happen and we are very good at picking out patterns where none actually exist (e.g. stellar constellations). BUT in this case, and unbeknownst to us --- for entirely different reasons, people have been suggesting for 25 years that J1415+1320 is a lensed object!

Perlman et al. 2002 AJ, 124, 2401

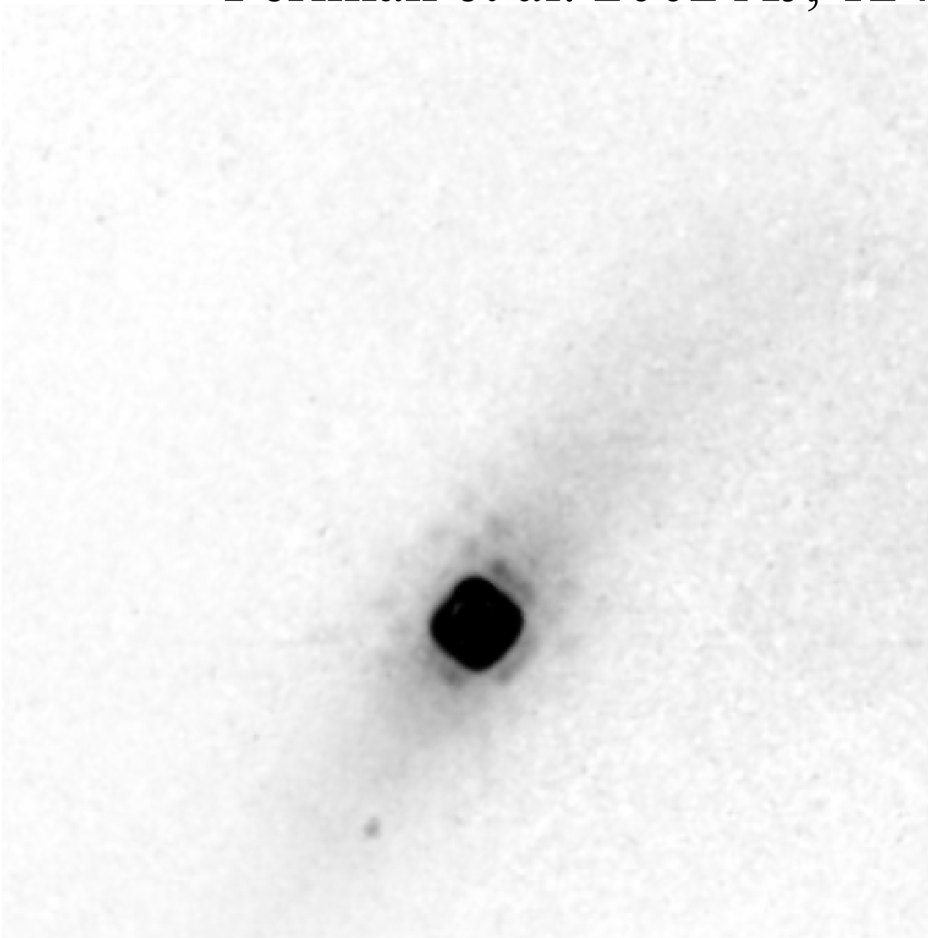

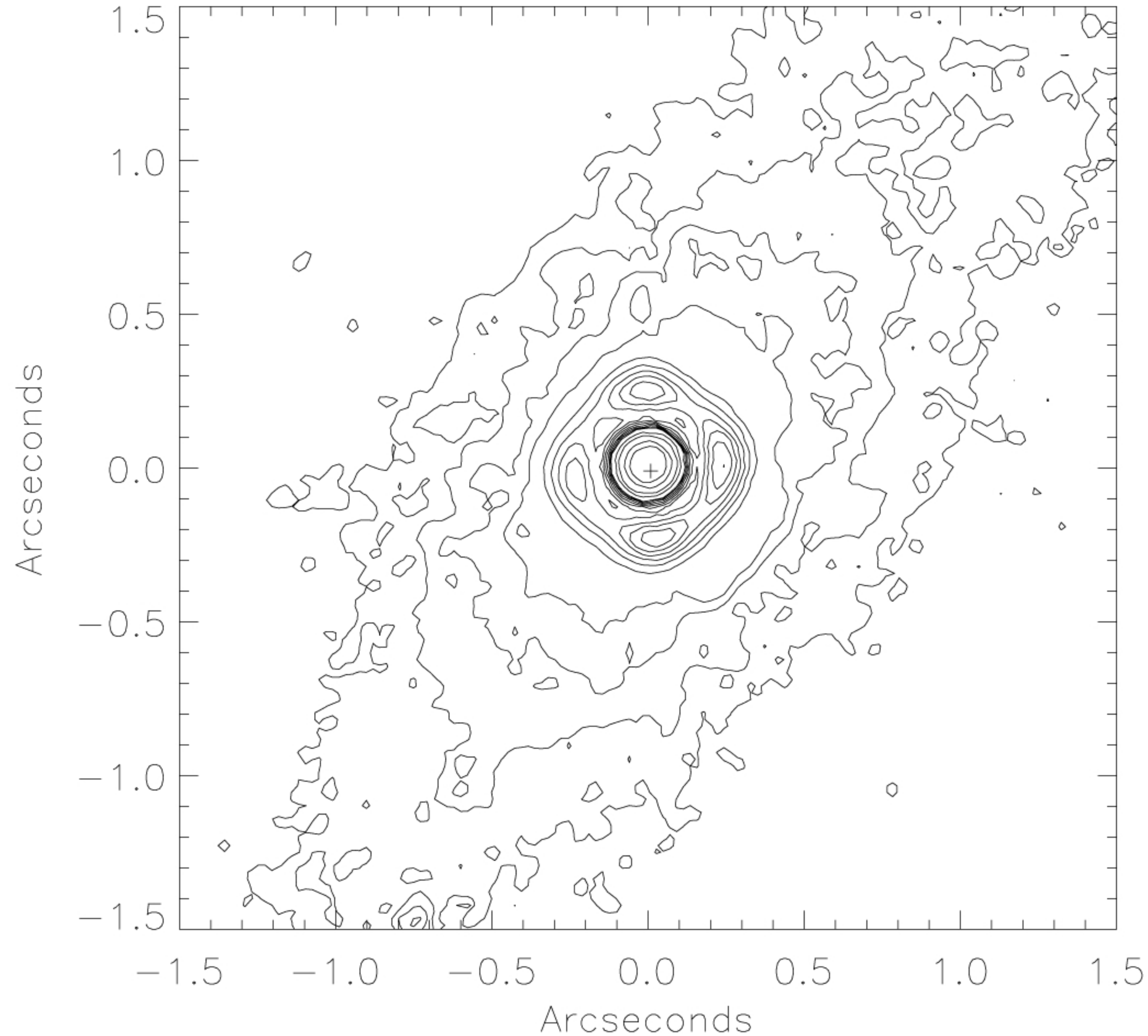

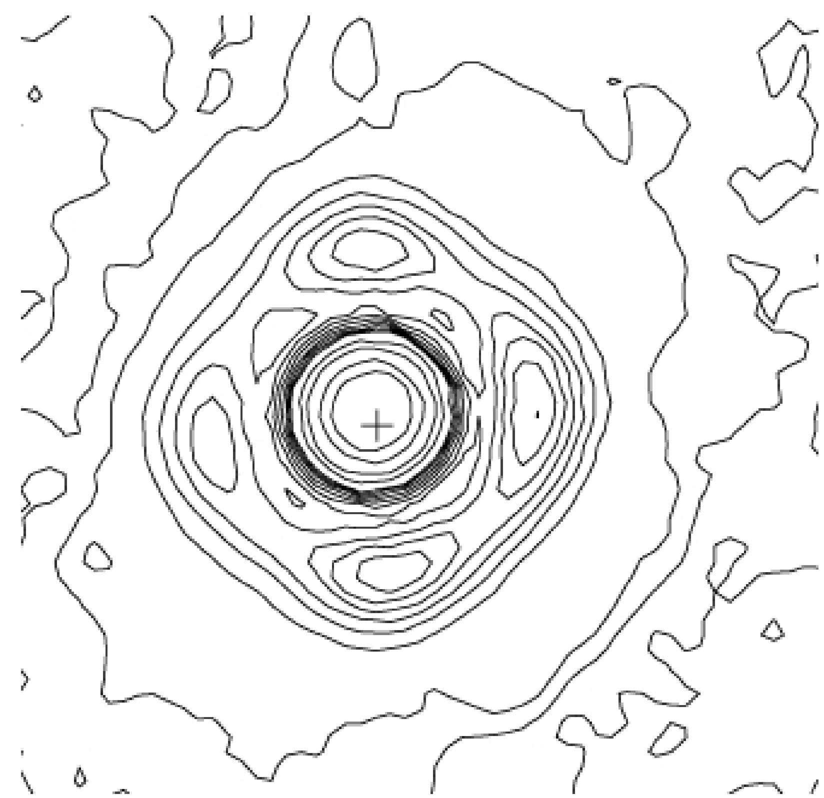

The offset in position is 13 milli-arcseconds, i.e. ~50 pc ----
the probability is only .006, or one in 170, of such an alignment after taking into account the magnification
How concerned should we be given that this is *a posteriori* statistics?

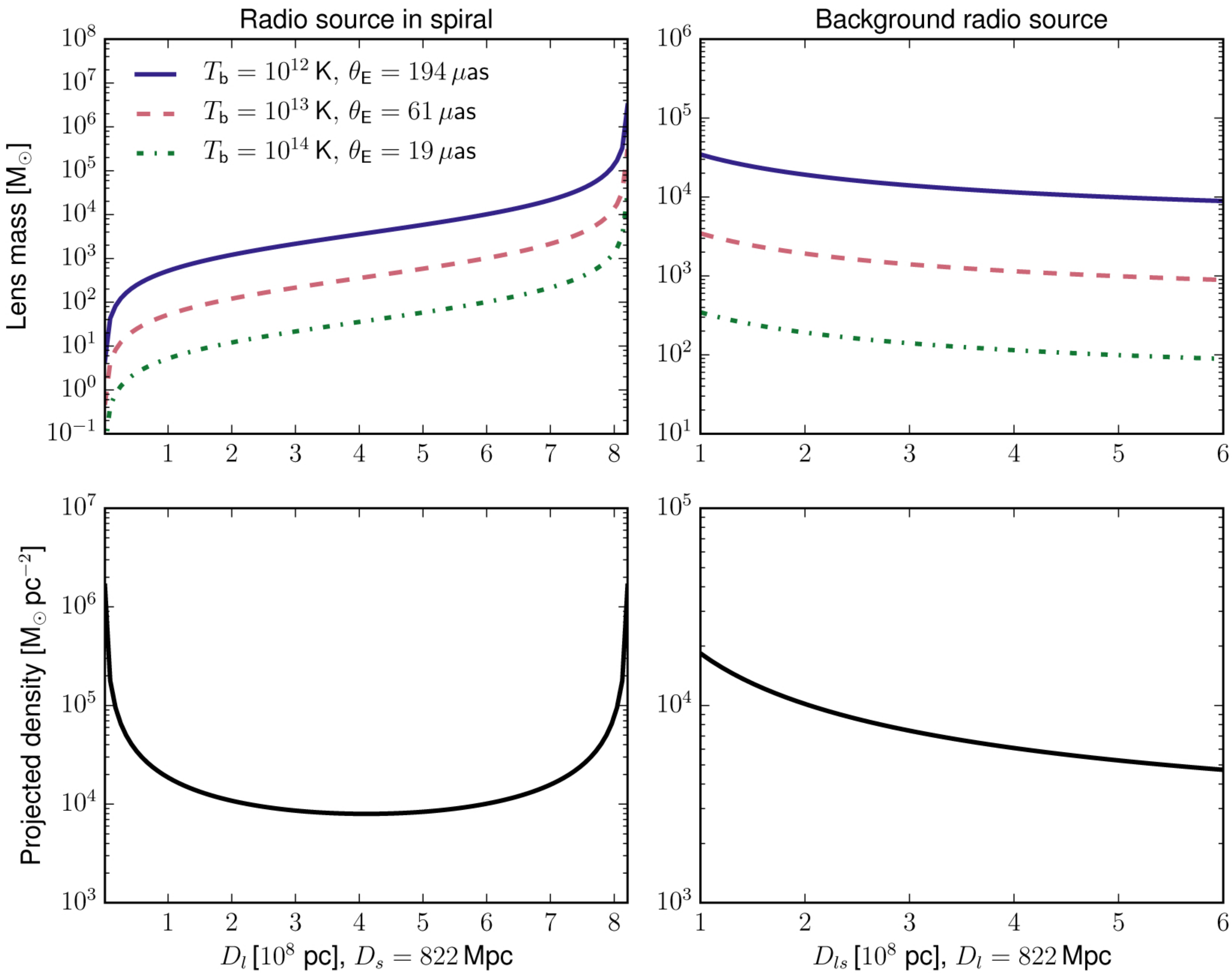
Radio source in spiral
Background radio source
$T_b = 10^{12}$ K, $\theta_E = 194\,\mu$as
$T_b = 10^{13}$ K, $\theta_E = 61\,\mu$as
$T_b = 10^{14}$ K, $\theta_E = 19\,\mu$as
Lens mass [$M_\odot$]
Projected density [$M_\odot$ pc^{-2}]
D_l [10^8 pc], $D_s = 822$ Mpc
D_{ls} [10^8 pc], $D_l = 822$ Mpc

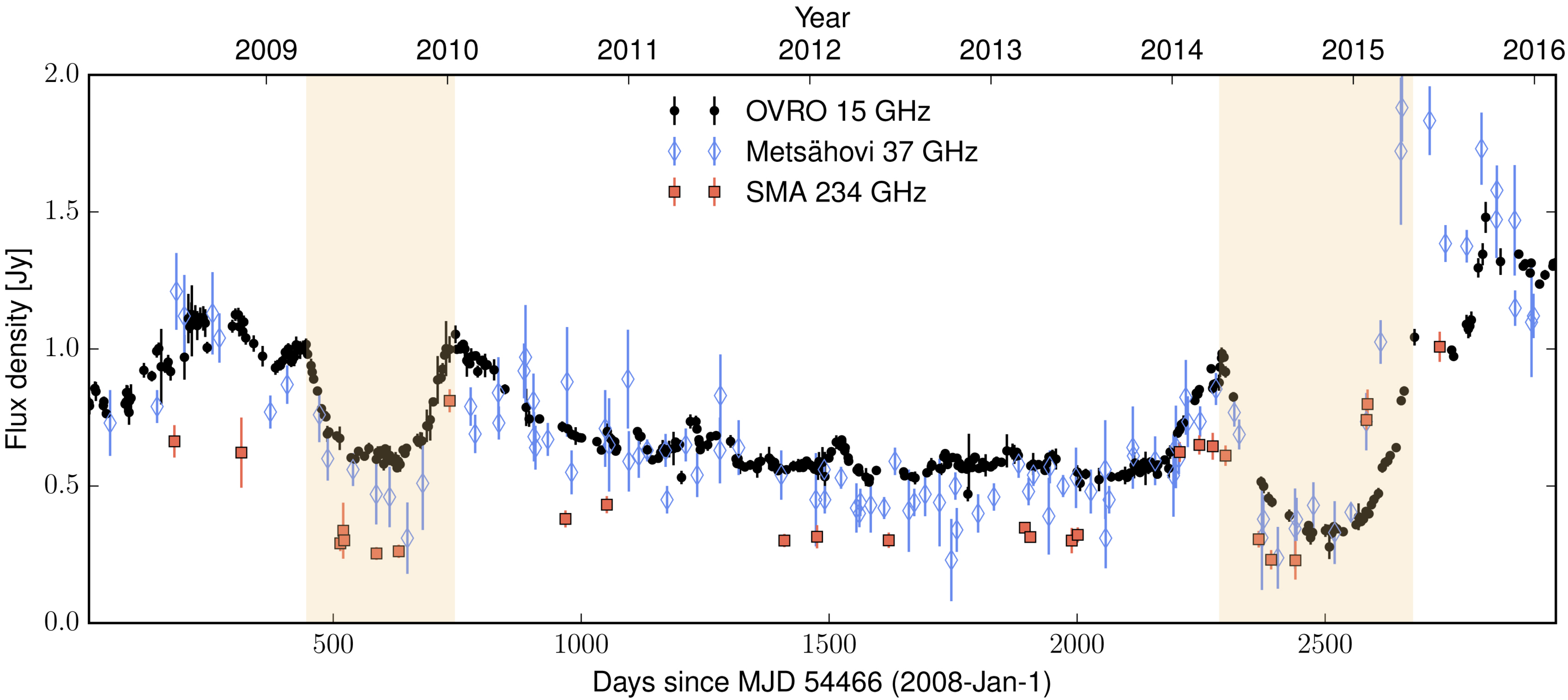

Note that the high frequency variations appear to precede the low frequency variations

For decades with VLBI we've been observing flat-spectrum cores at one end of steep-spectrum jets:

this + superluminal motion + the highly curved structures strongly suggested relativistic beaming of a jet pointed almost directly at us and as you observe at higher frequencies you drill down deeper into the jet

But does this always apply and does it apply at all energies? What about the gamma-ray emission?

3C 273

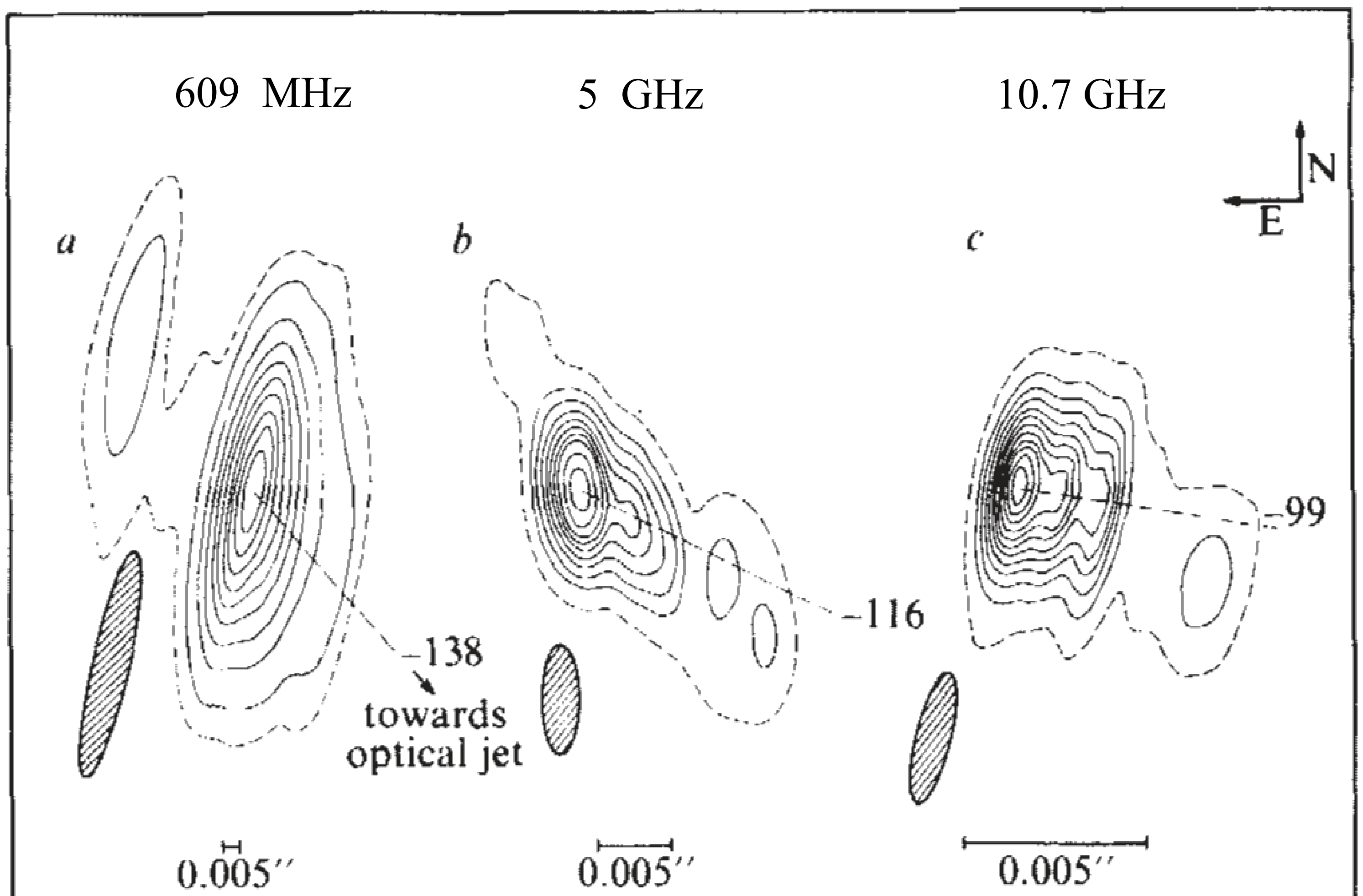

3C 345

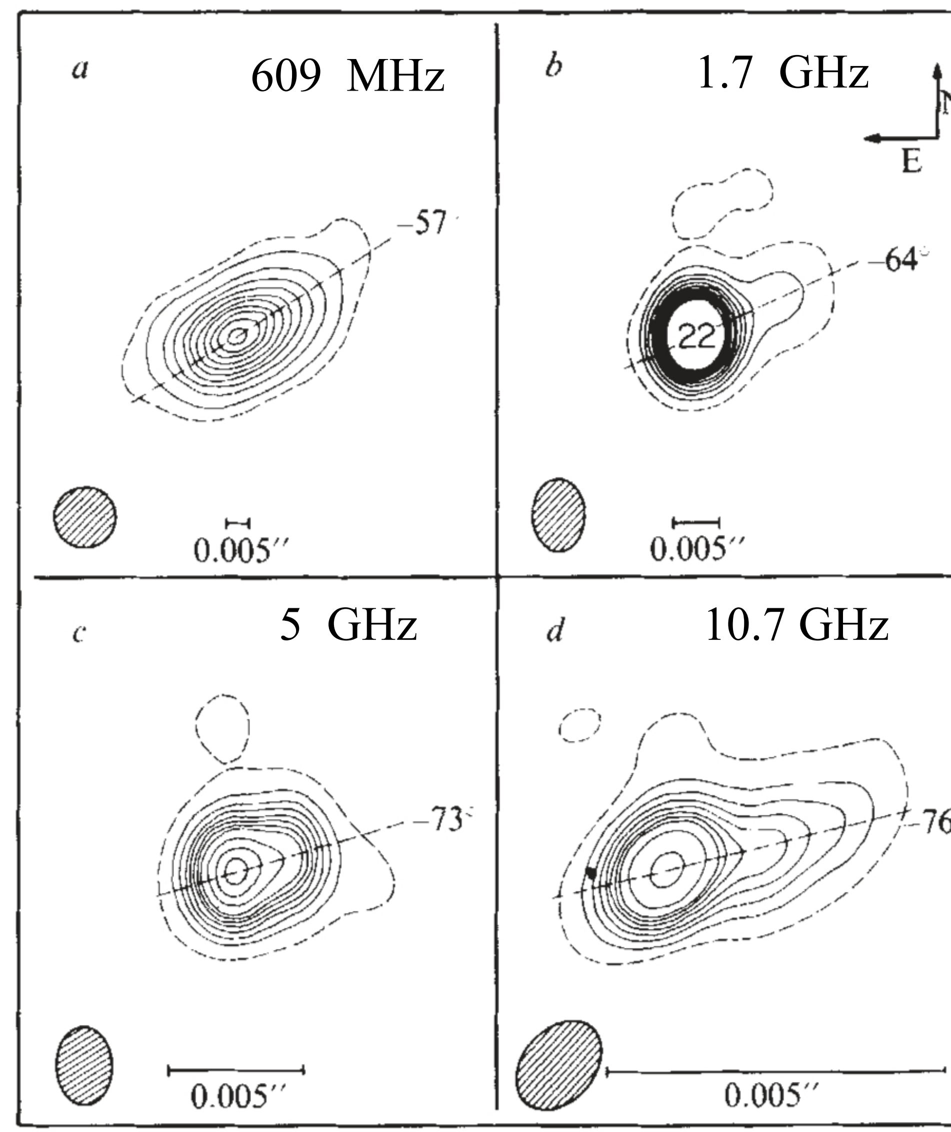

Readhead, Cohen, Pearson & Wilkinson 1978, Nature, 276, 768

At first we saw nothing to contradict this model in the observations, and when the CGRO EGRET observations at γ-ray energies came along it seemed highly probable in view both of their energy and very rapid variability that they are coming from even closer to the central engine

PAIR CASCADES IN EXTRAGALACTIC JETS. I. GAMMA RAYS

THE ASTROPHYSICAL JOURNAL, 441:79–95, 1995 March 1

R. D. BLANDFORD AND A. LEVINSON
Theoretical Astrophysics 130-33, Caltech, Pasadena, CA 91125
Received 1994 February 11; accepted 1991 September 9

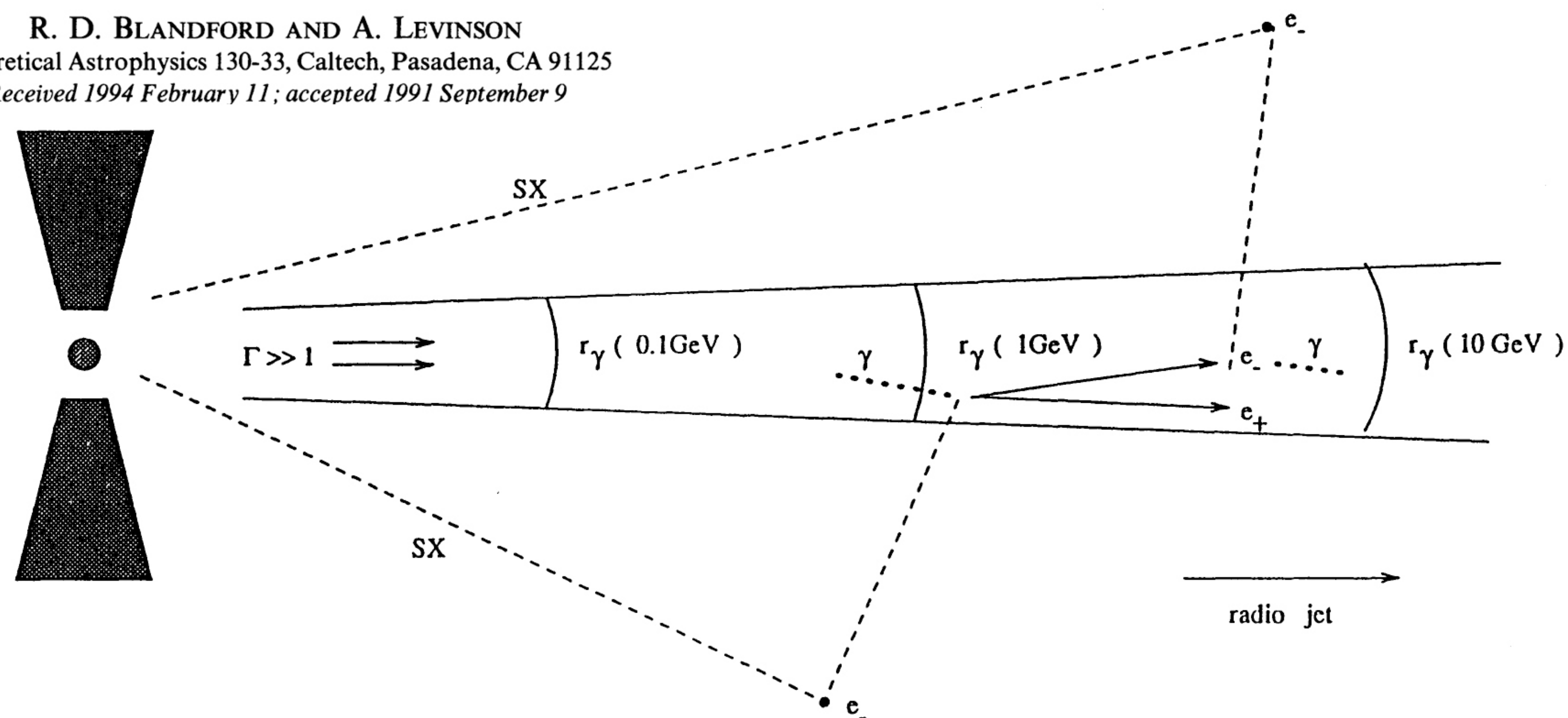

FIG. 6.—Schematic representation of the pair cascade model. A relativistic jet is formed parallel to the spin of a massive black hole orbited by a thick accretion disk. Soft X-ray photons denoted SX emitted near the black hole may be Thomson-scattered into the jet. There they can both combine with γ-rays to form electrons and positrons and be inverse Compton scattered by electrons and positrons to form γ-rays. In this way a pair cascade can develop. Also shown are the γ-spheres for $E_\gamma = 0.1, 1, 10$ GeV.

but Jorstad and Marscher had a different take on the γ-ray emission:

Jorstad, Marscher, et al. Ap.J. 556, 738, 2001

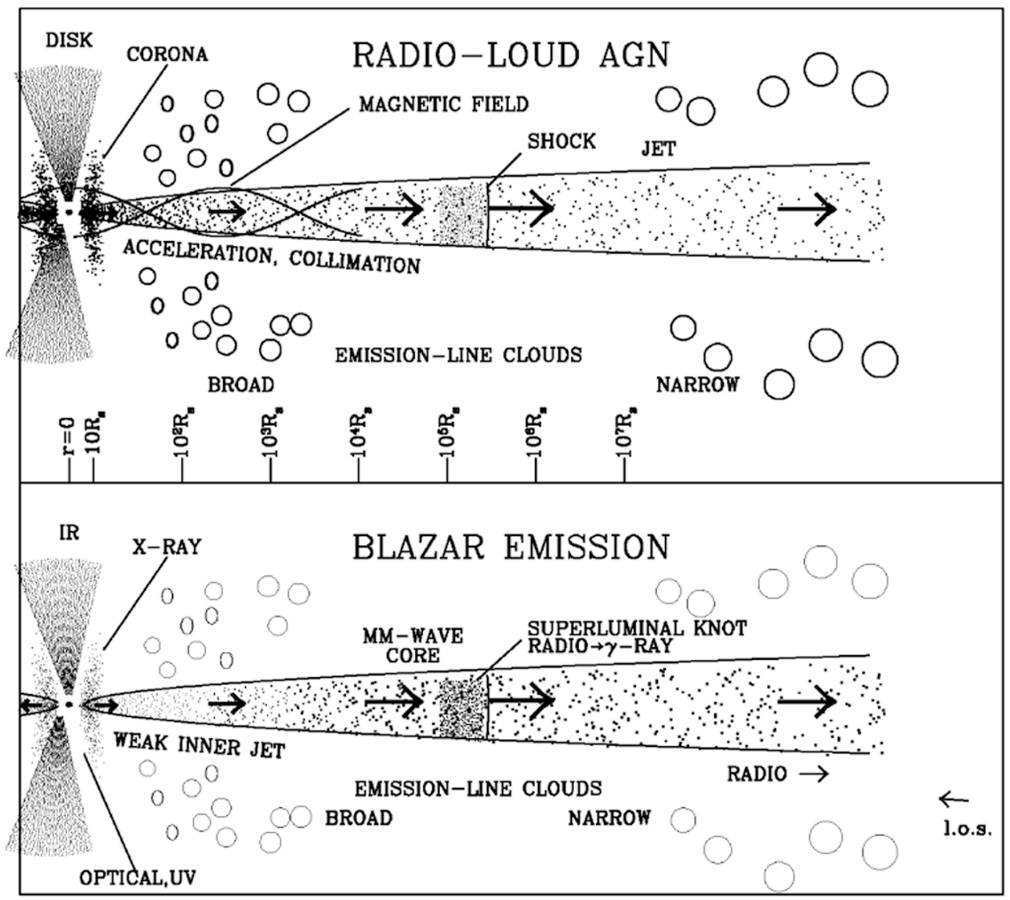

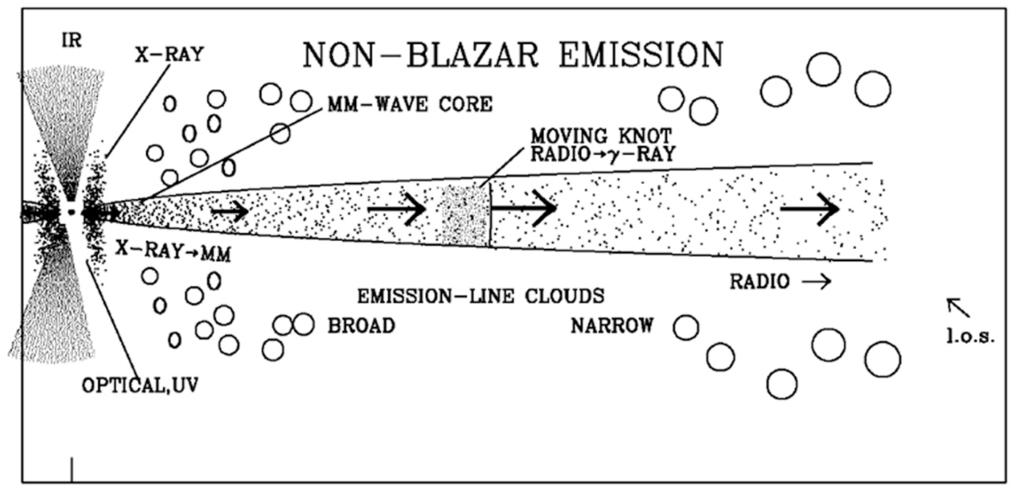

Quote from Abstract: "Our analysis . . . suggests that the γ-ray events occur in the superluminal radio knots. This implies that the γ-ray flares are caused by inverse Compton scattering by relativistic electrons in the parsec-scale regions of the jet rather than closer to the central engine."

Fig. 1 Rough sketch of the structure and emission regions of a radio-loud active galaxy with a relativistic jet. Note the logarithmic scale on the bottom for the distance down the jet. In the two emission panels—one for jets viewed almost end-on (a blazar) and the other for those seen at a wider angle (a typical radio galaxy)—the likely waveband of photons that can be emitted at each site is indicated. If the jet accelerates out to parsec scales, the inner jet between the mm-wave core and the black hole may be essentially invisible in blazars, while in radio galaxies bright emission might extend down to the base of the jet. (Adapted from Marscher 2005.)

Monthly Notices of the ROYAL ASTRONOMICAL SOCIETY
MNRAS **441,** 1899–1909 (2014)
doi:10.1093/mnras/stu540

Detection of significant cm to sub-mm band radio and γ-ray correlated variability in *Fermi* bright blazars

L. Fuhrmann,[1★] S. Larsson,[2] J. Chiang,[3] E. Angelakis,[1] J. A. Zensus,[1] I. Nestoras,[1] T. P. Krichbaum,[1] H. Ungerechts,[4] A. Sievers,[4] V. Pavlidou,[1] A. C. S. Readhead,[5] W. Max-Moerbeck[5] and T. J. Pearson[5]

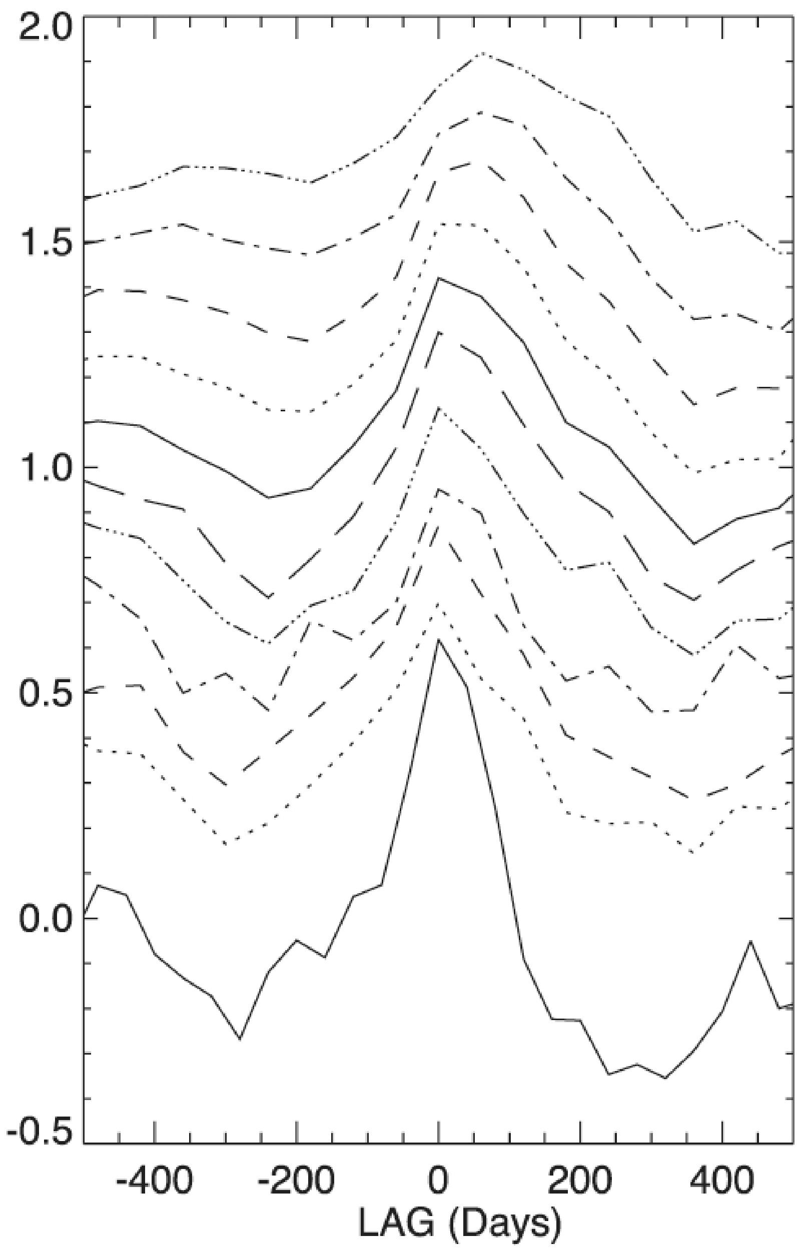

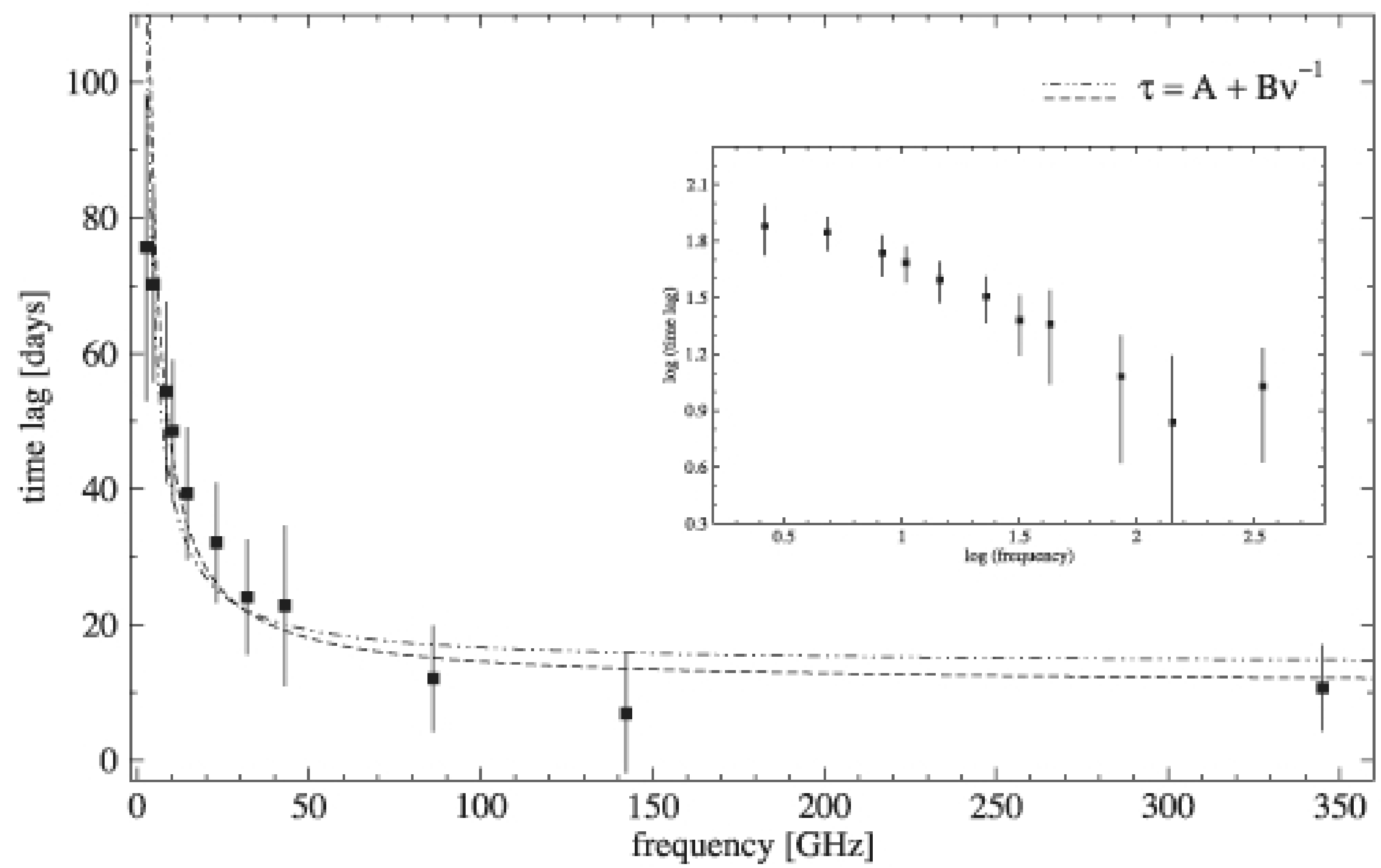

Conclusions:

1. If our gravitational lensing hypothesis for SAV behavior is confirmed, and furthermore if these objects are not anomalous, they could have profound implications for our interpretation of the relationship between the high-frequency and the low-frequency emission regions observed in AG jets.

2. The observed behavior is readily interpretable if the moving features are outwardly propagating particle acceleration/magnetic amplification fronts – i.e. shocks if the jet is plasma-dominated. The optically emitting electrons would cool close to the front and the centroid of their emission would cross any caustic ahead of the radio emission

3. Symmetric Achromatic provides a third observational approach to gravitational lensing and also provides micro-arcsecond resolution on the nuclei of some active galaxies.

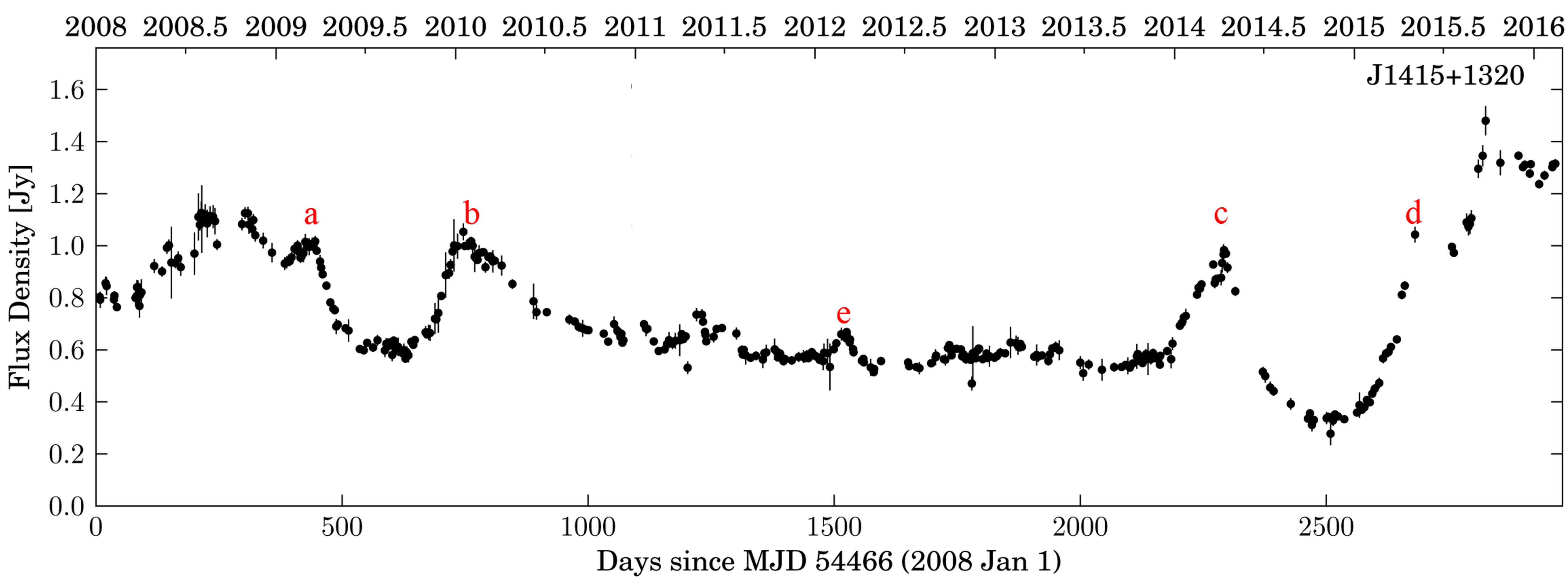

2008
2008.5
2009
2009.5
2010
2010.5
2011
2011.5
2012
2012.5
2013
2013.5
2014
2014.5
2015
2015.5
2016
J1415+1320
a
b
c
d
e
Flux Density [Jy]
0.0
0.2
0.4
0.6
0.8
1.0
1.2
1.4
1.6
0
500
1000
1500
2000
2500
Days since MJD 54466 (2008 Jan 1)

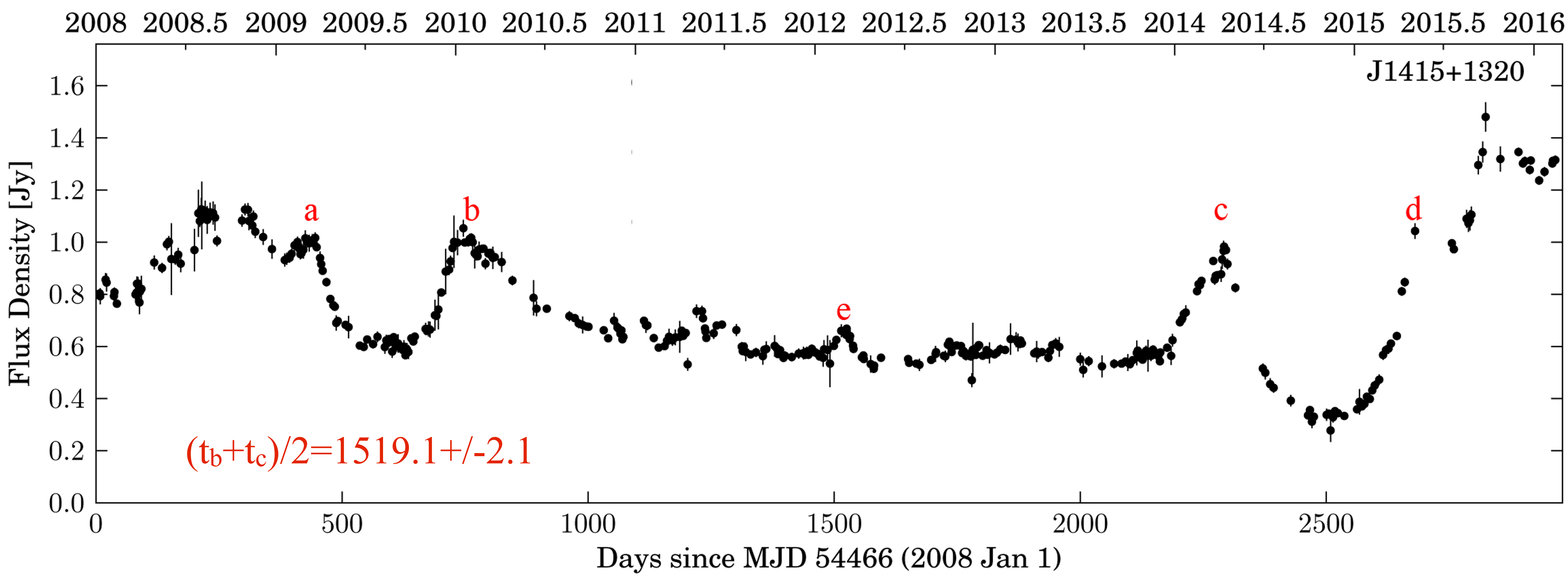

2008
2008.5
2009
2009.5
2010
2010.5
2011
2011.5
2012
2012.5
2013
2013.5
2014
2014.5
2015
2015.5
2016
J1415+1320
Flux Density [Jy]
1.6
1.4
1.2
1.0
0.8
0.6
0.4
0.2
0.0
a
b
c
d
e
(tb+tc)/2=1519.1+/-2.1
0
500
1000
1500
2000
2500
Days since MJD 54466 (2008 Jan 1)

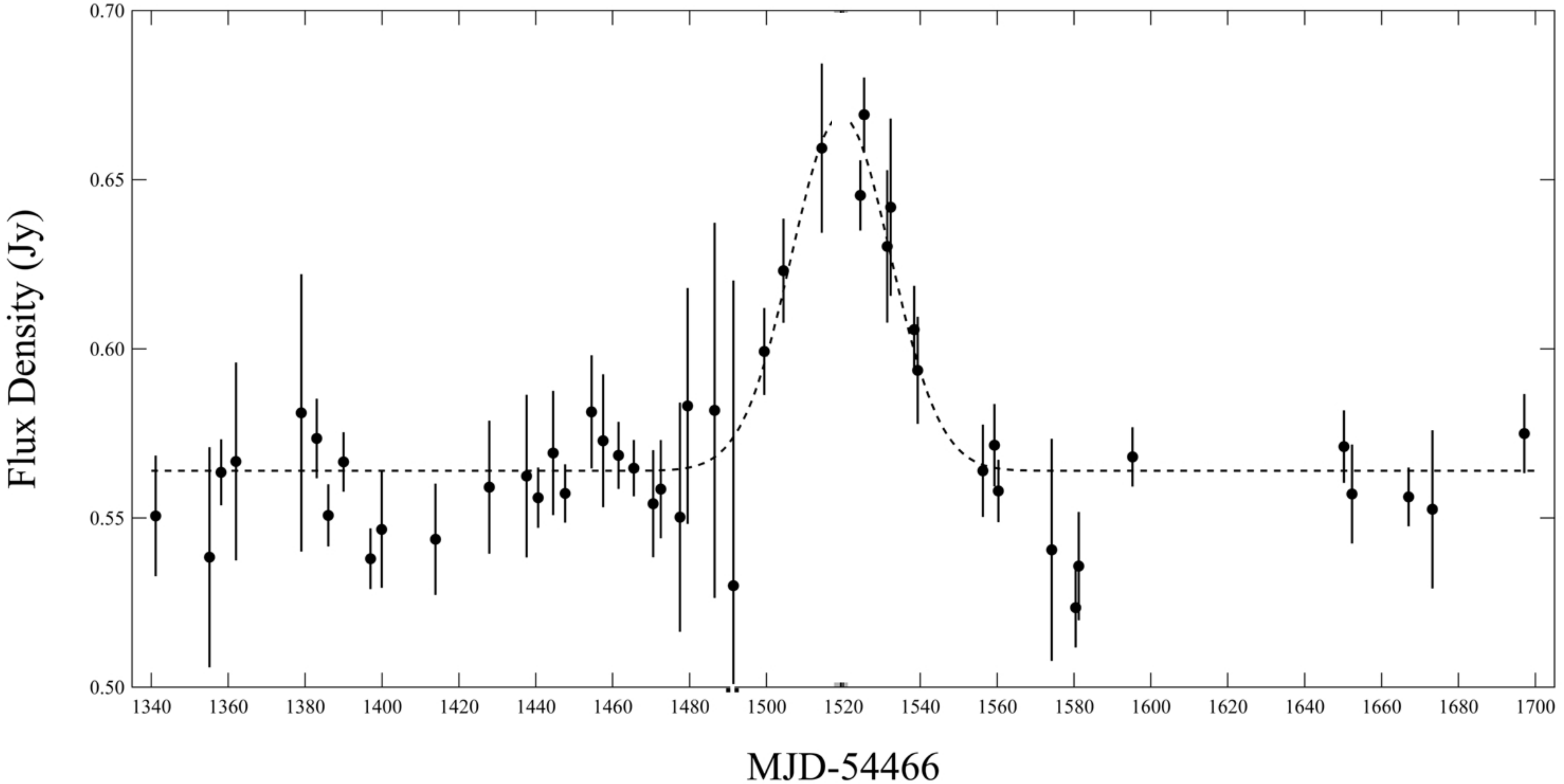

Flux Density (Jy)
MJD-54466

Figure 3

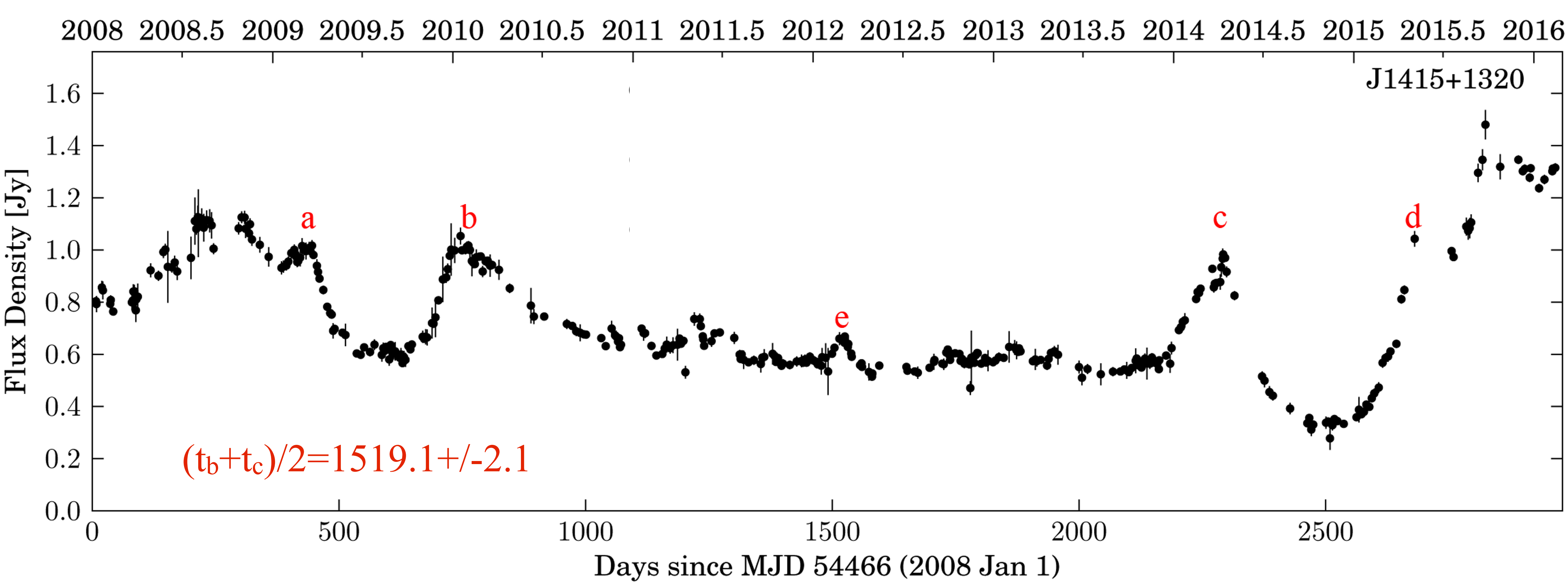

J1415+1320
a
b
c
d
e
$(t_b+t_c)/2=1519.1+/-2.1$
Flux Density [Jy]
Days since MJD 54466 (2008 Jan 1)

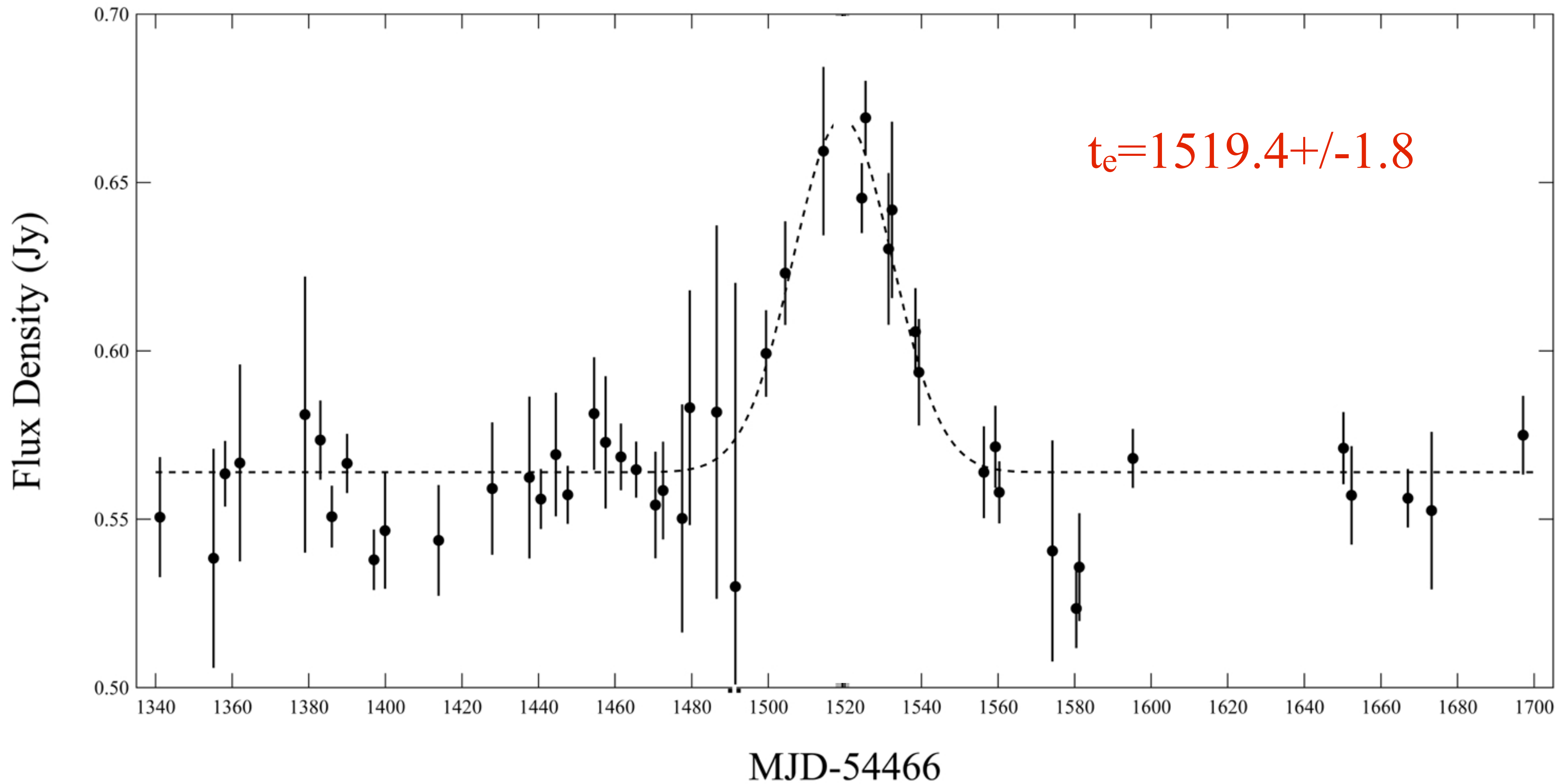
te=1519.4+/-1.8
Flux Density (Jy)
MJD-54466

Figure 3

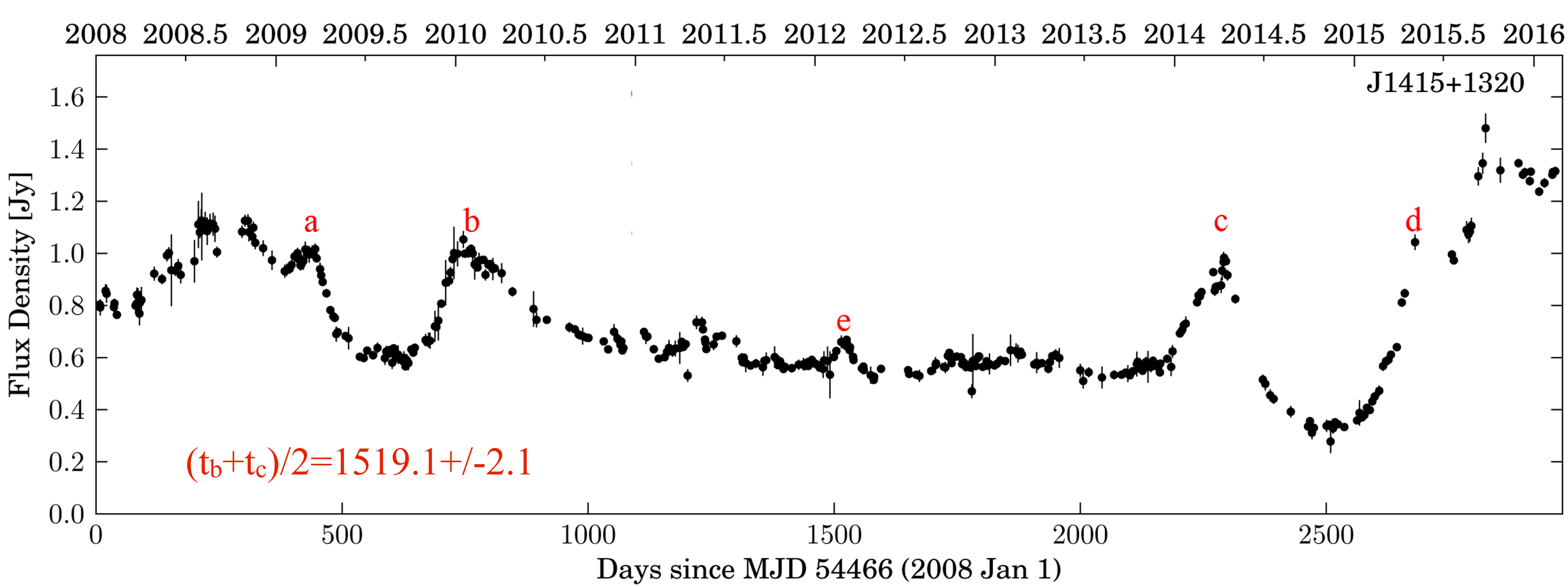
J1415+1320
a
b
c
d
e
(tb+tc)/2=1519.1+/-2.1
Flux Density [Jy]
Days since MJD 54466 (2008 Jan 1)

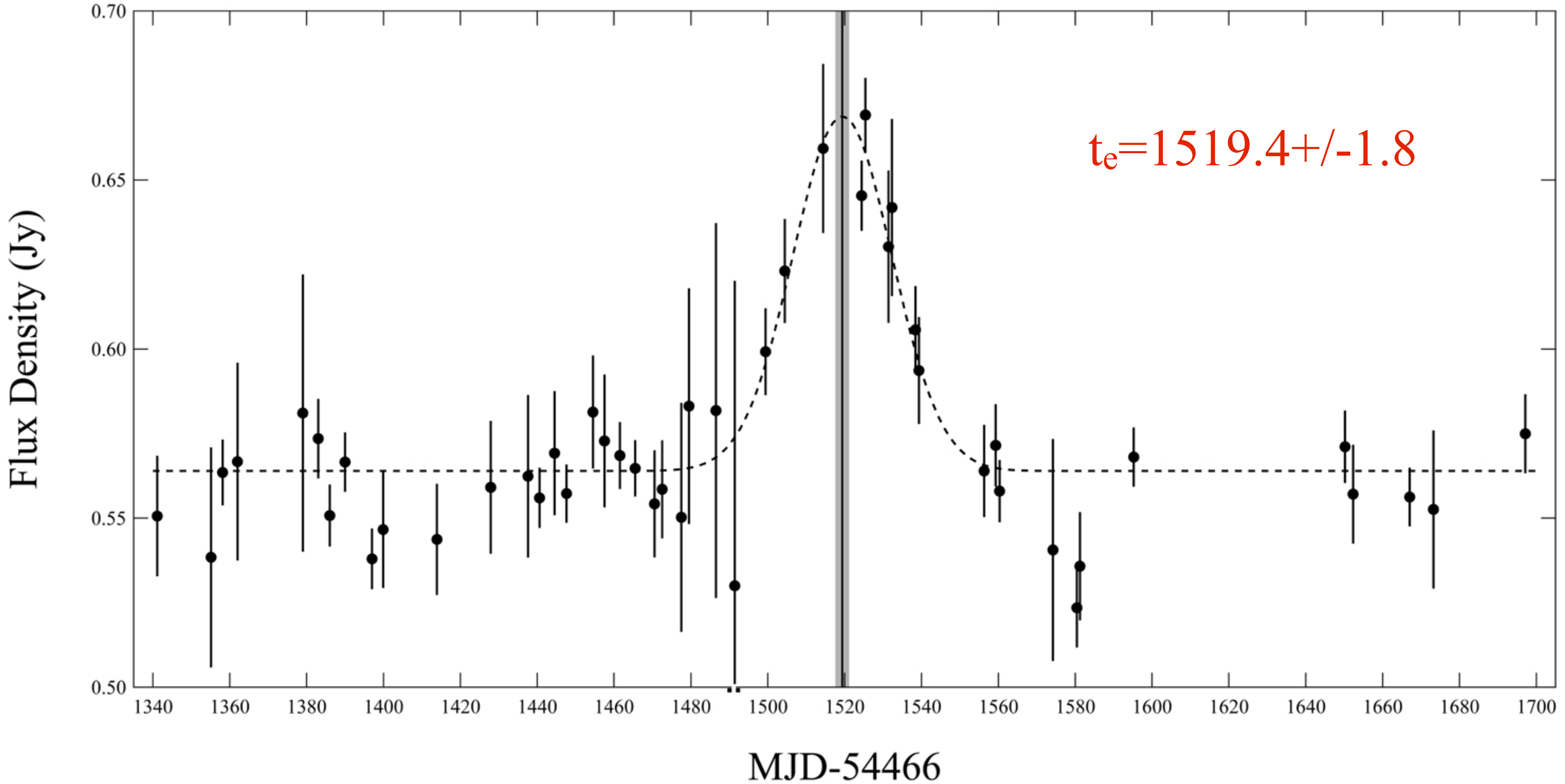

t_e=1519.4+/-1.8
Flux Density (Jy)
MJD-54466

Figure 3

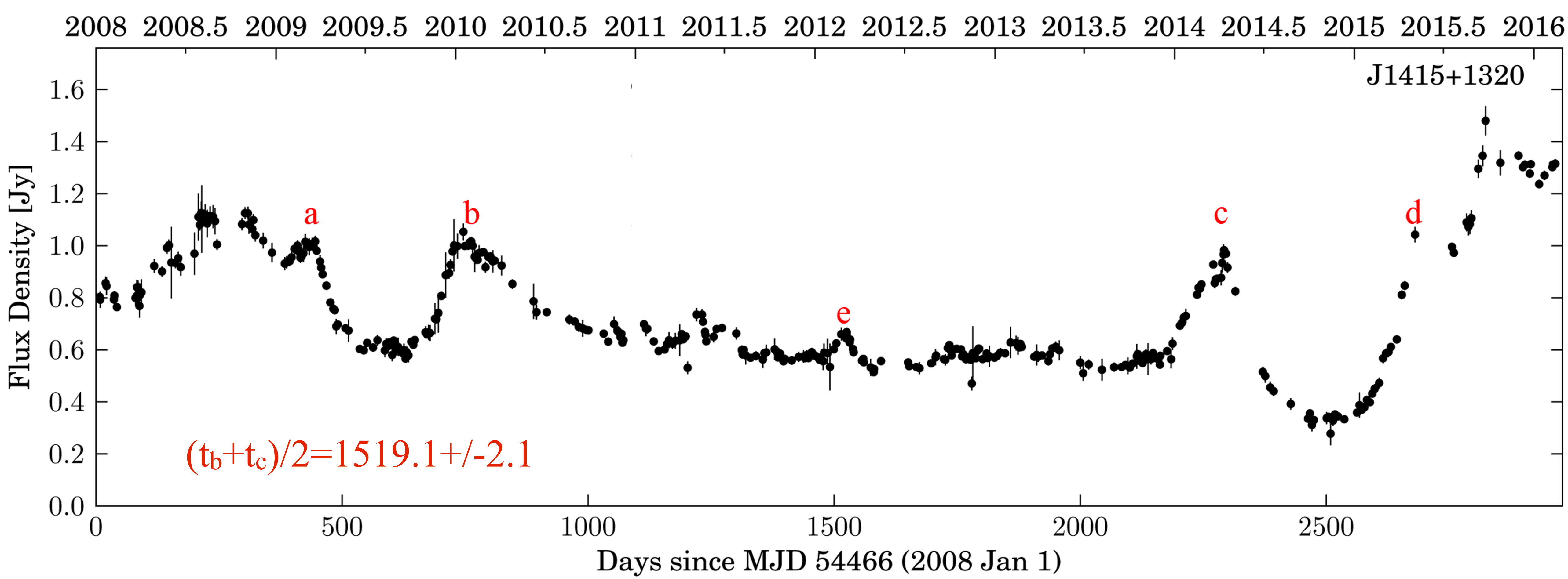

J1415+1320
a
b
c
d
e
$(t_b+t_c)/2$=1519.1+/-2.1
Flux Density [Jy]
Days since MJD 54466 (2008 Jan 1)